Volume 49
Number 28
28 July 2025
Pages 12019–12454

NJC

New Journal of Chemistry

A journal for new directions in chemistry

rsc.li/njc

ISSN 1144-0546

PERSPECTIVE

Kathryn M. Wolfe, Michael J. Grant, Irene E. Park and Gregory C. Welch

Tris(pentafluorophenyl)borane: leveraging historical and emerging work to identify alternatives for organic electronic applications

ROYAL SOCIETY OF CHEMISTRY

cnrs

NJC

ROYAL SOCIETY OF CHEMISTRY

PERSPECTIVE

View Article Online
View Journal | View Issue

Cite this: *New J. Chem.*, 2025, **49**, 12032

Tris(pentafluorophenyl)borane: leveraging historical and emerging work to identify alternatives for organic electronic applications

Kathryn M. Wolfe, Michael J. Grant, Irene E. Park and Gregory C. Welch *

Received 31st March 2025,
Accepted 27th May 2025

DOI: 10.1039/d5nj01430a

rsc.li/njc

Tris(pentafluorophenyl)borane ($B(C_6F_5)_3$) is a versatile Lewis acid now having played a key role in the development of boron-based Lewis acid chemistry. The borane has found utility in many applications ranging from a co-catalyst for olefin-polymerization to a dopant for organic (semi-)conductors. Highlighted within are historical advances of $B(C_6F_5)_3$ utilization in the realms of molecular transformations and frustrated Lewis pairs (FLPs). Applications of $B(C_6F_5)_3$ in various electronic devices is upcoming and presented, as well emerging dopant strategies for organic-based electronic applications are included. This perspective is completed by presenting other known Lewis acids with respective properties relevant for dopant applications in organic electronics.

1. Introduction

Tris(pentafluorophenyl)borane ($B(C_6F_5)_3$; Fig. 1) is a popular boron-based Lewis acid that has seen applications in many branches of science and engineering. With a 3-coordinate neutral structure there is an empty p-orbital on boron which can accept lone pairs of electrons, thus enabling reactivity. The Lewis acidity of $B(C_6F_5)_3$ is influenced by the three electron withdrawing pentafluorophenyl substituents that remove electron density away from boron and make the atom more acidic. The bulky pentafluorophenyl groups sterically encumber the boron center and introduces intermolecular interactions, which renders the compound a solid at room temperature with increased air and moisture stability compared to halide BX_3 (X = F, Cl, Br) counterparts. These properties make $B(C_6F_5)_3$ a potent yet stable Lewis acid, and therefore has been widely used both academically and industrially.[1] First synthesized in the early 1960's,[2] $B(C_6F_5)_3$ received little attention until the early 1990's when the compound was employed as a co-catalyst for the polymerization of olefins.[3–6] Following this, the volume of research and industrial application involving $B(C_6F_5)_3$ as a catalyst for molecular transformations was exponential. Around this time $B(C_6F_5)_3$ was also being applied in electronic devices, such as lithium batteries, with reports dating back as early as the 1990's.[7] Then in the mid 2000's, the discovery of frustrated Lewis pairs (FLPs), based on the combination of $B(C_6F_5)_3$ with sterically bulky phosphines, re-popularized the chemistry of this borane and led to the first reports of metal-free hydrogenation using hydrogen gas (H_2) and the subsequent sequestration of many other small molecules (*e.g.* CO_2, N_2O, olefins).[8–11] While the chemistry of $B(C_6F_5)_3$ for molecular transformations[1,6,12–14] and FLPs[9–11,15] has been extensively reviewed, the use of $B(C_6F_5)_3$ as a p-type dopant for organic (semi-)conductors with reports of increased stability and efficiency of organic electronic devices is emerging.

Within we first highlight established applications of $B(C_6F_5)_3$ in the realms of organic/organometallic molecular transformations and FLPs. The reported interactions, properties, and reactivity are critical to consider when applying $B(C_6F_5)_3$ as a p-type dopant in organic electronics, as the role of the Lewis acid has been somewhat elusive and debated, and thus these accounts provide valuable insight. A variety of electronic devices, including batteries, organic transistors, solar cells, *etc.*, are reviewed with relevant dopant mechanisms, emerging applications, and dopant strategies. Lastly, we present alternate borane- and borate-based Lewis acids with the respective properties relevant for dopant applications in organic electronics. Our perspective is that while the utility and scope of $B(C_6F_5)_3$ is impressive, the variety of materials applied in organic electronics is so vast that alternate Lewis acids need to be considered as $B(C_6F_5)_3$ will not harbour the optimal properties for every set of materials and device architectures that develop.

2. Molecular transformations using $B(C_6F_5)_3$

2.1. Overview

The empty p-orbital on the boron of $B(C_6F_5)_3$ can accept a pair of electrons and thus can activate Lewis basic sites on compounds to promote catalytic reactions & organic/organometallic

Department of Chemistry, University of Calgary, 2500 University Drive N.W., Calgary, Alberta, T2N 1N4, Canada. E-mail: gregory.welch@ucalgary.ca; Tel: +1-403-210-7603

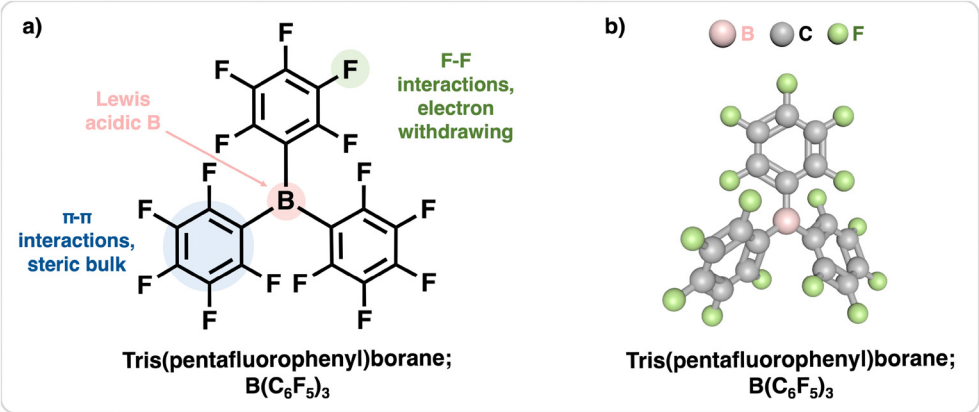

Fig. 1 Structural representations of $B(C_6F_5)_3$. (a) Line drawing of $B(C_6F_5)_3$ with highlights of F atoms for electron withdrawing effects and F–F interactions, phenyl rings for π–π interactions and providing steric bulk, and B atom as the Lewis acidic site. (b) 3D model of $B(C_6F_5)_3$ for visual representation of the propeller style conformation.

transformations. Some important reactions & transformations involving $B(C_6F_5)_3$ include olefin polymerization,[1,5,6] aldol-type Michael reactions,[16] hydrosilylations,[17,18] Piers–Rubinsztajn reactions,[17,19,20] allylstannations,[21–23] and Diels–Alder reactions.[24–27] Unlike other boron/halogen containing Lewis acids (BX_3, X = F, Cl, Br), the pentafluorophenyl groups on $B(C_6F_5)_3$ increase the sterics about the boron center, embodies B–C bonds that are less prone to hydrolysis, and promotes intermolecular interactions which allows for stable and isolable intermediates/products in a plethora of catalytic reactions. This resulted in mechanistic studies on Lewis acid catalyzed and co-catalysed reactions which were previously not achievable with traditional boron/halogen containing Lewis acids. Furthermore, the high thermal stability of $B(C_6F_5)_3$ (stable up to 270 °C) is ideal for reactions that require higher temperatures in which traditional metal catalysts would degrade. There are comprehensive reviews on the various organic and organometallic transformations that $B(C_6F_5)_3$ is capable of catalyzing and/or plays a key role in ref. 13 and 28, therefore, this section merely highlights enlightening studies using $B(C_6F_5)_3$ in various molecular transformations and FLPs. Reactions involving $B(C_6F_5)_3$ in the presence of water are also included as $B(C_6F_5)_3{\cdot}H_2O$ adducts are an attractive p-type dopant for organic electronic materials (*vide infra*).

2.2. Historical molecular transformations using $B(C_6F_5)_3$

In 1991, both the groups of Marks and Robinson separately demonstrated highly active and productive olefin polymerization using $B(C_6F_5)_3$ as a co-catalyst with alkyl group-IV metallocenes, specifically dimethyl zirconocenes (Fig. 2a).[3,29] When paired with metallocenes, the Lewis acidic $B(C_6F_5)_3$ can abstract an alkyl group and is rendered anionic and the metal center cationic enabling coordination–insertion polymerization. Following this discovery, a plethora of reports using $B(C_6F_5)_3$ as a co-catalyst for olefin polymerization emerged throughout the 1990's and beyond.[3–6,29]

In 1993, $B(C_6F_5)_3$ was explored as a catalyst for aldol-type and Michael reactions, which were previously achieved with alternate Lewis acids, however, these reactions suffered from poor yields if even trace amounts of water were present.[16] With $B(C_6F_5)_3$ being somewhat water and air-stable, high yielding aldol-type and Michael reactions were achieved and resulted in the coupling of various silyl enol ethers and aldehydes (Fig. 2b). Hydrosilylation of carbonyls is used for the preparation of silylethers, and typically uses metal catalysts to do so. However, in 1996, Piers and Parks demonstrated the catalytic activity of $B(C_6F_5)_3$ for the hydrosilylation of aryl carbonyls (Fig. 2c), to which $B(C_6F_5)_3$ was reported as being comparable with traditional metal catalysts used in terms of selectivity and conversion rates.[30] Later, hydrosilylation of imines using $B(C_6F_5)_3$ was also demonstrated.[35] In 1998, Maruoka and coworkers reported allylation and reduction of an *ortho*-anisaldehyde using $B(C_6F_5)_3$ and an allyl tributyltin reagent in a competitive reaction with *para*-anisaldehyde, where the allylation of the *ortho*-anisaldehyde resulted in a >20 : 1 favour over the *para*-anisaldehyde (Fig. 2d).[31] The authors suggested the reaction proceeds *via* pentacoordinate $B(C_6F_5)_3$ adducts with the *ortho*-anisaldehyde, a highly unusual reaction as this requires chelation of a boron-based Lewis acid, something that is notoriously difficult to do. However, Piers and coworkers later elucidated the mechanism: $B(C_6F_5)_3$ abstracts the allyl group from the tin reagent, producing the activated "$SnBu_3^+$" species which then catalyzes the reaction thus suggesting hypercoordination of the borane is not necessary.[21,36]

Developed in the 2000's, the Piers–Rubinsztajn reaction is one that involves the synthesis of alkoxysilanes and the respective polymers. It was first noted by Piers and Parks in 1996 that a small amount of silyl ethers were transformed into silyl alkanes in the presence of $B(C_6F_5)_3$ when attempting to reduce aromatic carbonyl compounds.[30] This lead to Rubinsztajn and Cella investigating the formation of siloxane polymers using $B(C_6F_5)_3$.[33] Shortly after, the Piers–Rubinsztajn reaction was formulated and has since been widely used for the synthesis of polymeric siloxanes (Fig. 2f).[17,19,20] These polymers are composed of strong Si–O bonds, which provides the bulk material with high chemical resistance and thermal stability but at the consequence of requiring harsh conditions for degradation or recycling. However, the depolymerization of

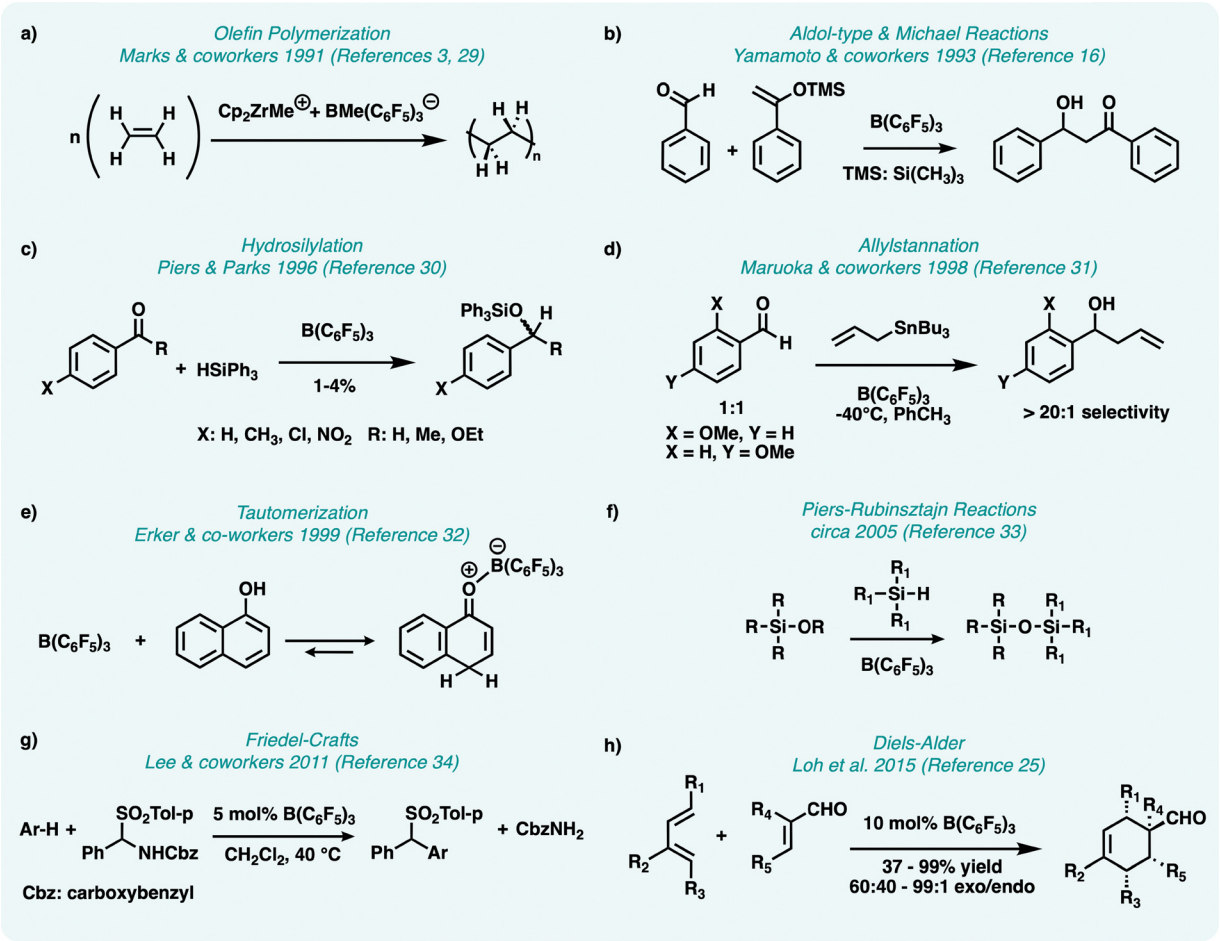

Fig. 2 Critical reactions involving $B(C_6F_5)_3$ for catalysis & chemical transformations. (a) Olefin polymerization is achieved using Cp_2ZrMe^+ + $BMe(C_6F_5)_3^-$,[3,29] (b) Adol-type and Michael reactions utilizing aldehydes and silyl enol ethers are catalyzed by $B(C_6F_5)_3$,[16] (c) hydrosilylation of aryl carbonyls are catalyzed by $B(C_6F_5)_3$,[30] (d) allylstannations of *ortho*-anisaldehydes are favoured over *para*-anisaldehydes by >20 : 1 in the presence of $(B(C_6F_5)_3)$,[31] (e) tautomerization of aromatic enols can be done by coordination of the boron on $B(C_6F_5)_3$ with the oxygen on the enol,[32] (f) Piers–Rubinsztajn reactions see siloxane formation using hydrosilanes and alkoxysilanes in the presence of catalytic $B(C_6F_5)_3$,[33] (g) Friedel–Crafts reactions using 1,2,4-trimethoxy benzene was successfully alkylated with a *N*-benzyloxycarbonylamino phenyl *p*-tolylsulfone in the presence of catalytic $B(C_6F_5)_3$,[34] (h) Diels–Alder *exo*-selective isomers are formed open chain-dienes and α,β-unsaturated enals in the presence of catalytic $B(C_6F_5)_3$.[25]

polydimethylsiloxane using reagents $B(C_6F_5)_3$ and dimethyl carbonate under mild conditions was more recently reported.[37] This demonstrates the versatility of $B(C_6F_5)_3$ for both the synthesis and sustainable degradation of organosiloxanes.

Tautomerization of aromatic enols are difficult due to breaking aromaticity, however, due to stable $B(C_6F_5)_3$-carbonyl adducts, the tautomerization of naphthol with $B(C_6F_5)_3$ for isolation of the keto isomer was shown to be possible (Fig. 2e).[32] Following this, several pyrrole based tautomers were made and put to use in Ziegler–Natta catalysis chemistry as Brønsted acid activators for highly efficient polymerizations.[38–41] Due to the ability to form adducts with carbonyl and imine containing compounds, it was then discovered that $B(C_6F_5)_3$ can catalyze other important C–C coupling reactions. Indeed, Diels–Alder reactions of 2-cycloalkenones can be catalyzed by $B(C_6F_5)_3$, however, like other Lewis acids these reactions resulted in high ratios of the *endo* product.[24] Then in 2015, Loh and coworkers demonstrated the use of $B(C_6F_5)_3$ for *exo*-selective isomers using open chain-dienes and α,β-unsaturated enals as the dienophiles (Fig. 2h).[25] It was hypothesized that due to the bulky nature of $B(C_6F_5)_3$, sterics cause the favour of the *exo*-product with ratios ranging from 60 : 40 to 99 : 1, which was later supported by Soós and coworkers in 2018.[26] Additionally, $B(C_6F_5)_3$ is capable of catalyzing Friedel–Crafts reactions, showcasing yet another example of making C–C bond formation more efficient. A reaction of this type was first reported in 2011, where 1,2,4-trimethoxy benzene was successfully alkylated with a *N*-benzyloxycarbonylamino phenyl *p*-tolylsulfone in the presence of $B(C_6F_5)_3$ with high yields (Fig. 2g).[34]

2.3. Frustrated Lewis pairs involving $B(C_6F_5)_3$

Frustrated Lewis pairs (FLPs) can be described as compounds that contain Lewis base/acid pairs with sufficient steric hinderance to prevent Lewis adduct formation *via* dative bonding. The seminal discovery of FLPs (first publication in 2006) provided the next sequence of impactful research involving $B(C_6F_5)_3$. The serendipitous discovery of FLPs came from a unusual reaction

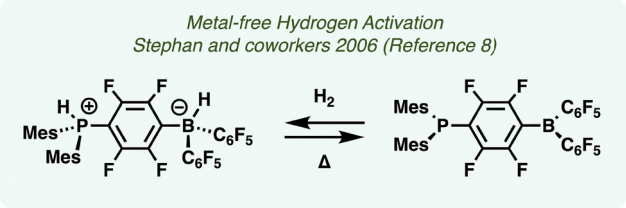

Fig. 3 The seminal discovery of FLPs; $(C_6H_2Me_3)_2PH(C_6F_4)BH(C_6F_5)_2$ liberates H_2 when heated (to ~100 °C) to give the phosphino-borane $(C_6H_2Me_3)_2P(C_6F_4)B(C_6F_5)_2$, a process which is reversible upon cooling.[8]

of $B(C_6F_5)_3$ with the sterically bulky phosphine bismesitylphosphine ($(C_6H_2Me_3)_2PH$) to form the air & moisture stable white zwitterionic solid, $(C_6H_2Me_3)_2PH(C_6F_4)BF(C_6F_5)_2$.[8] Treatment of this compound with Me_2SiHCl resulted in the exchange of a fluorine atom for a hydride at the boron and gave $(C_6H_2Me_3)_2PH(C_6F_4)BH(C_6F_5)_2$. This compound contained both a proton (on the phosphorus) and hydride (on the boron) which when gently heated (~100 °C) released H_2 gas and gave the phosphino-borane $(C_6H_2Me_3)_2P(C_6F_4)B(C_6F_5)_2$ (Fig. 3), which was bright orange in color owing to intramolecular charge transfer characteristics. The process of H_2 liberation was found to be reversible and thus this resulted in the first ever report of metal-free hydrogen activation.[8] By retaining the Lewis basicity and acidity within the $(C_6H_2Me_3)_2P(C_6F_4)B(C_6F_5)_2$ molecule, electron density can be donated and accepted simultaneously and allowed for reversible heterolytic cleavage and liberation of H_2 at moderate (25 °C) and high (>100 °C) temperatures, respectively. Upon further investigation of the interaction (or lack thereof) of bulky phosphines (PR_3, R = i-Pr, Cy & PHR'_2, R′ = *t*-Bu, $C_6H_2Me_3$-2,4,6) with $B(C_6F_5)_3$, the term FLP was coined.[42] Subsequently a diverse and rapid emergence of research involving $B(C_6F_5)_3$ based FLPs for many reactions, including metal-free hydrogenation, hydroamination, activation of various small molecules, and dehydrogenation has been extensively reviewed.[9–11,15,43–45] Furthermore, many variations of FLPs have been made, where both the Lewis acid and Lewis base have been exchanged.[10,15] This section aims to highlight select molecular transformations catalyzed by FLPs using $B(C_6F_5)_3$ as the Lewis acid component.

Metal-free hydrogenation has positive implications for some important industries, such as the food & beverage and petrochemical industries, where the use of metal catalysts in these industries can be costly. For example, hydrogenation is responsible for the manufacturing of food products such as oils, shortenings, and spreads. Following the discovery of FLPs as a catalyst for metal-free hydrogenation, useful transformations such as the hydrogenation of alkenes/olefins/alkynes (Fig. 4a),[46–49] aromatics,[50] carbonyls (Fig. 4b),[51–53] imines/nitriles/enamines (Fig. 4c and d),[54–56] silyl enol ethers (Fig. 4f),[57] and oximes (Fig. 4e)[58] have been reported using $B(C_6F_5)_3$ as the Lewis acid component.

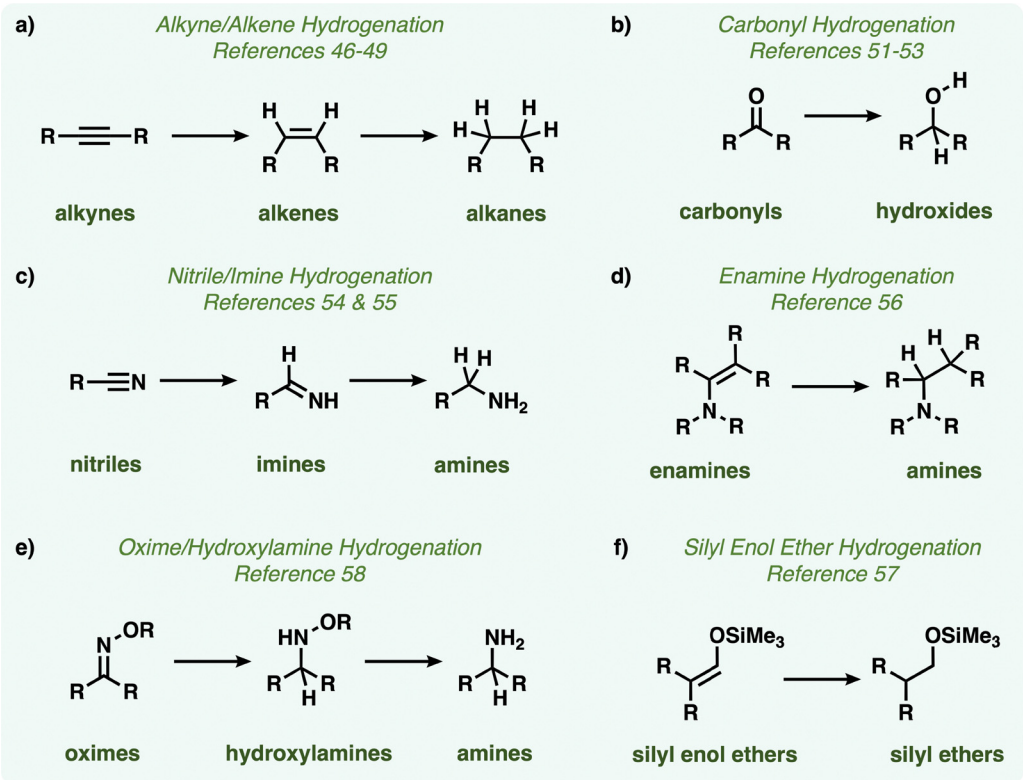

Fig. 4 Metal-free hydrogenation using $B(C_6F_5)_3$ FLPs. (a) $B(C_6F_5)_3$ FLPs are capable of reducing alkynes to alkenes, and upon further treatment from alkenes to alkanes.[46–49] (b) $B(C_6F_5)_3$ based FLPs can reduce carbonyls to primary alcohols.[51–53] (c) $B(C_6F_5)_3$ based FLPs can reduce nitriles into imines, and then into amines.[54,55] (d) $B(C_6F_5)_3$ based FLPs can reduce enamines into amines.[56] (e) $B(C_6F_5)_3$ based FLPs can reduce oximes to hydroxylamines and then amines.[58] (f) $B(C_6F_5)_3$ based FLPs can reduce silyl enol ethers into silyl ethers.[57]

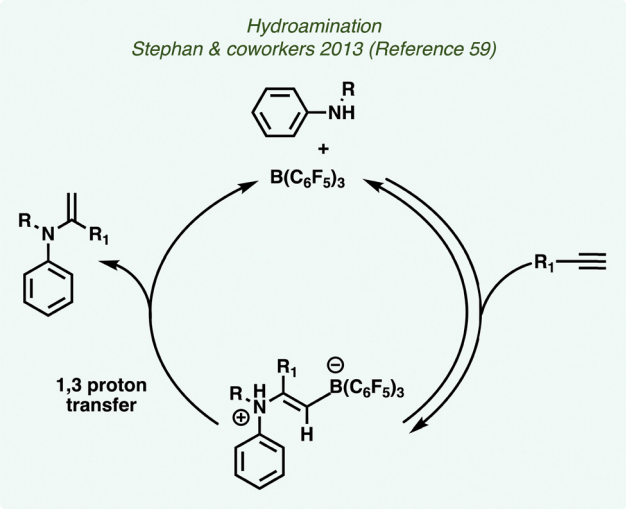

Fig. 5 Hydroamination using $B(C_6F_5)_3$ as an FLP.[59] When the combination of $B(C_6F_5)_3$ and an aryl amine is treated with alkynes it creates a zwitterionic FLP intermediate, and then a 1,3 proton transfer induces the release of an aryl enamine product and regeneration of $B(C_6F_5)_3$.

Hydroamination reactions are relevant for many synthetic chemists, as they can be employed using amines and alkenes/alkynes intermolecularly or intramolecularly, where the latter results in N-heterocycle formation. Stephan and coworkers demonstrated the first account of using $B(C_6F_5)_3$ based FLPs for hydroamination reactions using aryl amines and terminal alkynes in an intermolecular fashion to produce an aryl enamine (Fig. 5).[59] Later, the same authors expanded the scope of $B(C_6F_5)_3$ based FLPs for hydroamination using aryl amines and terminal alkynes in both an inter- and intramolecular fashion, producing a plethora of compounds including a series of N-heterocycles.[60] However, instead of forming the imine N-heterocycles, the intramolecular hydroamination reactions were performed under a H_2 atmosphere, resulting in one-pot hydroamination/hydrogenation reactions further demonstrating versatility of $B(C_6F_5)_3$ based FLPs.

Other than activating H_2 for metal-free hydrogenation, capturing and activating alternate small molecules such as CO,[61–63] CO_2,[64–69] N_2O,[70] NO,[71] and SO_2,[72] alkenes,[43] alkynes,[73–75] and disulphides[76] using FLPs is highly sought after. We refer the reader to a recent review involving FLPs capturing and converting CO_2.[69] In brief, Stephan and Erker reported the first use of FLP chemistry for the sequestration of CO_2, where the FLP P*t*Bu$_3$ + $B(C_6F_5)_3$ and FLP complex $(Me_3C_6H_2)_2PCH_2CH_2B(C_6F_5)_2$, can capture and liberate CO_2 reversibly (Fig. 6a).[64] Later, Kumacheva and coworkers determined the thermodynamics of the capture and liberation of CO_2 *via* FLPs by a novel micro fluidics approach that provided a means for future thermodynamic characterization of FLP CO_2 sequestrations and other reactions of the like.[77] The first conversion of CO_2 to methanol *via* FLPs was reported by O'Hare and coworkers, however, thermolysis to produce free methanol resulted in the decomposition of $B(C_6F_5)_3$.[65] In 2010, Piers and coworkers reported CO_2 conversion using a 2,2,6,6-tetramethylpiperidine/$B(C_6F_5)_3$ FLP with triethylsilane for a deoxygenative reduction of CO_2 to CH_4.[66] Other than CO_2 activation, using the same P*t*Bu$_3$ & $B(C_6F_5)_3$ FLP for CO (Fig. 6b),[61] N_2O (Fig. 6c),[70] and SO_2 (Fig. 6d)[72] activation has been successful, where all reactions result in complexation of the small molecules with the P*t*Bu$_3$ & $B(C_6F_5)_3$ pair by bridging them and producing solids.

2.4. Emerging applications of $B(C_6F_5)_3$ in the presence of H_2O for molecular transformations

Upon exposure to water, $B(C_6F_5)_3$ forms oxygen bridged borate adducts and complexes (Fig. 7a) and can decompose into boronic acids and boroxines, especially upon heating.[78] Therefore, chemists working with $B(C_6F_5)_3$ typically ensure a moisture free environment for storage and reaction conditions.

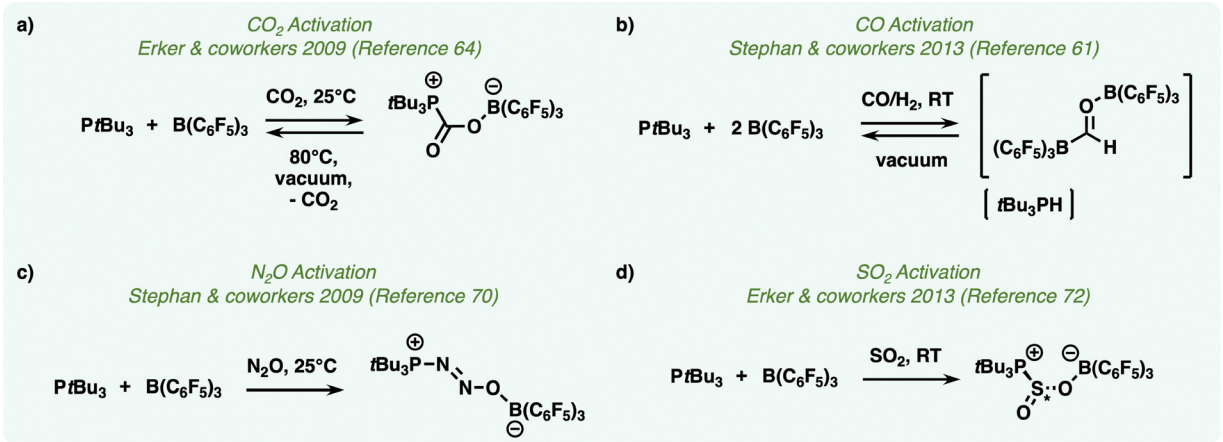

Fig. 6 Small molecule activation using $B(C_6F_5)_3$ FLPs. (a) CO_2 activation & capture using P*t*Bu$_3$ and $B(C_6F_5)_3$ at 25 °C results in a P*t*Bu$_3$CO$_2$B$(C_6F_5)_3$ complex, where CO_2 can be liberated at 80 °C under vacuum.[64] (b) CO activation & capture using P*t*Bu$_3$ and 2[$B(C_6F_5)_3$] at room temperature in the presence of H_2 to form a formyl borate derivative, which can be reversed to release CO upon placing under vacuum.[61] (c) P*t*Bu$_3$, $B(C_6F_5)_3$, & N_2O form a bridged $B(C_6F_5)_3$–N_2O–P*t*Bu$_3$ species in a *trans* configuration upon combining the reagents and heating at 25 °C.[70] (d) P*t*Bu$_3$, $B(C_6F_5)_3$, & SO_2 react at room temperature to form a bridged zwitterionic $B^-(C_6F_5)_3$–SO_2–P^+*t*Bu$_3$ adduct.[72]

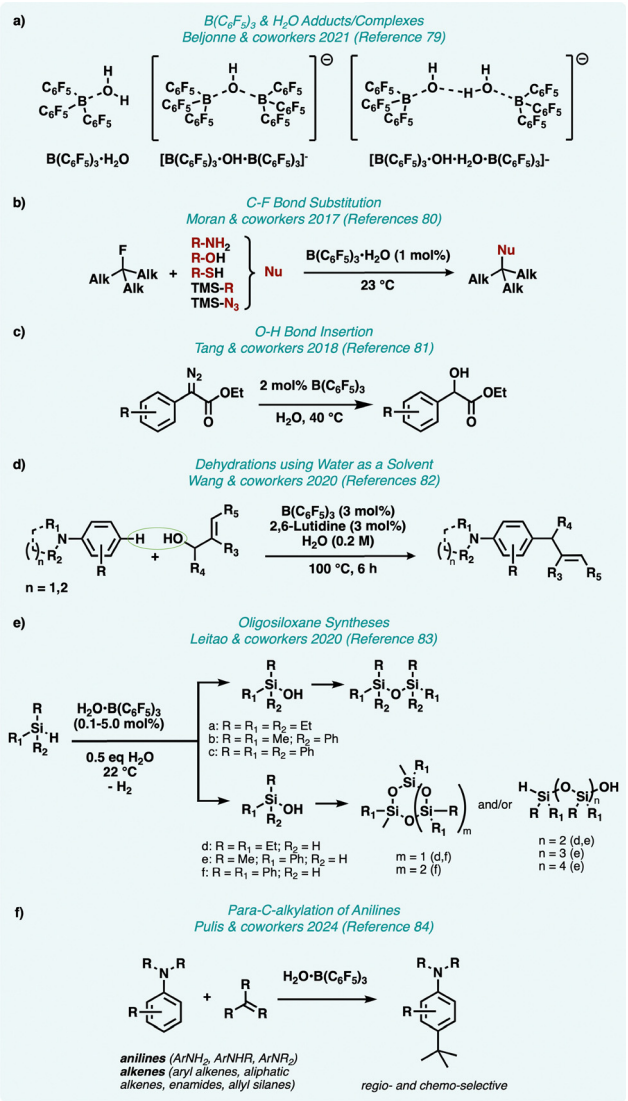

Fig. 7 $B(C_6F_5)_3$ in the presence of H_2O for molecular transformations; (a) adducts of $B(C_6F_5)_3$ with H_2O: $B(C_6F_5)_3{\cdot}H_2O$, $[B(C_6F_5)_3{\cdot}OH{\cdot}B(C_6F_5)_3]^-$, and $[B(C_6F_5)_3{\cdot}OH{\cdot}H_2O{\cdot}B(C_6F_5)_3]^-$,[79] (b) C–F bond substitution of alkanes is catalyzed by $B(C_6F_5)_3{\cdot}H_2O$ (1 mol%) at room temperature to afford an array of C-, N-, O-, and S-substituted products,[80] (c) $B(C_6F_5)_3$ in H_2O affords O–H bond insertion for α-diazoesters to form α-hydroxyesters at moderate temperatures (40 °C),[81] (d) dehydration reactions involving allylation of electron-rich arenes and allyl alcohols using $B(C_6F_5)_3$ in water,[82] (e) syntheses of oligosiloxanes using $H_2O{\cdot}B(C_6F_5)_3$ as a catalyst for the conversion of hydrosilanes and tethered hydrosilanes to make oligomeric siloxanes,[83] (f) regio- and chemo-selective *para*-alkylation of anilines using $H_2O{\cdot}B(C_6F_5)_3$.[84]

However, there are emerging applications of adducts involving $B(C_6F_5)_3$ and water ($B(C_6F_5)_3{\cdot}H_2O$; Fig. 7a) which transform $B(C_6F_5)_3$ from a Lewis acid to a potent Brønsted acid. This results in altered reactivity and applications, including as a p-type dopant for organic electronics (*vide infra*).[79] Note, considering the study done by Beljonne and coworkers, upon deprotonation of $B(C_6F_5)_3{\cdot}H_2O$, it is likely that the resulting $[B(C_6F_5)_3{\cdot}OH]^-$ anion complexes with free $B(C_6F_5)_3$ and $B(C_6F_5)_3{\cdot}H_2O$ to form the energetically favoured complexes $[B(C_6F_5)_3{\cdot}OH{\cdot}B(C_6F_5)_3]^-$ and $[B(C_6F_5)_3{\cdot}OH{\cdot}H_2OB(C_6F_5)_3]^-$ (Fig. 7a), respectively.[79]

Efforts to break C–F bonds under benign conditions have persisted, one example being defluorination functionalization of tertiary aliphatic fluorides mediated by a $H_2O{\cdot}B(C_6F_5)_3$ adduct. In 2017, Moran and coworkers reported that 1 mol% of the adduct was capable of catalyzing C–F bond substitution of aliphatic fluorides at room temperature using various heteroatomic nucleophiles to afford a range of S-, O-, N-, and C-substituted products in good yields (Fig. 7b).[80] The authors previously reported a Friedel–Crafts autocatalytic mechanism, where initiation occurs by abstraction of the fluoride ion by a $B(C_6F_5)_3{\cdot}H_2O$ adduct (*via* F–H coordination) resulting in a aliphatic carbocation free to react with a plethora of nucleophiles, and is the proposed mechanism for this work.[85]

Molecular transformations using $B(C_6F_5)_3$ and water as the solvent is emerging, in 2018 $B(C_6F_5)_3$ was found to catalyze O–H bond insertion in α-diazoesters to form α-hydroxyesters using $B(C_6F_5)_3$ in water (Fig. 7c).[81] In 2020, Wang and coworkers reported the allylation of electron-rich arenes and allyl alcohols using $B(C_6F_5)_3$ in water, and provided a series of indoles coupled to 1,3-diphenylallyl alcohol.[82] These reactions are proposed to proceed by an FLP of $B(C_6F_5)_3$ and 2,6-lutidine, which then reacts to abstract the hydroxyl group of 1,3-diphenylallyl alcohol to provide a reactive allyl cation and $[B(C_6F_5)_3{:}OH]^-$ (Fig. 7d). In 2021, Wang and coworkers continued this work by allylation of 1,3-diketones or β-ketone esters with allyl alcohols in water.[86] The authors propose this proceeds by adduct formation and thus activation of the ketone *via* adduct formation between the carbonyl and $B(C_6F_5)_3$, which renders the $-CH_2$ group bridging the diketone acidic and upon deprotonation forms a reactive carbocation.

While reactions involving $B(C_6F_5)_3$ and water have been demonstrated, excess water can still be problematic as the Brønsted acidity is expected to decrease.[78,79] This can be mediated by adding controlled amounts of water to a reaction mixture to form $B(C_6F_5)_3{\cdot}H_2O$, or by adding the premade adduct directly. This has been demonstrated for the synthesis of oligosiloxanes using $B(C_6F_5)_3{\cdot}H_2O$ as a catalyst by Leitao and coworkers, who reported the conversion of hydrosilanes and tethered hydrosilanes to make oligomeric siloxanes using controlled mol percentages of $B(C_6F_5)_3{\cdot}H_2O$ (Fig. 7e).[83] Pulis and coworkers reported on the *para*-alkylation of anilines, where the $H_2O{\cdot}B(C_6F_5)_3$ adduct was added to the reaction directly for highly selective *para-C*-alkylation over the *N*-alkylation and *ortho-C*-alkylation pathways (Fig. 7f).[84] The authors suggest this mechanism proceeds by protonation of the alkyl functional group by $B(C_6F_5)_3{\cdot}H_2O$ to form a reactive carbocation.

3. Applications of $B(C_6F_5)_3$ in electronic devices

3.1. Overview

Society relies heavily on electronic devices, with an indication that dependence on such technology is forever increasing. Some examples of on-going research in this field are batteries/energy storage, energy conversion, lighting displays, and sensors.

$B(C_6F_5)_3$ has seen research and application in this field; however, the function of $B(C_6F_5)_3$ varies significantly, further highlighting the vast scope and utilization of the compound. While the incorporation of boron into organic electronic materials is classic,[87–90] the use of $B(C_6F_5)_3$ is emerging and has proved to be fruitful. This section serves to highlight various roles of $B(C_6F_5)_3$ in electronic devices, more specifically for its role in batteries, organic electronics, and emerging applications.

3.2. Incorporating $B(C_6F_5)_3$ in batteries

3.2.1 Overview. Rechargeable batteries are commonly used in electronic devices such as mobile phones and electric vehicles.[91,92] These applications are currently dominated by lithium-ion batteries (LIBs) owing to their high power density, excellent performances, and long cycling stability.[93] However, current LIBs have persistent safety issues, such as overheating which results in fires, which limits the realization of large-scale implementation and further market expansion.[94] Thermal, electrical, and mechanical stress can trigger thermal runaway reactions in LIBs, resulting from the uncontrollable electrochemical reactions from the decomposition of liquid electrolyte containing Li-salts and flammable organic solvents.[94–96] To address this problem, additives, such as anion receptors, are introduced to facilitate complex formation with anions to prevent ion-pairing of the salt and mitigates the risk of the salt reacting within the electrolyte.[97] This section highlights

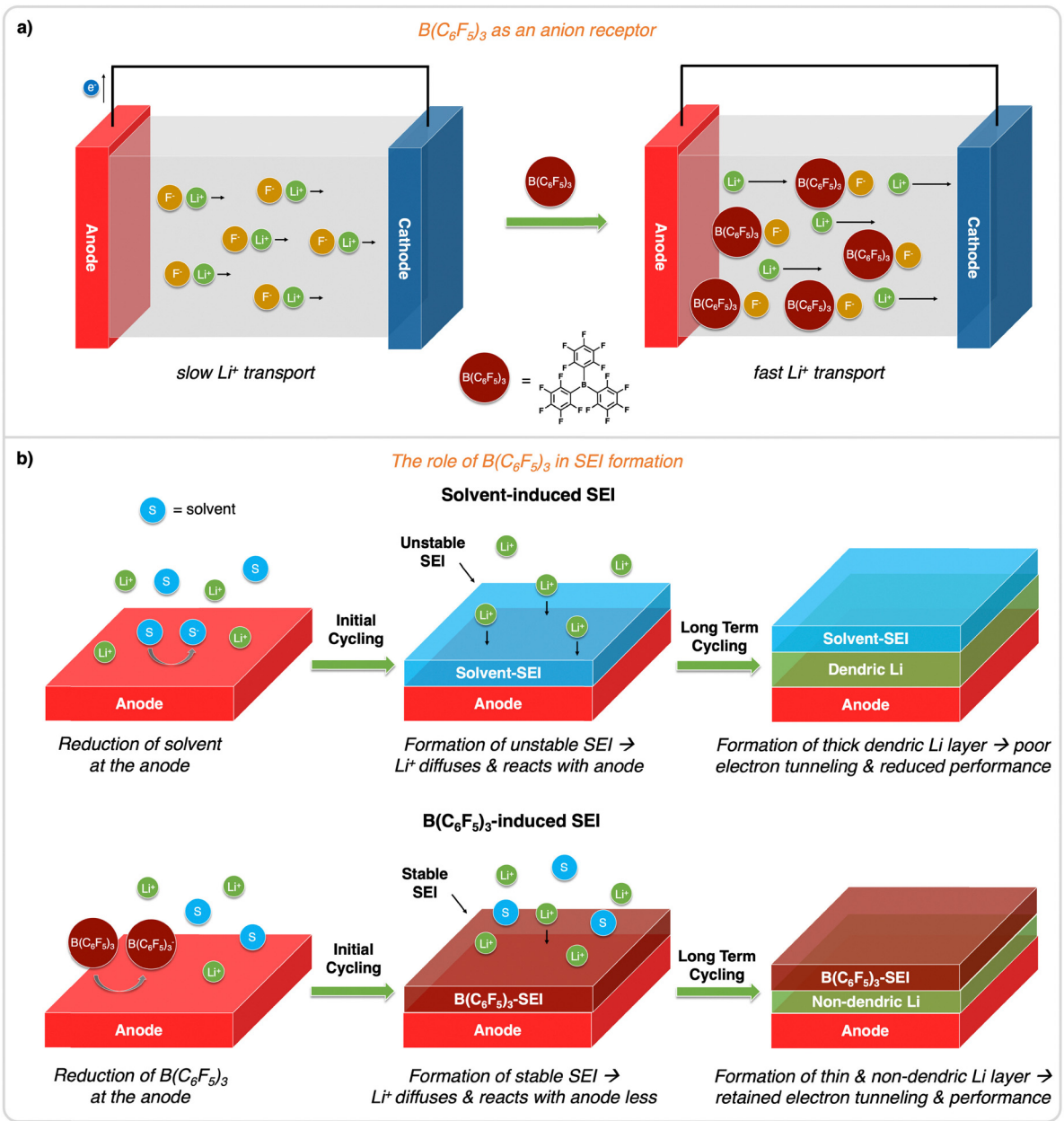

Fig. 8 The role of $B(C_6F_5)_3$ in LIBs. (a) $B(C_6F_5)_3$ as an anion receptor, which serves to aid in dissolution of LiF salts and increase the movement of Li^+. (b) $B(C_6F_5)_3$ as a sacrificial additive to LIBs to induce ideal SEI on the anode.

early and emerging work involving incorporating $B(C_6F_5)_3$ (Fig. 8) in batteries.

3.2.2 Early applications in lithium ion batteries. In 1998, $B(C_6F_5)_3$ saw its first application in LIBs as an electrolyte additive, serving as an anion receptor to assist in the dissolution of insoluble LiF salts in organic solvents (Fig. 8a), resulting in high ionic conductivity from higher salt concentrations in electrolyte.[7] The dissociation of the LiF salt is achieved by scavenging of F-ions by $B(C_6F_5)_3$ (forming stable B–F bonds), and as well anion migration is hindered due to the low mobility of the large complexes, allowing for improved Li ion movement.[7,98] Following this, several papers reported that addition of $B(C_6F_5)_3$ improved cycling performance and thermal stability of LIBs due to strong anion coordination along with formation of a passivation film, referred to as solid electrolyte interphase (SEI) on the surface of the electrode (Fig. 8b).[97,99–104] The SEI layer is critical to performance as it serves to prevent surface-reduction of electrolytic solvents,[105] and to protect anodes from Li dendrite growth.[106] However, SEI growth results in consumption of active electrolyte materials, leading to decreases in power density and increases in resistance over time.[107] Even though large concentrations of $B(C_6F_5)_3$ can benefit from higher ionic conductivity, controlled addition of $B(C_6F_5)_3$ is important to ensure longevity of the cycling performance of LIBs.[108] In addition to SEI formation, $B(C_6F_5)_3$ was used as a polymerization initiator for the solvent 1,4-dioxolane to achieve a solid-state polymer electrolyte, which is unlike liquid electrolytes that are prone to leakage which raises safety concerns.[98] It was also suggested that $B(C_6F_5)_3$ acts as flame retardant in LIBs due to the fluorine free radical generation from thermal decomposition that acts as a trap for highly reactive radical species such as $H^{\bullet}$ and $OH^{\bullet}$.[98] $B(C_6F_5)_3$ has thus seen success as an electrolyte additive in rechargeable lithium–metal batteries,[98,109–111] metal–gas batteries (*e.g.*, lithium–sulfur hexafluoride batteries),[112] and lithium–oxygen batteries.[113]

3.2.3 Emerging applications in sodium ion batteries. $B(C_6F_5)_3$-containing electrolytes for sodium-ion batteries (SIB) or -metal batteries (SMB) is emerging,[114,115] which are attractive alternatives to LIBs due to the natural abundance and low-cost of sodium compared to lithium.[116] $B(C_6F_5)_3$ was recently used as an electrolyte additive in SIBs by Chou and coworkers, who reported that the strong coordination of $B(C_6F_5)_3$ with ClO_4^- anions allowed for the free movement of Na^+ leading to high conductivity and overall performance.[115] This coordination led to an increase of organic solvents in the inner solvation sheath of sodium ions, resulting in fewer free solvents within the electrolyte. Although free solvents partake in SEI formation, controlling the rate is challenging, which can lead to a reduction in battery efficiency over time. Therefore, the decrease in the availability of free solvent molecules promoted preferential oxidation to decompose $B(C_6F_5)_3$ over free solvents, which led to overall enhanced oxidation stability. This process formed a beneficial NaF-rich solid electrolyte interphase (SEI) on a $Na_3V_2(PO_4)_3$ cathode, contributing to excellent electrochemical performances at high operating temperature of 60 °C. In another study, the fabrication of (quasi)solid-state electrolyte SMB was achieved with $B(C_6F_5)_3$ induced polymerization of 1,4-dioxolane solvent, in addition to the control of solvation environment resulting in a great stability with over 1000 cycles at low temperature of −20 °C.[114]

3.3. $B(C_6F_5)_3$ as a dopant in organic electronics

3.3.1. Overview. Doping organic materials has been employed since the discovery of conductive polymers in the 1970's,[117] where chemical doping enhances conductivity by increasing free electron movement through the introduction of small amounts of electron-rich moieties (n-type doping) or by creating holes with electron-poor moieties (p-type doping). A staple p-type dopant for organic materials is the electron accepting 2,3,5,6-tetrafluoro-7,7,8,8-tetracyanoquinodimethane (F_4-TCNQ).[118] However, application of F_4-TCNQ is limited due its lack of solubility resulting in energy intensive thermal evaporation for processing[119–121] and the need for organic materials with a large highest occupied molecular orbital (HOMO) energy level to allow for efficient integer charge

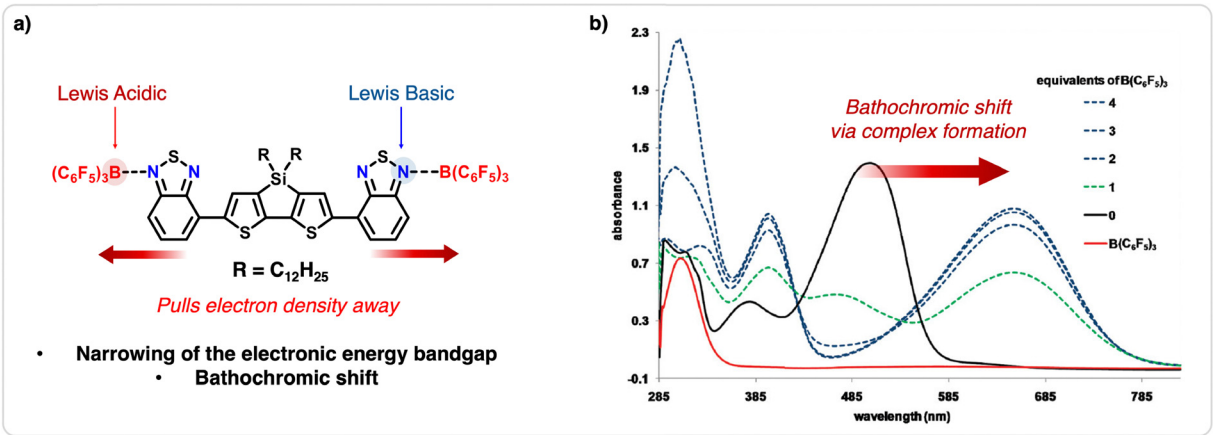

Fig. 9 Bazan and coworkers demonstrate how $B(C_6F_5)_3$ can tune the electronic gap of benzothiadiazole (BT) & $DTSC_{12}$ based oligomers.[128] (a) When added in stoichiometric amounts, $B(C_6F_5)_3$ forms a complex with the nitrogen on the BT unit of the BT/DTS_{C12} based oligomers. (b) Modified from Bazan and coworkers,[128] increasing the stoichiometric equivalence of $B(C_6F_5)_3$ (red line is neat $B(C_6F_5)_3$) in relation to the BT/DTS_{C12} oligomers (black line is neat $BT/DTSC_{12}$), a bathochromic shift is observed for the λ_{max} of the BT/DTS_{C12} spectra.

transfer (ICT), which is not always viable or suitable across various types of devices.[122–124] $B(C_6F_5)_3$ has advantageous properties over F_4TCNQ: (1) superior solubility in organic solvents which enables solution processing, (2) increased thermal, oxygen, and water stability,[1,125,126] and (3) can dope organic materials *via* multiple mechanisms enabling material use with a wide range of HOMO energy levels.[127]

Early applications using $B(C_6F_5)_3$ for organic semi-conductor modification was carried out by Bazan and coworkers, where modulated optical properties and electronic energy levels was achieved without synthetic modification (Fig. 9b).[128–130] Oligomers consisting of a dithienosilole (R = $C_{12}H_{25}$; DTS_{C12}) core capped with two benzothiadiazole (BT) units were combined with stoichiometric amounts of $B(C_6F_5)_3$, resulting in Lewis acid–base complexes involving the boron on $B(C_6F_5)_3$ and the nitrogen of the BT units (Fig. 9a).[128] This pulled electron density away from the π-system of the BT unit towards the Lewis acid, increasing donor–acceptor charge transfer character of the system, resulting in an overall narrowing of the energy gap and red-shifting of the optical absorption (Fig. 9b). The work was expanded on by complexing $B(C_6F_5)_3$ with various Lewis basic polymers,[129] with eventual applications in organic light emitting diodes (OLEDs).[130]

Nguyen and coworkers first reported on the p-doping effect of $B(C_6F_5)_3$ on a pyridine-based copolymer for hole-only diode devices in 2014, and observed an enhancement of hole-mobility by two orders of magnitude compared to their pristine counterparts.[125] Following this, many accounts of doping organics with $B(C_6F_5)_3$ for use in electronics started to emerge, particularly for solution-processed organic electronic devices. Taking advantage of the unique synergistic effect of $B(C_6F_5)_3$ doping on modifying optoelectronic properties and solid-state morphologies of organic materials, the application area has broadened to the bulk heterojunctions (BHJs) in organic photovoltaics (OPVs),[131–135] hole transporting layers (HTLs) in perovskite solar cells (PSCs),[136,137] organic thermoelectrics (OTEs),[138–142] organic thin-film transistor (OTFT)-based sensors,[143–147] and organic photodetectors (OPDs).[143,145] This section includes a mini review of $B(C_6F_5)_3$ as a p-type dopant for the active organic components in organic electronics, proposed mechanisms, emerging applications, and new dopant strategies. For more detailed reviews regarding the effect of doping active organic components, please refer to the reviews by Anthopoulos and coworkers,[148] Koch and coworkers,[123] and Baumgartner and coworkers.[149]

3.3.2. Doping mechanisms of $B(C_6F_5)_3$ with organics. Doping mechanisms involving $B(C_6F_5)_3$ across various organic electronic devices remained elusive for some time. Early work done by Nguyen and coworkers[125] and Heeney and coworkers[127] show that $B(C_6F_5)_3$ doped organic materials do not exhibit typical integer charge transfer (ICT; Fig. 10a) characteristics. ICT requires the HOMO energy level of the hole transport material to be destabilized relative to that of the lowest unoccupied molecular orbital (LUMO) of the p-dopant for efficient charge transfer. However, these authors reported that their materials possessed stabilized HOMO energy levels relative to that of the LUMO energy level of $B(C_6F_5)_3$, but that upon application doping was indeed occurring and noted unpaired electrons *via* polaron (p-type carriers) absorbances in the IR region and electron paramagnetic resonance (EPR) signals.[125,127] Nguyen and coworkers suggested that $B(C_6F_5)_3$ forms adducts with Lewis basic moieties in organic π-conjugated materials, and instead doping *via* charge transfer

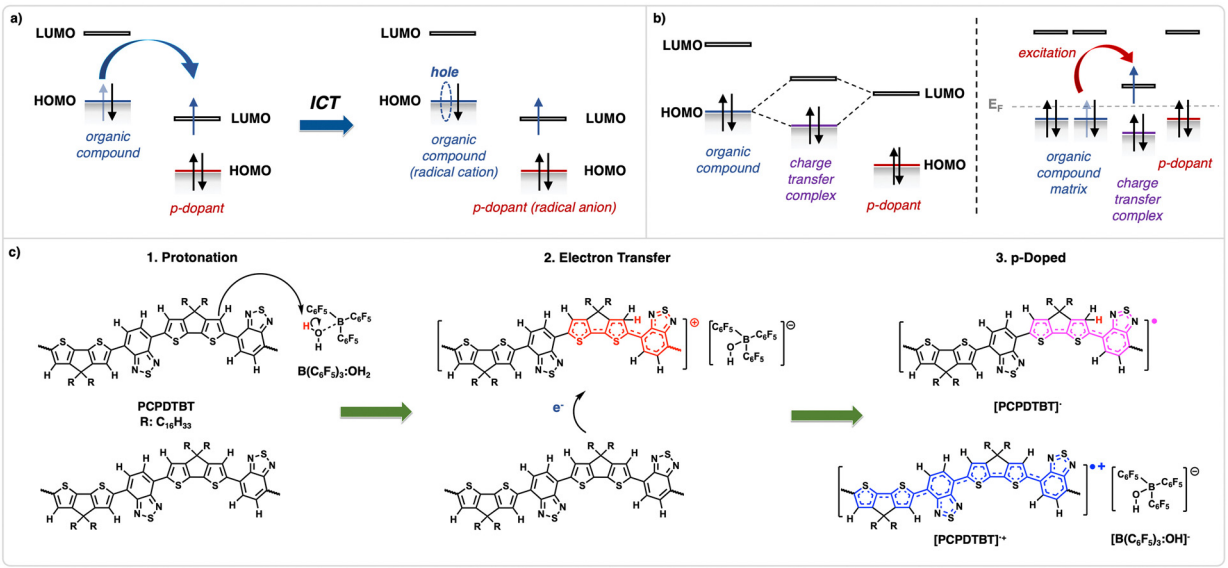

Fig. 10 Possible doping mechanisms in organic electronics by $B(C_6F_5)_3$. (a) Integer charge transfer (ICT) works to abstract an electron from the organic compound, allowing for increased hole transport throughout the material. (b) Charge transfer complex formation (CTC) results in orbital hybridization and an electron transfer into a charge transfer hybrid orbital (c) Brønsted acid doping in organic materials can occur when in the presence of $B(C_6F_5)_3$ and H_2O, and occurs in three main steps: (i) protonation of a π-conjugated system in the presence of the proposed $B(C_6F_5)_3{\cdot}OH_2{\cdot}B(C_6F_5)_3$ complex (ii) electron transfer from a neighbouring π-conjugated system, and (iii) formation of a neutral protonated radical species, [PCPDTBT-H]•, and "p-doped" delocalized cationic radical species, $[PCPDTBT]^{\bullet+}$, balanced with the counter ion, $[B(C_6F_5)_3{\cdot}OH]^-$.[151]

complexation (CTC; Fig. 10b) occurs. Heeney and coworkers supported this by reporting frontier-orbital hybridization from B–N bond formation which lead to the strongly electrophilic "pyrazinium" like cations, inducing empty states into the band gap which is similar to CTC doping mechanism suggested by Salzmann and coworkers.[150] Another example is doping poly(3-hexylthiophene) (P3HT) with $B(C_6F_5)_3$, where P3HT exhibits an estimated HOMO energy level of −5.1 eV and $B(C_6F_5)_3$ a LUMO energy level of −4.8 eV.[126] It was in 2020 that $B(C_6F_5)_3$ was proposed to induce p-doping *via* Brønsted acid doping (Fig. 10c) upon the formation of the Brønsted acid complex, $B(C_6F_5)_3{\cdot}H_2O$, in the presence of water.[151] Using DFT calculations, the authors proposed a mechanism which is as follows: (1) the formation of Brønsted acid, $B(C_6F_5)_3{\cdot}H_2O$ complex, which protonates the polymer backbone, in this case forming a positively charged protonated polymer $[PCPDTBT\text{-}H]^+$ and anionic $[B(C_6F_5)_3{\cdot}OH]^-$, (2) electron transfer from the neutral polymer to the $[PCPDTBT\text{-}H]^+$, and (3) formation of a neutral protonated radical species, $[PCPDTBT\text{-}H]^\bullet$, and "p-doped" delocalized cationic radical species, $[PCPDTBT]^{\bullet+}$, effectively neutralized with the counter ion, $[B(C_6F_5)_3{\cdot}OH]^-$. An additional Brønsted acid doping mechanism was proposed where the $B(C_6F_5)_3{\cdot}H_2O$ complex will likely to protonate the carbon on the 1 position of the cyclopentadithiophene instead of position 3,[79] as previously suggested by Nguyen and coworkers.[151]

Later, Beljonne and coworkers suggested that more energetically favorable bridged anion complexes, such as $[B(C_6F_5)_3{\cdot}OH{\cdot}B(C_6F_5)_3]^-$ and $[B(C_6F_5)_3{\cdot}OH{\cdot}OH_2{\cdot}B(C_6F_5)_3]^-$, were more feasible to have formed than the monomeric species $[B(C_6F_5)_3{\cdot}OH]^-$, as per DFT calculations.[79] In addition, Brønsted acid doping processes are entropically driven by the loss of H_2 gas to counter the highly endergonic process, where H_2 gas was successfully detected by Beverina and coworkers in 2023.[152] This mechanism accounted for the single signal seen in the EPR of these doped systems, as the result is a single spin-carrying species in the form of a radical cation. A follow up study on P3HT doped by $B(C_6F_5)_3$ was done to include EPR experiments, where a single EPR signature was indeed observed.[153] While Brønsted acid doping with $B(C_6F_5)_3$ can occur in the presence of water, if the organic material being doped contains Lewis basic moieties, it should be noted that Brønsted acid and CTC doping compete, however, Brønsted acid doping has been deemed as the more effective doping approach.[140] Therefore, in designing organic systems doped with $B(C_6F_5)_3$, one must define a target doping mechanism and consider the presence of water and/or Lewis basic moieties. Note, many early studies reviewed within do not elucidate doping mechanisms at play and instead speculate with minimal supporting data.

3.3.3. Organic photovoltaic devices. OPVs offer an appealing approach to harnessing solar energy due to solution processability and a lightweight, flexible design. The mechanism of action involves the absorption of photons by "donor" organic molecules, leading to an excited state which can result in a transfer of an electron to "acceptor" organic molecules (channel I process) or *vice versa* (channel II process).[154] This results in free charges that generate an electrical current when sandwiched between a cathode and anode. Typically, the donor and acceptor compounds are solution-processed and coated from the same solution, forming an intermixed film with domains of either donor or acceptor compounds, constituting the bulk heterojunction (BHJ) in OPVs (Fig. 11a). Additionally, OPVs tend to incorporate other organic material layers as electron or hole transporting layers, facilitating the movement of charges to the preferred electrodes for efficient current generation.

Both the BHJ and organic-based electron/hole transporting layers can undergo doping to enhance performance. Instances of using $B(C_6F_5)_3$ to augment OPV device performance have been reported, specifically when utilized in the BHJ. One example is the work of Ma and coworkers, where the authors utilized Lewis basic donor polymers (PCE10) with fullerene ($PC_{71}BM$) acceptors in the BHJ of OPVs,[131] and then added $B(C_6F_5)_3$ to induce doping in the donor PCE10 polymers. Not only did $B(C_6F_5)_3$ dope the PCE10 polymers, albeit mechanisms unknown, highly ordered nanostructures were observed with increased charge transport and thereby device performance for an increase in power conversion efficiency (PCE) from 8.9% to 9.6%. Chen and coworkers designed and synthesized a pyrazine-

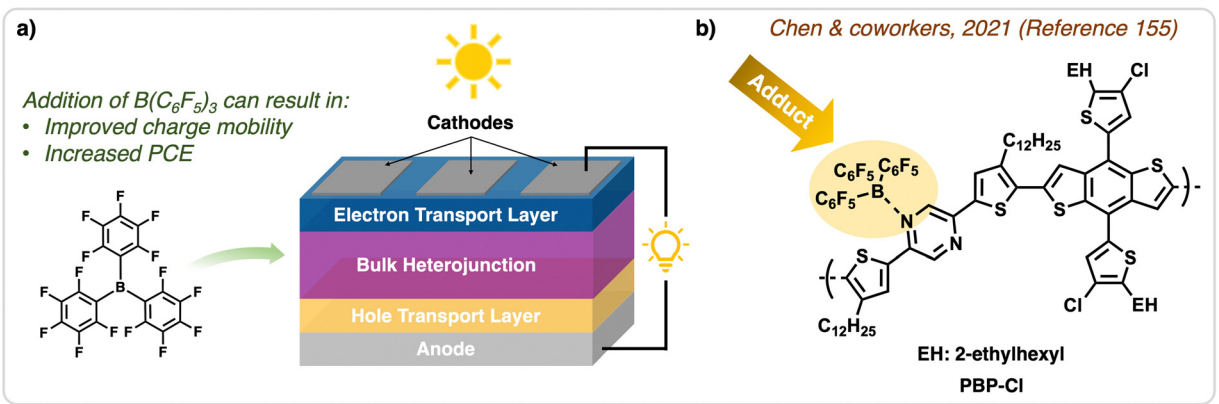

Fig. 11 Application of $B(C_6F_5)_3$ in OPVs. (a) Structure of an OPV used to harvest and convert solar radiation into current, $B(C_6F_5)_3$ can be incorporated into the BHJ for increased charge mobilities and PCEs. (b) In the work done by Chen & coworkers,[155] adduct formation between the boron of $B(C_6F_5)_3$ with the nitrogen on the pyrazine-based polymer, PBP-Cl, is observed, which was applied to OPVs for enhanced performance.

based donor polymer (PBP-Cl) to induce intermolecular B–N coordination for CTC doping with $B(C_6F_5)_3$ in BHJ of OPVs (Fig. 11b), where Y6 was used a non-fullerene acceptor.[155] By adding a trace amount of $B(C_6F_5)_3$ at 0.05 wt% relative to PBP-Cl in the BHJ, increased hole mobilities were observed with PCEs improving from 13.7% to 15.2%. Despite this, morphological alteration in the BHJ due to the presence of dopants can be detrimental, especially when the presence of dopants breaks up intermolecular interactions of the donor and/or acceptor species that are designed to induce favorable orientations that result in efficient charge transport in these types of devices.[155–157] Realizing this, in 2019 Ma and coworkers applied a different approach by employing a planar heterojunction (PHJ), where the donor and acceptor materials are coated individually and subsequentially. In this work, the best device performance was observed when $B(C_6F_5)_3$ was employed at the donor–acceptor interface, thereby residing between the donor and acceptor layers, and resulted an increase to PCE from 1.20% to 1.39%.[132] The authors also doped a PCE10/$PC_{71}BM$ BHJ by vapor annealing which resulted in an overall improved photovoltaic performance, marking an increase to PCE from 8.6% to 9.4%.[133] Various studies that utilize $B(C_6F_5)_3$ as a dopant are continuously being published, with many of them putting an efforts into modifying the formation of favorable BHJ morphology.[134,135] Notable is the doping of the electron transporting layers, where employing the $H_2O{\cdot}B(C_6F_5)_3$ complex as a dopant for the known cathode interlayer material, (*N*,*N*-dimethyl-ammonium *N*-oxide)propyl perylene diimide (PDINO) resulted in high performance OPVs with a PCE of 17.7%. The authors utilized DFT to show that the complex coordinates to the *N*-oxide terminal unit of PDINO by the boron core, thus displacing the water moiety.[158] Furthermore, Kelvin probe force microscopy and ultra-violet photoelectron spectroscopy of $PDINO{\cdot}B(C_6F_5)_3$ thin films determined the work function of the films were lowered upon increasing levels of the $H_2O{\cdot}B(C_6F_5)_3$ complex, enabling a smaller energy mismatch with the Y6 BHJ acceptor material.

3.3.4. Organic thermoelectric devices. OTEs, as depicted in Fig. 12a, are devices that convert heat into electricity, showing promising applications in flexible thermoelectric generators for waste heat recovery and wearable cooling/heating devices.[159] Materials used in OTEs utilize temperature gradients to generate electrical potentials through the diffusion of charge-carriers from the hot to the cold side, known as the Seebeck effect. The efficiency of thermoelectrics is quantified by the dimensionless figure-of-merit, $ZT = S^2\sigma T/\kappa$, where ZT at a given absolute temperature (T) is directly proportional to electrical conductivity (σ) and Seebeck coefficient (S), and inversely proportional to thermal conductivity (κ). In contrast to inorganic semiconductors, organic semiconducting materials have intrinsically low κ owing to strong electron–phonon coupling and low electrical conductivity.[160,161] Therefore, recent focus has been on enhancing power factor ($S^2\sigma$) mainly *via* doping.[162–164]

Jang and coworkers utilized $B(C_6F_5)_3$ as a Lewis acid dopant in inert atmosphere and as a Brønsted acid dopant in air to p-dope poly(3-hexylthiophene) (P3HT) through a one-step solution mixing method.[139] The Brønsted acid doping induced a conformational change in P3HT that resulted in a quinoidal structure, promoting backbone planarity (Fig. 12b). This structural change resulted in improved intra/inter-chain charge transport, reflected by the enhanced σ of 33.0 S cm^{-1} compared to Lewis acid-doped P3HT films at 0.020 S cm^{-1}. This outcome showcases the doping efficiency and air-stability of $B(C_6F_5)_3$ when employed as a Brønsted acid dopant. In the case of strong Lewis basic polymers, the competition between Brønsted acid and CTC doping in ambient atmosphere can limit doping efficiency. Consequently, in 2022 Jang and coworkers thermally annealed doped polymer films (PCDTPT) at 120 °C, transitioning from Lewis acid/base adducts (CTC) to Brønsted acid doping. This resulted in an increase in σ by three orders of magnitude reaching power factor of 8.48 μW m^{-1} K^{-2}.[140] They suggested that the Lewis acid–base interaction of $B(C_6F_5)_3$ with PCDTPT can be thermally disrupted to form Brønsted acidic $B(C_6F_5)_3{\cdot}H_2O$ complexes, and when employed with the weak Lewis basic polymer (PCDTBT), CTC doping was effectively suppressed and Brønsted acid doping increased to achieve a high power factor of 49.6 μW m^{-1} K^{-2}.

Despite the impressive increase in performance resulting from $B(C_6F_5)_3$ by doping *via* CTC or Brønsted acid doping, $B(C_6F_5)_3$ (and $B(C_6F_5)_3$ water complexes) are bulky and can

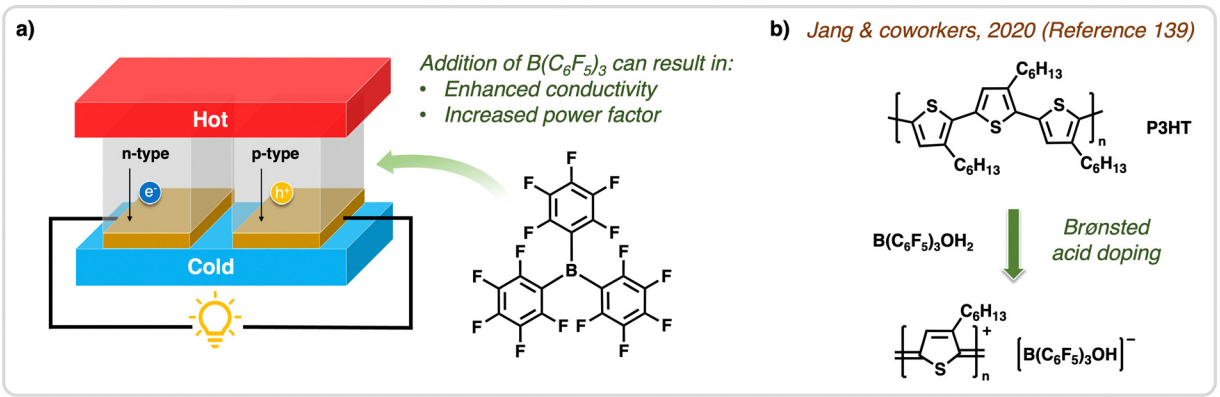

Fig. 12 Application of $B(C_6F_5)_3$ in OTEs. (a) Structure of an organic thermoelectric device used to convert heat into current. Using $B(C_6F_5)_3$ to p-dope OTEs results in enhanced conductivity and increases the power factor of the devices. (b) In the work done by Jang & coworkers,[139] Brønsted acid doping was observed when mixing $B(C_6F_5)_3$ (in the presence of water) with P3HT, which was used for OTEs and resulted in enhanced conductivity.

disrupt the solid-state morphology of organic thin films. Cho and coworkers addressed this challenge posed by the steric bulk of $B(C_6F_5)_3$ dopants,[142] where they employed sequential doping by dissolving $B(C_6F_5)_3$ in the non-polar aliphatic solvent, hexanes, and then dipped their prepared organic semiconducting films into the solution. This method allowed $B(C_6F_5)_3$ to diffuse into a semi-crystalline polymer film made up of poly[2,5-bis(3-tetradecylthiophen-2-yl)thieno[3,2-*b*]thiophene] (PBTTT) without disrupting the crystallinity of the film. The authors propose that hexanes can intercalate with the side chains of the PBTTT polymer but not the backbone, therefore, this method of subsequential doping resulted in deposition of the $B(C_6F_5)_3$ dopant in the lamellar spacing of PBTTT. Compared to solution-mixed doping, this method effectively suppressed dopant-induced disorder, resulting in a narrower density of states and reduced charge traps. The outcome was an impressive electrical conductivity (σ) of 230 S cm^{-1} and power factor of 140 μW m^{-1} K^{-2}, ranking among the highest values reported for $B(C_6F_5)_3$-doped organic polymer films. OTE devices doping using $B(C_6F_5)_3$ has therefore seen success,[157] including noncontact mode (IR irradiation) OTEs,[165] and self-healable and stretchable OTEs.[166]

3.3.5. Organic thin-film transistors. OTFTs are devices composed of a semiconducting channel positioned between two electrodes in the presence of a gate with various possible architectures/configurations. In simplified terms, noting that mechanisms are actually quite complex, when a bias is applied the semiconducting channel activates and generates current. An example is depicted in Fig. 13a, which illustrates a top-contact bottom-gate configuration. Similar to their inorganic counterparts, doping of the semiconducting channel is frequently employed to enhance performance, including improvements in charge generation, charge mobility, and overall conductivity. OTFTs exhibit potential in sensor applications, where analytes or external stimuli can induce electronic and/or morphological changes to the organic semiconducting channel. These changes result in measurable alterations to channel current.[167]

Early work in this field was done by Heeney and coworkers who were able to achieve 11-fold enhancement of hole-mobility in pyrazine-based copolymer OTFTs.[127] These devices were highly sensitive to dopant concentrations due to the bulky nature of $B(C_6F_5)_3$ complex, which disrupts solid-state morphology thereby affecting charge transport properties.[125,127] However, with careful optimization of the stoichiometric amount of $B(C_6F_5)_3$ added, the organic materials can simultaneously undergo p-doping and induced long-range crystallization resulting in enhanced hole-mobility, which was observed by Anthopoulos and co-workers in 2018.[168] This work explored several systems of organic molecular and polymeric materials for applications in OTFTs, more specifically they compared molecular and polymeric materials to blends of molecular polymeric materials in the presence of $B(C_6F_5)_3$. The most notable system was that of the polymer C_{16}-IDT-BT blended with the small molecule C_8-BTBT, where upon doping with $B(C_6F_5)_3$ the resulting OTFT devices reached a maximum of 11 cm^2 V^{-1} s^{-1} (Fig. 13b).

OTFTs are commonly studied for their application as sensors, particularly gas sensors. In 2012, Katz and coworkers fabricated OTFT-based NH_3 gas sensor using Lewis basic, copper phthalocyanine (CuPc) and $B(C_6F_5)_3$ as an active layer.[144] Upon the exposure to NH_3 gas, which is a stronger Lewis base than CuPc, $B(C_6F_5)_3$ effectively formed a Lewis acid–base complex with NH_3 resulting in a pronounced changes to the current, achieving a low limit of detection (LOD) of 0.35 ppm. However, it should be noted as per the correction to this work that there is a possibility of $B(C_6F_5)_3$ forming an adduct with trace water, which can act as a Brønsted acid p-dopant and thereby also affects the observed current in these devices.[169] Another study done in 2020 by Kim and coworkers fabricating solution-processed OTFT-based NH_3 gas sensor using poly(3-hexylthiophene) (P3HT) doped with $B(C_6F_5)_3$ as an active layer showed enhancement of current response.[147] This OTFT-based NH_3 gas sensor was more selective towards NH_3 compared to acetone, methanol, and dichloromethane, where they attributed to the strong Lewis acid ($B(C_6F_5)_3$) and Lewis base (NH_3) interaction for CTC type doping.

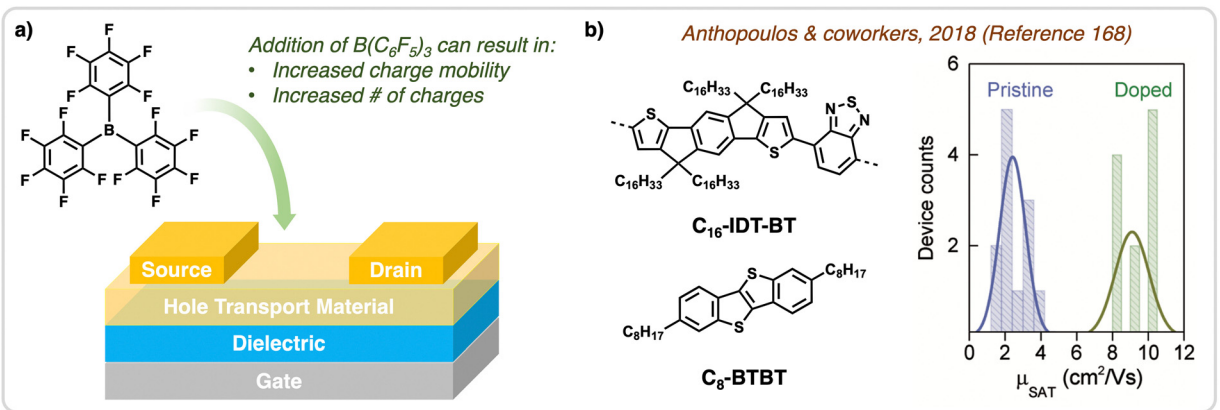

Fig. 13 Application of $B(C_6F_5)_3$ in OTFTs. (a) Structure of a type of OTFTs, specifically a bottom-gate top-contact OTFT. Doping hole transporting materials with $B(C_6F_5)_3$ in OTFTs results in an improvement in charge mobility and increases the number of charges generated. (b) Modified from Anthopoulos & co-workers,[168] when the mixture of hole transporting materials, C_{16}-IDT-BT & C_8-BTBT, were doped with $B(C_6F_5)_3$ and applied in OTFTs hole mobilities increased to 11 cm^2 V^{-1} s^{-1}.

3.3.6. Organic photodetectors. OPDs are devices capable of detecting light by converting light signals into electrical signals, and harbour several different types of architectures such as phototransistors, photodiodes, and photoconductors.[170] For example, organic phototransistors (OPTRs) are essentially OTFTs that undergoes a change in device on-current upon exposing the organic layer to incident light by means of altering the charge carrier density. $B(C_6F_5)_3$ has found applications in hole transporting OPTRs (Fig. 14a) owing to its polaron absorption peak in the IR region.[126,171] Typically, OPTRs are limited to visible-light with a few reports of ultraviolet (UV) and near-infrared (NIR), however, Kim and coworkers were the first to report shortwave infrared (SWIR, 1400–3300 nm) OPTRs utilizing a triphenylamine-based polymer (PolyTPD) doped with $B(C_6F_5)_3$ which the authors claim results in radical formation *via* ICT (Fig. 14b).[143] The combination of PolyTPD and $B(C_6F_5)_3$ allowed for an appropriate doping-induced energy offset between the HOMO energy level of PolyTPD and LUMO energy level of $B(C_6F_5)_3$, which corresponds to the SWIR wavelength range. As a result, doped PolyTPD:$B(C_6F_5)_3$ films exhibited a broad optical absorption peak between 1000–3300 nm, allowing for the detection of SWIR, specifically at 1500 nm for 583.4 mA W^{-1}, 2000 nm at 695.4 mA W^{-1}, and 2500 nm at 829.4 mA W^{-1}. This type of radical formation with a Lewis base as a single electron donor and Lewis acid as a single electron acceptor has been probed using FLP chemistry,[172] where the disassociated radicals have been termed frustrated radical pairs. In this work perhaps $B(C_6F_5)_3$ acts as a radical anion, however, further investigation is needed.

Another example of using $B(C_6F_5)_3$ as a dopant in OPDs was reported by Someya and Anthopoulos in 2021, where an organic photodiode with a bulk heterojunction consisting of a diketopyrrolopyrrole & thiophene based donor polymer (PMDPP3T) with a fullerene acceptor ($PC_{61}BM$), and was doped by $B(C_6F_5)_3$ alongside n-type organic dopants.[145] The authors controlled doping concentration (0.02 wt%) to achieve enhanced photocurrent and NIR detectivity, without increasing dark current. This is notable as doping often increases dark current, which can result in rapid device degradation under ambient conditions.

3.3.7. Emerging applications in organic electronics. While the application of $B(C_6F_5)_3$ in electronics has been established for doping organics in OPVs, OTEs, and OTFTs, applications of $B(C_6F_5)_3$ continue to expand in this realm. This section serves to highlight some emerging and innovative approaches to using $B(C_6F_5)_3$ in electronics, where new methods and types of devices are explored.

In regard to emerging electrochemical device applications, Abe and coworkers reported a new method for enhancing electrochemiluminescence (ECL) by Lewis acid–base pairing complexation of $B(C_6F_5)_3$ with organic donor–acceptor (D–A) diads. This complexation served to stabilize electrogenerated radicals, preventing the formation of unstable radicals which can lead to unwanted chemical reactions.[173] In the study, pyridal (py) functionalized benzothienobenzothiophene (BTBT) D–A diads were used as the active component, forming dative B–N bonds with $B(C_6F_5)_3$. They report that van der Waals interaction between H···F of py and $-C_6F_5$ groups restricted the rotational motion, maintaining a planar configuration during the excited intramolecular charge transfer state. This restriction effectively inhibited non-radiative decay. Additionally, the strong electron-withdrawing coordination of $B(C_6F_5)_3$ facilitated efficient charge separation. Moreover, single crystals of py-BTBT diads revealed highly ordered 1D columnar π-stacks in the solid state, contributing to efficient singlet exciton delocalization. Therefore, the py-BTBT diads demonstrated improved radical stability with a 156-fold increase in ECL intensity. $B(C_6F_5)_3$ was reported to not only dope the organic material and induce favorable morphology changes in the solid state, but also acted as an oxygen trap and thus increased the stability of the organic electrochemical transistor (OECT) devices over several cycles.[174]

Another promising usage of $B(C_6F_5)_3$ was to enhance the photophysical properties of organic light-emitting films, which was done by Huang and coworkers in 2023.[175] They employed supramolecular diarylfluorene compounds functionalized with pyridine as a host material and $B(C_6F_5)_3$ as a guest material to explore B–N coordination and the effect on emission of the host material. By casting this material into films, they observed Förster resonance energy transfer (FRET) from the host material to the coordinated $B(C_6F_5)_3$ which resulted in longer fluorescence lifetime. In addition, according to DFT, the HOMO and LUMO of the $B(C_6F_5)_3$-coordinated molecule is highly

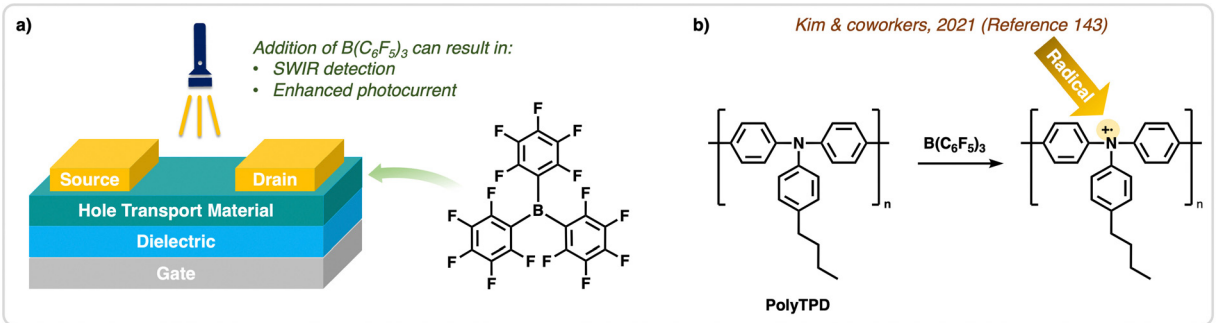

Fig. 14 Application of $B(C_6F_5)_3$ in OPTRs. (a) Structure of organic phototransistor devices used to detect various wavelengths of light. Addition of $B(C_6F_5)_3$ in these types of devices can result in SWIR detection and enhanced photocurrent. (b) In the work done by Kim & coworkers,[143] doping of PolyTPD with $B(C_6F_5)_3$ to generate radicals was done for applications in OPTRs.

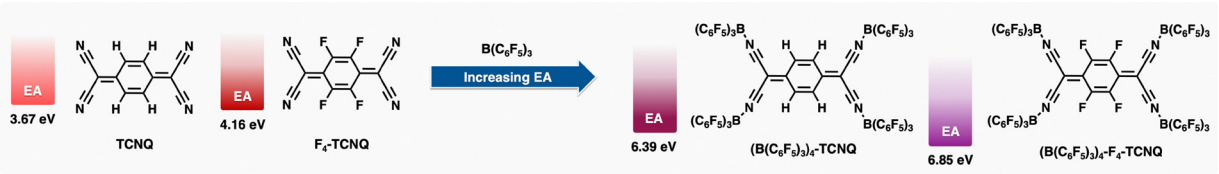

Fig. 15 Coordination of $B(C_6F_5)_3$ with the nitrogen on the –CN functional groups of TCNQ and F_4-TCNQ dramatically increases the EA and oxidation potential of the p-type dopants.[177]

delocalized, resulting in an intramolecular charge transfer state. Since the intramolecular charge transfer state is highly sensitive to polarity, changing the ratio of host to $B(C_6F_5)_3$ has led to wide range of fluorescence emission that are highly tunable even in the film. In addition, the blending of coordinated molecule has also led to enhanced PLQY (~30% to almost 80–90%) and conductivity (two orders of magnitude increase) of the films.

3.3.8. Emerging dopant strategies. While an effective-p-dopant alone, $B(C_6F_5)_3$ has also been utilized for increasing the performance of other p-dopants. $B(C_6F_5)_3$ adducts of 7,7,8,8-tetracyanoquinododimethane (TCNQ; Fig. 15) and derivatives have shown remarkably high oxidation power and have thus been of significant interest for doping as first reported by Malischewski and co-workers in 2022.[176] TCNQ·$4B(C_6F_5)_3$ could not be isolated, and instead was treated with ferrocene or decamethylcobaltacene to give a dianion, or thianthrene or tris(4-bromophenyl)amine to give a radical anion. The instantaneous oxidation of thianthrene gives an estimated reduction potential for TCNQ·$4B(C_6F_5)_3$ as >0.9 V *vs.* Fc/Fc^+. DFT calculations estimate the electron affinity to be 6.04 eV (583 kJ mol^{-1}), closely matching experimental estimates. Koch and co-workers then carried on this work, investigating derivatives based on F_4TCNQ (Fig. 15) and 1,3,4,5,7,8-hexafluorotetracyano-naphthoquinodimethane (F_6TCNNQ).[177] Fluorination proved an effective strategy for increasing electron affinity even further, as electron affinities for F_4TCNQ·$4B(C_6F_5)_3$ and F_6TCNNQ·$4B(C_6F_5)_3$ were calculated as 6.85 eV (661 kJ mol^{-1}) and 6.88 eV (664 kJ mol^{-1}), respectively.

Koch and co-workers investigated the utility of TCNQ·$4B(C_6F_5)_3$ and derivatives as dopants for organic polymers: three p-type organic polymers were evaluated for doping with F_4TCNQ·$4B(C_6F_5)_3$, poly(3-hexylthiophene) (P3HT), methylated poly(*para*-phenylene) (MeLPPP), and poly(9,9-dioctylfluorene-*alt*-benzothiadiazole) (F8BT).[177] For both P3HT and MeLPPP, thin film and solution spectroscopic studies showed significant doping with F_4TCNQ·$4B(C_6F_5)_3$, evident from the appearance of polaron-related absorption. At the same ratio of either $B(C_6F_5)_3$ or TCNQ, neither polymer showed any evidence of doping. F8BT, a polymer with a very high ionization energy (*circa* 5.9 eV) was not doped by F_4TCNQ·$4B(C_6F_5)_3$, but F_6TCNNQ·$4B(C_6F_5)_3$ did show considerable doping at a 1 : 10 dopant ratio. Further, it was determined that at very low dopant ratios, 1 : 100 or 1 : 50, F_4TCNQ·$4B(C_6F_5)_3$ dopes P3HT more effectively than F_4TCNQ alone, improving conductivity by a factor of ~1000 relative to F_4TCNQ-doped P3HT. This work was eloquently expanded upon by Campoy-Quiles and co-workers, who investigated over 20 additional organic semiconductors.[178] Nearly all these semiconductors demonstrated better conductivity when doped with F_4TCNQ·$4B(C_6F_5)_3$ compared to BCF or F4TCNQ alone, including notable examples Y6 and other NFAs and PM6, suggesting incorporation into the BHJ of OPV devices could be very promising. Lastly, owing to its large molecular volume, F_4TCNQ·$4B(C_6F_5)_3$ shows improved thermal de-doping performance and consequently improved stability at elevated temperatures.

4. Alternate Lewis acids for doping organics

4.1. Overview & perspective

The application of Lewis acids to enhance electronic device performance by doping requires specific structure–property relationships; upon reviewing molecular transformations and electronics to which $B(C_6F_5)_3$ is applied several target properties stand out. First, the strength of the Lewis acid is critical for reactivity and performance, and in the case of doping increasing Lewis acidity is hypothesized to enhance p-doping mechanisms such as Brønsted acid doping, adduct formation/CTC doping, and complexation with other dopants. Second, the steric bulk and intermolecular interactions of $B(C_6F_5)_3$ with organic materials prevents migration in the solid-state as a means of improving stability. Third, $B(C_6F_5)_3$ is solution processable in a range of organic solvents, which is ideal for devices fabricated by coating/printing methods. Fourth, it is stable and has distinguishable properties that are easily analyzed with common instrumentation, such as NMR spectroscopy, for in depth structural and mechanistic studies. Each aforementioned property plays a key role; for example, while increasing Lewis acidity may lead to better doping efficiencies if a Lewis acid is incompatible with target organic compounds due to a lack of intermolecular interactions it may migrate in processed films and reduce stability and efficiency over time. There are no clear trends for applying Lewis acids as dopants for organic compounds as a whole, as it depends on the materials, device architecture, and role of the Lewis acid. Therefore, this section presents alternates to $B(C_6F_5)_3$, and when available, relevant properties to encourage a more effective and systematic approach to selecting an appropriate dopant for niche systems.

For notable alternatives to $B(C_6F_5)_3$ presented within, Lewis acidity based on the Gutmann–Beckett (GB) method, fluoride ion affinity (FIA), and hydride ion affinity (HIA) is provided

when available. Note, variability of these values across studies is common, therefore, relative strength to that of $B(C_6F_5)_3$ for each compound/study is provided when available. The Gutmann–Beckett method involves complexation of a Lewis acid with a phosphine oxide, typically triethylphosphine oxide, and subsequent evaluation of the chemical shifts in ^{31}P-NMR spectra. Lewis acidity can be determined *via* relative correlations of $\Delta\delta$ of P where a higher $\Delta\delta$ indicates a stronger Lewis acid. FIA is a computational method that determines the binding energy or enthalpy change when a fluoride ion (F^-) binds to a Lewis acid and is typically reported in kJ mol^{-1}. The stronger the Lewis acid, the larger the value, and if a Lewis acid has a FIA greater than that of antimony pentafluoride (SbF_5, 493 kJ mol^{-1}) it is considered to be a Lewis super acid (LSA).[179,180] Similar to FIA is HIA, which computes the binding energy/enthalpy change when a hydride ion (H^-) binds to a Lewis acid and is reported in kJ mol^{-1}. Electronic characteristics such as calculated LUMO energy levels, formal reductions, and electron affinity are provided when available. Lastly, sterics are considered by including calculated buried volumes (%V_{bur}) of Lewis acid anions, typically fluoride ion adducts, where the %V_{bur} is the volume of the ligands that surround a boron center. Note, sterics need to be considered in the context of FLPs when selecting a dopant (for CTC), where using the method of Radius and coworkers[181] may define any Lewis acid/base interactions present when doping various organic compounds and compositions. Within are select tri-substituted aryl boranes, carboranyl boranes, and borates and the relative aforementioned properties to be applied for (1) identifying appropriate boron-based Lewis acid for organic electronic applications, (2) to better understand the effect of these types of Lewis acid dopants, and (3) to encourage new dopant and/or active material component designs.

4.2. Tri-substituted aryl boranes & borates

Triphenyl borane ($B(C_6H_5)_3$; Fig. 16a), being the non-fluorinated analog of $B(C_6F_5)_3$, exhibits 65%,[182] 78%,[183] and 74%[183] relative Lewis acidity (RLA) in relation to $B(C_6F_5)_3$ using the GB method, FIA, and HIA, respectively, and the LUMO energy level of $B(C_6H_5)_3$ is destabilized by 1.52 eV[183] relative to $B(C_6F_5)_3$ (Table 1). Despite this, $B(C_6H_5)_3$ has seen many applications in molecular transformations,[184] and is less sterically encumbered than $B(C_6F_5)_3$ by 5.8% (%V_{bur}). Increasing the degree of phenyl fluorination, as seen for $B(C_6H_3\text{-}2,6\text{-}F_2)_3$, $B(C_6H_2\text{-}2,4,6\text{-}F_3)_3$, and $B(C_6H\text{-}2,3,5,6\text{-}F_4)_3$ (Fig. 16a), results in RLAs (by GB method) of 82%,[185] 88%,[186] and 98%,[186] respectively, with LUMO energy levels destabilized relative to $B(C_6F_5)_3$ by 0.91 eV, 0.74 eV, and 0.21 eV, respectively (Table 1). The %V_{bur} reported for $B(C_6H_3\text{-}2,6\text{-}F_2)_3$ and $B(C_6H_2\text{-}2,4,6\text{-}F_3)_3$ indicates sterics about the boron center are near identical to that of $B(C_6F_5)_3$, an expected result when having fluorine substituted 2-positions on all phenyls in these compounds.[187] One method to increase withdrawing behaviour on triaryl borane phenyl groups beyond perfluorination is to install trifluoromethyl groups ($-CF_3$), as is seen with BAr^F, BTolF, and $B(FMes)_3$ (Fig. 16a). Indeed, RLAs (by GB method) of BAr^F, BTolF, and $B(FMes)_3$ are 106%, 108%, and 122%, respectively (Table 1). However, the electron affinity of BAr^F relative to $B(C_6F_5)_3$ is destabilized by 0.24 eV,[188] while the LUMO energy level of BTolF relative to $B(C_6F_5)_3$ is stabilized by 0.59 eV.[189] For %V_{bur}, BAr^F is less encumbered relative to $B(C_6F_5)_3$ by 5.2%,[181] and $B(Fmes)_3$ is greatly encumbered relative to $B(C_6F_5)_3$ with an increase to %V_{bur} of 26.9%.[181] Substituting perfluorinated phenyls with perchlorinated phenyls in $B(C_6F_5)_3$ is seen for $B(C_6Cl_5)(C_6F_5)_2$, $B(C_6Cl_5)_2(C_6F_5)$, and $B(C_6Cl_5)_3$ (Fig. 16a). Here, the C_6Cl_5 substituents are more electron withdrawing than C_6F_5 substituents due to the decrease in π-back-donation from Cl relative to that of F, and is apparent by the formal reductions of $B(C_6Cl_5)(C_6F_5)_2$, $B(C_6Cl_5)_2(C_6F_5)$, and $B(C_6Cl_5)_3$ being −1.87 V, −1.55 V, and −1.48 V, respectively (Table 1).[190] However, Lewis acidity is both electronic and steric dependent, where using the GB method the RLAs of $B(C_6Cl_5)(C_6F_5)_2$, $B(C_6Cl_5)_2(C_6F_5)$, and $B(C_6Cl_5)_3$ are 96%, 93%, and 0%, respectively.[190] While the GB method for $B(C_6Cl_5)_3$ is 0 due to a lack of complexation with triethylphosphine oxide, a RLA using FIA resulted in 89% relative to that of $B(C_6F_5)_3$ which indicates $B(C_6Cl_5)_3$ will complex with small Lewis bases.[191] The RLAs are supported when considering %V_{bur}, where $B(C_6Cl_5)(C_6F_5)_2$, $B(C_6Cl_5)_2(C_6F_5)$, and $B(C_6Cl_5)_3$ are encumbered by 4.3%, 7.9%, and 11.3% relative to $B(C_6F_5)_3$, respectively.[190]

Altering aryl substituents is another method to influence the Lewis acidity, electronics, and sterics about the boron in tri-substituted boranes. Borafluorene Lewis acids, such as $B(C_{12}H_8)(C_6H_5)$ and $B(C_{12}F_8)(C_6F_5)$ (Fig. 16b), contain antiaromatic five membered borole rings that influence the electronics, sterics, and thereby Lewis acidity relative to $B(C_6H_5)_3$ and $B(C_6F_5)_3$, respectively. Comparing $B(C_{12}H_8)(C_6H_5)$ to $B(C_6H_5)_3$ the RLA (by FIA), LUMO, and %V_{bur} is 103%,[183] 0.50 eV stabilized,[183] and decreased by 5.8%,[181] respectively (Table 1). While $B(C_6F_5)_3$ is a stronger Lewis acid than $B(C_{12}H_8)(C_6H_5)$, it is apparent that borafluorene substitution can slightly increase Lewis acidity while decreasing sterics. This is supported by comparing $B(C_{12}F_8)(C_6F_5)$ to $B(C_6F_5)_3$ the RLA (by FIA), LUMO, and %V_{bur} which is 101%, 0.26 eV stabilized, and decreased by 5.4%, respectively (Table 1).[183] One example of a bridged borane is provided, $B_2(C_6F_5)_2(C_6F_4)_2$ (Fig. 16b), which bears a six-membered central ring that bridges two C_6F_4 groups *via* two C_6F_5 substituted boranes. The RLA (by FIA) is 105% and the LUMO enegry level is 0.75 eV stabilized (Table 1).[197] Expanding π-conjugation is another approach to afford alternate tri-substituted boranes, two examples being $B(C_{12}F_9)_3$ and $B(C_{10}F_7)_3$ (Fig. 16b). When comparing $B(C_{12}F_9)_3$ to $B(C_6F_5)_3$, the RLA (by FIA) is 95%,[197] the LUMO is stabilized by 0.02 eV,[197] and %V_{bur} is increased by 24%,[181] indicating a substantial increase in sterics while maintaining Lewis acidity (Table 1). However, when comparing $B(C_{10}F_7)_3$ with $B(C_6F_5)_3$, the RLA (by FIA) is 106%,[197] the LUMO is destabilized by 0.02 eV,[197] and %V_{bur} is increased by 0.01%, indicating sterics are maintained while slightly increasing Lewis acidity (Table 1).[181]

Worth noting are select triaryl borates, which differ from boranes by an oxygen atom that links the central boron and carbon atoms of aryl substituents. $B(OC_6H_5)_3$ (Fig. 16c) compared to $B(C_6F_5)_3$ reveals a RLA (by FIA) of 77%, a LUMO energy

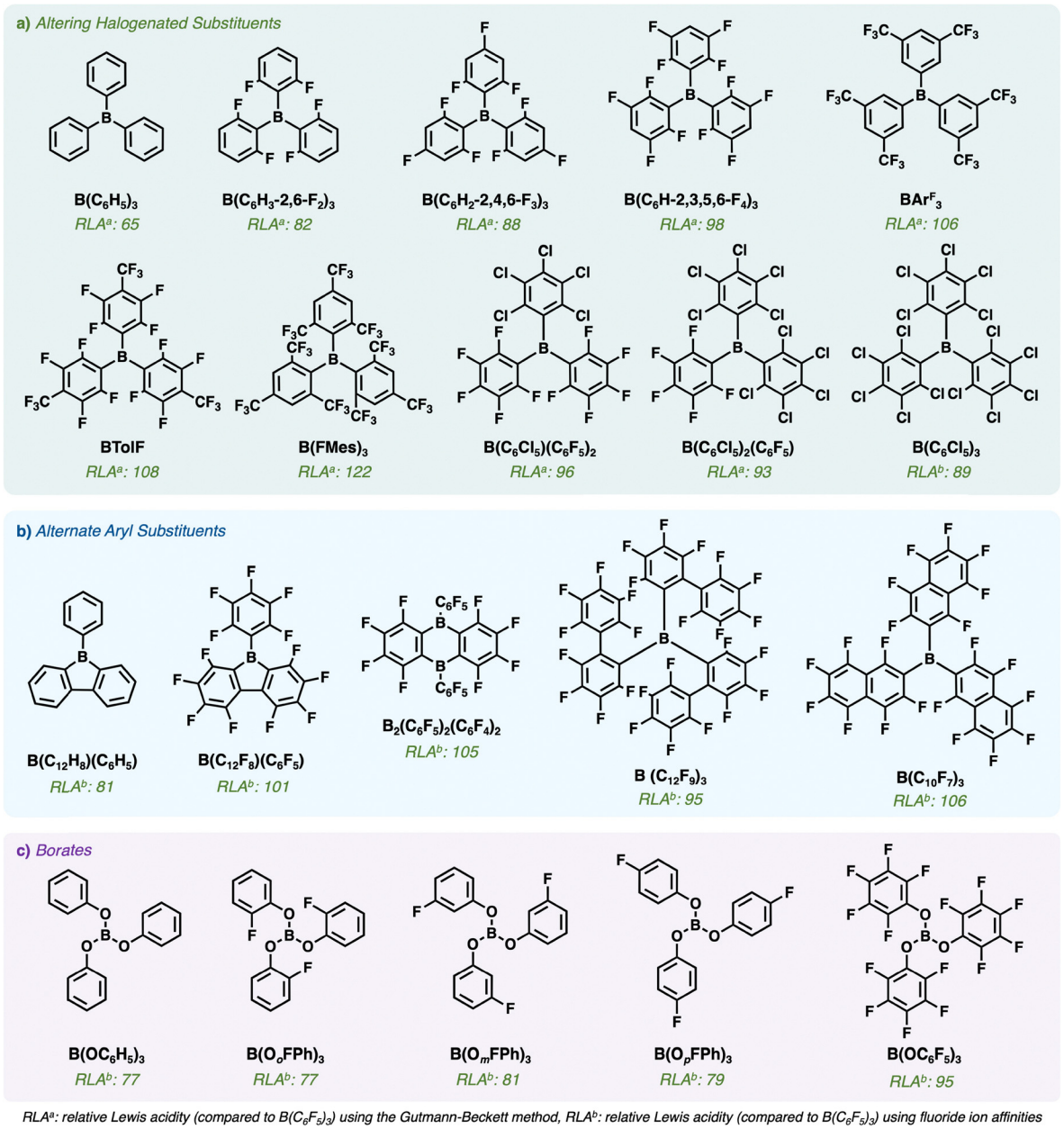

Fig. 16 Various tri-substituted aryl boranes & borates. (a) Altering halogenated (fluorine, chlorine) aryl substituents, where increasing the degree of fluorination on phenyl substituents results in increasing Lewis acidity, however, replacing perfluorinated phenyls with perchlorinated phenyls results in a decrease in Lewis acidity. (b) Alternate aryl substituents. (c) Various aryl borates. *RLA[a]: relative Lewis acidity (compared to $B(C_6F_5)_3$) using the Gutmann–Beckett method, RLA[b]: relative Lewis acidity (compared to $B(C_6F_5)_3$) using fluoride ion affinities.

level that is destabilized by 3.04 eV, and $\%V_{bur}$ that indicates 10.5% less encumbrance (Table 1).[198] Further, $B(OC_6F_5)_3$ (Fig. 16c) compared to $B(C_6F_5)_3$ reveals a RLA (by FIA) of 95%,[198] a LUMO energy level that is destabilized by 2.16 eV,[198] and is 5.0% less encumbered (Table 1).[181] While this suggests that both sterics and Lewis acidity is decreased when comparing borates to boranes, using the GB method to measure the Lewis acidity of $B(OC_6F_5)_3$ relative to that of $B(C_6F_5)_3$ affords a RLA of 114%, suggesting the borate counterpart is significantly more Lewis acidic. Furthermore, the RLA (by GB method) for $B(C_6H_5)_3$ to $B(C_6F_5)_3$ is 65%, which is lower than the RLA of $B(OC_6H_5)_3$ to $B(C_6F_5)_3$ at 77% and suggests that the presence of the bridging oxygen does increase Lewis acidity. Notable for triaryl borates is the variability in properties when considering *ortho*-, *meta*-, and *para*-substitution of fluorine on $B(OC_6H_5)_3$ affording $B(O_oFC_6H_4)_3$, $B(O_mFC_6H_4)_3$, and $B(O_pFC_6H_4)_3$, respectively (Fig. 16c). In terms of RLA (to $B(C_6F_5)_3$ by FIA), $B(O_oFC_6H_4)_3$, $B(O_mFC_6H_4)_3$, and $B(O_pFC_6H_4)_3$ afford values of 77%, 81%, and 79%, respectively (Table 1).[198] In terms of LUMO energy levels relative to $B(C_6F_5)_3$, $B(O_oFC_6H_4)_3$, $B(O_mFC_6H_4)_3$, and $B(O_pFC_6H_4)_3$ afford destabilizations of 2.68 eV, 2.67 eV, and 2.57 eV, respectively.[198] Lastly, the $\%V_{bur}$ compared to that of $B(C_6F_5)_3$ for $B(O_oFC_6H_4)_3$,

Table 1 Lewis acidity, electronic, and steric factors of tri-substituted aryl boranes & borates

Aryl Borane	Lewis Acidity	RLA	Electronics	Sterics
$B(C_6F_5)_3$	Due to variability across studies, relative $B(C_6F_5)_3$ data for each compound/study is reported			
$B(C_6H_5)_3$	GB $\Delta\delta$: 19.6 (C_6D_6), ^{b}30.2 (C_6D_6)[182]	GB $\Delta\delta$: 65		
	FIA: 354, ^{b}452[183]	FIA: 78	LUMO: −2.02[183]	BV: 53.1[181]
	HIA: 360, ^{b}484[183]	HIA: 74	^{b}LUMO: −3.52[183]	^{b}BV: 58.9[181]
$B(C_6H_3\text{-}2,6\text{-}F_2)_3$	GB $\Delta\delta$: 21.2 (CD_2Cl_2), ^{b}25.8 (CD_2Cl_2)[185]	GB $\Delta\delta$: 82	LUMO: −2.39[187]	^{a}BV: 58.0[187]
	FIA: 368, ^{b}457[187]	FIA: 81	^{b}LUMO: −3.30[187]	^{a,b}BV: 59.4[187]
$B(C_6H_2\text{-}2,4,6\text{-}F_3)_3$	GB $\Delta\delta$: 30.5 ($CDCl_3$), ^{b}34.8 ($CDCl_3$)[186]	GB $\Delta\delta$: 88	LUMO: −2.56[187]	^{a}BV: 58.0[187]
	FIA: 390, ^{b}457[187]	FIA: 85	^{b}LUMO: −3.30[187]	^{a,b}BV: 59.4[187]
$B(C_6H\text{-}2,3,5,6\text{-}F_4)_3$	GB $\Delta\delta$: 34.0 ($CDCl_3$), ^{b}34.8 ($CDCl_3$)[186]	GB $\Delta\delta$: 98	LUMO: −2.59[192]	NR
			^{b}LUMO: −2.80[192]	
$BAr^F{}_3$	GB $\Delta\delta$: 28.2 (CD_2Cl_2), ^{b}26.6 (CD_2Cl_2)[193]	GB $\Delta\delta$: 106	EA: −2.79[188]	BV: 53.7[181]
			^{b}EA: −3.03[188] 5/22/2025 10:05:00 AM	^{b}BV: 58.9[181]
BTolF	GB $\Delta\delta$: 31.9 (C_6D_6), 29.0 (CD_2Cl_2), ^{b}29.5 (C_6D_6), ^{b}26.5 (CD_2Cl_2)[194]	GB $\Delta\delta$: 108 (C_6D_6) & 109 (CD_2Cl_2)	LUMO: −4.09[189] ^{b}LUMO: −3.50[189]	NR
$B(FMes)_3$	GB $\Delta\delta$ = 44.21 (calculated) ^{b}36.34 (calculated)[195]	GB $\Delta\delta$: 122	NR	BV: 85.8[181]
				^{b}BV: 58.9[181]
$B(C_6Cl_5)(C_6F_5)_2$	GB $\Delta\delta$: 32.5 (CD_2Cl_2), ^{b}33.7 (CD_2Cl_2)[190]	GB $\Delta\delta$: 96	FR: −1.87[190]	BV: 63.2[181]
			^{b}FR: −1.97[190]	^{b}BV: 58.9[181]
$B(C_6Cl_5)_2(C_6F_5)$	GB $\Delta\delta$: 31.2 (CD_2Cl_2), ^{b}33.7 (CD_2Cl_2)[190]	GB $\Delta\delta$: 93	FR: −1.55[190]	BV: 66.8[181]
			^{b}FR: −1.97[190]	^{b}BV: 58.9[181]
$B(C_6Cl_5)_3$	GB $\Delta\delta$: 0 (CD_2Cl_2) ^{b}33.7 (CD_2Cl_2)[191]	GB $\Delta\delta$: 0	FR: −1.48[190]	BV: 70.2[181]
	FIA: 366, ^{b}413[191]	FIA: 89	^{b}FR: −1.97[190]	^{b}BV: 58.9[181]
$B(C_{12}H_8)(C_6H_5)$	GB $\Delta\delta$: 33.1 (C_6D_6), ^{b}NR[196]			
	FIA: 366, ^{b}452[183]	FIA: 81	LUMO: −2.52[183]	BV: 47.3[181]
	HIA: 382, ^{b}484[183]	HIA: 79	^{b}LUMO: −3.52[183]	^{b}BV: 58.9[181]
$B(C_{12}F_8)(C_6F_5)$	FIA: 457, ^{b}452[183]	FIA: 101	LUMO: −3.78[183]	^{a}BV: 52.7[183]
	HIA: 491, ^{b}484[183]	HIA: 101	^{b}LUMO: −3.52[183]	^{a,b}BV: 58.1[183]
$B_2(C_6F_5)_2(C_6F_4)_2$	FIA: 477, ^{b}452[197]	FIA: 105	LUMO: −4.68[197]	NR
	HIA: 514, ^{b}484[197]	HIA: 106	^{b}LUMO: −3.93[197]	
$B(C_{12}F_9)_3$	FIA: 431, ^{b}452[197]	FIA: 95	LUMO: −3.95[197]	BV: 82.9[181]
	HIA: 452, ^{b}484[197]	HIA: 93	^{b}LUMO: −3.93[197]	^{b}BV: 58.9[181]
$B(C_{10}F_7)_3$	FIA: 483, ^{b}452[197]	FIA: 106	LUMO: −3.91[197]	BV: 58.8[181]
	HIA: 519, ^{b}484[197]	HIA: 107	^{b}LUMO: −3.93[197]	^{b}BV: 58.9[181]
$B(OC_6H_5)_3$	GB $\Delta\delta$: 23.0 (C_6D_6) ^{b}30.2 (C_6D_6)[182]	GB $\Delta\delta$: 76		
	FIA: 350, ^{b}454[198]	FIA: 77	LUMO: −0.39[198]	^{a}BV: 49.2[198]
	HIA: 323, ^{b}497[198]	HIA: 65	^{b}LUMO: −3.43[198]	^{a,b}BV: 59.7[198]
$B(OC_6F_5)_3$	GB $\Delta\delta$ = 34.5 (C_6D_6) ^{b}30.2 (C_6D_6)[182]	GB $\Delta\delta$: 114		
	FIA: 431, ^{b}454[198]	FIA: 95	LUMO: −1.27[198]	BV: 54.9[181]
	HIA: 411, ^{b}497[198]	HIA: 83	^{b}LUMO: −3.43[198]	^{b}BV: 58.9[181]
$B(O_oFC_6H_4)_3$	GB $\Delta\delta$ = 23.8 ($CDCl_3$) ^{b}NR[198]			
	FIA: 351, ^{b}454[198]	FIA: 77	LUMO: −0.75[198]	^{a}BV: 50.7[198]
	HIA: 339, ^{b}497[198]	HIA: 68	^{b}LUMO: −3.43[198]	^{a,b}BV: 59.7[198]
$B(O_mFC_6H_4)_3$	GB $\Delta\delta$ = 22.0 ($CDCl_3$) ^{b}NR[198]			
	FIA: 368, ^{b}454[198]	FIA: 81	LUMO: −0.76[198]	^{a}BV: 43.3[198]
	HIA: 340, ^{b}497[198]	HIA: 68	^{b}LUMO: −3.43[198]	^{a,b}BV: 59.7[198]
$B(O_pFC_6H_4)_3$	GB $\Delta\delta$ = 14.1 ($CDCl_3$) ^{b}NR[198]			
	FIA: 359, ^{b}454[198]	FIA: 79	LUMO: −0.86[198]	^{a}BV: 43.4
	HIA: 329, ^{b}497[198]	HIA: 66	^{b}LUMO: −3.43[198,199]	^{a,b}BV: 59.7[198]

GB $\Delta\delta$ = Gutmann–Beckett Method ^{31}P $\Delta\delta$ (ppm), FIA = fluoride ion affinity (kJ mol^{-1}), HIA = hydride ion affinity (kJ mol^{-1}), LUMO = calculated LUMO energy (eV), FR = formal reduction potential experimentally found using cyclic voltammetry (V), BV = buried volume of Lewis acids adducts with a fluoride ion $[LA–F]^-$. ^{a} BV is calculated using F-ion adduct cartesian coordinates obtained from associated references and the SambVca 2.1 web application,[199] EA = calculated electron affinity (eV), RLA = relative Lewis acidity compared to $B(C_6F_5)_3$ (%). ^{b} Relative $B(C_6F_5)_3$ data, NR = not reported or relevant data not available.

$B(O_mFC_6H_4)_3$, and $B(O_pFC_6H_4)_3$ exhibits less encumbrance by 9.0%, 16.4%, and 16.3%, respectively.[198] This suggests that *meta*-substitution results in the highest Lewis acidity while being the least sterically encumbered.

4.3. Carborane substituted boranes

Carborane substituents on boranes are an emerging strategy for producing Lewis superacids (LSAs) with superior stability to their aryl counterparts. Carboranes are non-classically bonded polyhedral clusters of boron, carbon, and hydrogen atoms (Fig. 17a). Icosahedral *closo*-carboranes with the formula $C_2B_{10}H_{12}$ are the most common and can exist in three isomers: 1,2-, 1,7-, and 1,12-, referred to as *ortho* ($_O$Cb), *meta* ($_M$Cb), and *para* ($_P$Cb), respectively (Fig. 17a). All three isomers are very strongly electron withdrawing, and unlike aryl substituents cannot act as π-donors, making them promising candidates for the synthesis of highly Lewis acidic species. Computational studies in the Martin group found that carboranes are superior to aryl groups in general at increasing the Lewis acidity of boranes; for primary, secondary and tertiary boranes it is demonstrated that Lewis acidity follows the trend $B_OCb_XH_{3-X} > B_MCb_XH_{3-X} > B_PCb_XH_{3-X} > B(C_6F_5)_XH_{3-X} > B(C_6H_5)_XH_{3-X}$ (X = 1, 2, 3; Fig. 17c).[200] Early work with carboranyl substituents focused on perimeter substitution of triaryl boranes ($B(Mes)_2(_P\text{Ph}_O\text{Cb})$ & $B(2,6\text{-Me4-}_O\text{Cb})_3$; Fig. 17b) which resulted in increased Lewis acidity.[201,202] Towards applications, Park and coworkers applied these peripheral carboranyl-substituted triaryl boranes as fluoride ion sensors.[203] Considering the increase in Lewis acidity, stability, and emerging work, we preset select directly-bound *ortho*-carboranyl boranes,[189,204–220] many of which exceed the pentafluorophenyl analogues in terms of Lewis acidity and performance in chemical reactions.

The use of carborane as a directly-bound functional group towards the synthesis of Lewis acidic boranes has been spearheaded by Martin and coworkers.[189,200,218,221] Tris(*ortho*-carboranyl)borane (B_OCb_3, Fig. 17c), analogous to $B(C_6F_5)_3$, exhibits substantial increases to Lewis acidity when probed by the GB method, FIA, and HIA for RLAs of 115%, 134%, and 129%, respectively (Table 2).[200] Indeed, Lewis superacidity was confirmed computationally with an FIA of 605 kJ mol^{-1}.[180] In terms of electronics, relative to $B(C_6F_5)_3$ the LUMO energy level is stabilized by 0.49 eV. In terms of sterics, relative to $B(C_6F_5)_3$ B_OCb_3 sees an increase of 18.8% (%V_{bur}) and will preferentially forms FLPs over adducts.[221] Notable is the high thermal stability, with no decomposition when heated to 250 °C.

Two examples of mono-substituted carboranyl boranes include dimesityl(*ortho*-carboranyl)borane bearing either a H or Ph substituent on the carborane ($B(Mes)_{2o}$CbH & $B(Mes)_{2o}$CbPh; Fig. 17d). Computational investigation determined both were LSAs with FIAs of 556 kJ mol^{-1} for $B(Mes)_{2o}$CbH and 533 kJ mol^{-1} for $B(Mes)_{2o}$CbPh (Table 2).[204] LUMO energy levels were also computed for values of −2.13 eV for $B(Mes)_{2o}$CbH and −2.11 eV for $B(Mes)_{2o}$CbPh. Notably, both derivatives are water stable when considering aqueous workups in the syntheses, and while long-term experiments revealed

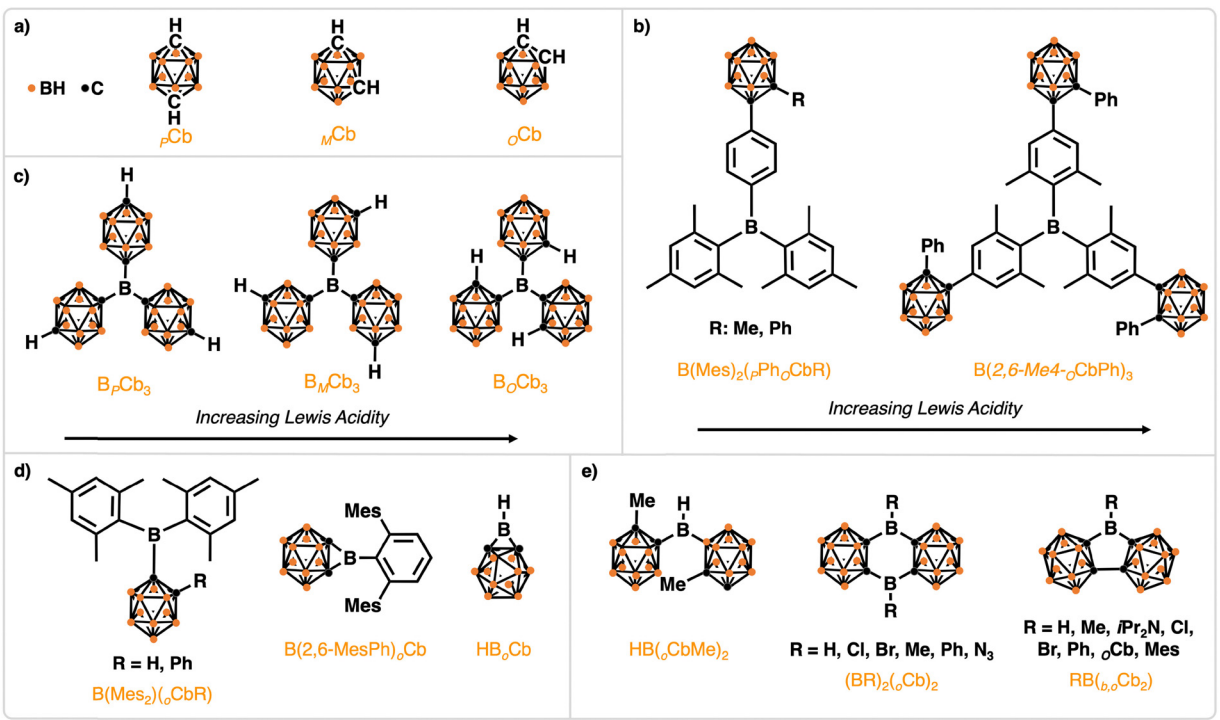

Fig. 17 Icosahedral *closo*-carboranes and carboranyl substituted boranes (Cb); (a) *ortho*-Cb ($_O$Cb), *meta*-Cb ($_M$Cb), and *para*-Cb ($_P$Cb), (b) triaryl boranes with peripheral carboranyl substituents $B(Mes)_2(_P\text{Ph}_O\text{CBR})$ & $B(2,6\text{-Me4-}_O\text{CbPh})_3$, (c) *ortho*-, *meta*-, and *para*-carboranyl tri-substituted boranes B_OCb_3, B_MCb_3, and B_PCb_3, (d) mono-substituted carboranyl boranes: $B(Mes_2)(_O\text{CbR})$, $B(2,6\text{-MesPh})_O\text{Cb}$, $HB_O\text{Cb}$, and (e) di-substituted carboranyl boranes: $HB(_O\text{CbMe})_2$, $(BR)_2(_O\text{Cb})_2$, $RB(_{b,O}\text{Cb}_2)$.

Table 2 Lewis acidity, electronic, and steric factors of carboranyl boranes

Borane	Lewis acidity	RLA	Electronics	Sterics
$B(C_6F_5)_3$	Due to variability across studies, relative $B(C_6F_5)_3$ data for each compound/study is reported			
B_oCb_3	GB $\Delta\delta$: 34.1 (C_6D_6), [b]29.7 $(C_6D_6)^{200}$ FIA: 605, [b]452[200] HIA: 622, [b]484[200]	GB $\Delta\delta$: 115 FIA: 134 HIA: 129	LUMO: −3.99[200] [b]LUMO: −3.50[200]	BV: 71.9[200] [b]BV: 53.1[200]
$B(Mes)_2(_OCbH)$	FIA: 556[204]	NR	LUMO: −2.13[204]	BV: NR
$B(Mes)_2(_OCbPh)$	FIA: 533[204]	NR	LUMO: −2.11[204]	BV: NR
$B(2,6\text{-}MesPh)_OCb$	FIA: 466, [c]474[207] HIA: 535, [b]546[207]	[c]FIA: 98 HIA: 98	LUMO: NR	BV: NR
HB_OCb	FIA: 512, [c]474[207] HIA: 580, [b]546[207]	[c]FIA: 108 HIA: 106	LUMO: NR	BV: NR
$HB(_oCbMe)_2$	GB $\Delta\delta$: 35.8 (C_6D_6), [b]29.7 $(C_6D_6)^{200}$ FIA: 527, [b]452[200] HIA: 540, [b]484[200]	GB $\Delta\delta$: 121 FIA: 117 HIA: 112	LUMO: −3.10[200] [b]LUMO: −3.50[200]	BV: 64.7[200] [b]BV: 53.1[200]
$(BH)_{2o}Cb_2$	FIA: 538, [c]474[214] HIA: 615, [b]546[214]	[c]FIA: 114 HIA: 113	LUMO: NR	[a]BV: 55.6[214]
$(BCl)_{2o}Cb_2$	GB $\Delta\delta$: 36.8 (C_6D_6), [b]26.6 $(C_6D_6)^{214}$ FIA: 535, [c]474[214] HIA: 601, [b]546[214]	GB $\Delta\delta$: 138 [c]FIA: 113 HIA: 110	LUMO: −1.50[214]	[a]BV: 60.6[214]
$(BBr)_{2o}Cb_2$	GB $\Delta\delta$: 40.8 (C_6D_6), [b]26.6 $(C_6D_6)^{214}$ FIA: 537, [c]474[214] HIA: 608, [b]546 [214]	GB $\Delta\delta$: 153 [c]FIA: 133 HIA: 111	LUMO: −1.57[214]	[a]BV: 61.4[214]
$(BMe)_{2o}Cb_2$	GB $\Delta\delta$: 32.6 (C_6D_6), [b]26.6 $(C_6D_6)^{214}$ FIA: 495, [c]474[214] HIA: 562, [b]546[214]	GB $\Delta\delta$: 123 [c]FIA: 104 HIA: 103	LUMO: −1.03[214]	[a]BV: 61.5[214]
$(BPh)_{2o}Cb_2$	GB $\Delta\delta$: 28.9 (C_6D_6), [b]26.6 $(C_6D_6)^{214}$ FIA: 523, [c]474[214] HIA: 592, [b]546[214]	GB $\Delta\delta$: 109 [c]FIA: 110 HIA: 108	LUMO: −1.18[214]	[a]BV: 66.2[214]
$(BN_3)_{2o}Cb_2$	GB $\Delta\delta$: 37.8 (C_6D_6), [b]26.6 $(C_6D_6)^{216}$ FIA: 515, [c]474[216] HIA: 578, [b]546[216]	GB $\Delta\delta$: 142 [c]FIA: 109 HIA: 106	LUMO: −1.33[216]	[a]BV: 59.2[216]
$iPr_2NB(_{b,O}Cb)$	GB $\Delta\delta$: 6.9 $(C_6D_6)^{213}$ FIA: 414, [c]474[217] HIA: 480, [b]546[217]	[c]FIA: 87 HIA:88	LUMO: −2.05[213]	[a]BV: 67.7[217]
$ClB(_{b,O}Cb)$	GB $\Delta\delta$: 40.3 (C_6D_6), [b]29.6 $(C_6D_6)^{217}$ FIA: 560, [c]474[217] HIA: 625, [b]546[217]	GB $\Delta\delta$: 136 [c]FIA: 118 HIA: 114	LUMO: NR	[a]BV: 55.5[217]
$BrB(_{b,O}Cb)$	GB $\Delta\delta$: 41.5 (C_6D_6), [b]29.6 $(C_6D_6)^{217}$ FIA: 565, [c]474[217] HIA: 635, [b]546[217]	GB $\Delta\delta$: 140 [c]FIA: 119 HIA: 116	LUMO: NR	[a]BV: 56.3[217]
$PhB(_{b,O}Cb)$	GB $\Delta\delta$: 34.3 (C_6D_6), [b]29.6 $(C_6D_6)^{217}$ FIA: 514, [c]474[217] HIA: 585, [b]546[217]	GB $\Delta\delta$: 116 [c]FIA: 108 HIA: 107	LUMO: −1.17[217]	[a]BV: 61.2[217]
$_OCbB(_{b,O}Cb)$	GB $\Delta\delta$: 34.9 (C_6D_6), [b]29.6 $(C_6D_6)^{212}$ FIA: 621, [c]475[212] HIA: 632, [b]484[212]	GB $\Delta\delta$: 118 [c]FIA: 131 HIA: 131	LUMO: −3.94[212] [b]LUMO: −3.52[212]	BV: 67.7[212]

GB $\Delta\delta$ = Gutmann–Beckett Method ^{31}P $\Delta\delta$ (ppm), FIA = fluoride ion affinity (kJ mol^{-1}), HIA = hydride ion affinity (kJ mol^{-1}), LUMO = calculated LUMO energy (eV), BV = buried volume of Lewis acids adducts with a fluoride ion $[LA\text{–}F]^-$. [a] BV is calculated using F–ion adduct cartesian coordinates obtained from associated references and the SambVca 2.1 web application,[199] RLA = relative Lewis acidity compared to $B(C_6F_5)_3$ (%). [b] Relative $B(C_6F_5)_3$ data. [c] Data is relative to SbF_5 rather than $B(C_6F_5)$, NR = not reported or relevant data not available.

hydrolysis on exposure to air over multiple weeks the carboranyl substituent remained bound to central boron. Another example of a mono-substituted carboranyl borane is the borirane, HB_OCb (Fig. 17d). While not a LSA, the FIA for HB_OCb is reported as 512 kJ mol^{-1} (Table 2), which is higher than typical reports for $B(C_6F_5)_3$ ($\sim$450–480 kJ mol^{-1}).[207] Note, several works have explored the properties and reactivity of these types of boriranes, including N-heterocyclic carbene stabilization.[205] For example, 5 and 7 membered ring-expansion products form when treated with aldehydes and ketones, respectively.[206–208,222,223] Computational investigation found the carboranyl borirane has higher ring strain than borirane, where this combined with the lack of π-delocalisation from the carborane leads to increased Lewis acidity.

Bis(1-methyl *ortho*-carboranyl)borane ($HB(_oCbMe)_2$, Fig. 17e) is an example of a di-substituted carboranyl borane and is analogous to Piers' borane. Lewis superacidity was confirmed computationally with FIA at 527 kJ mol^{-1} (exceeding SbF_5 at 493 kJ mol^{-1}; Table 2).[200] Electronically, the LUMO energy level of $HB(_oCbMe)_2$ is destabilized by 0.40 eV relative to $B(C_6F_5)_3$, and in terms of sterics is encumbered by 11.6% relative to $B(C_6F_5)_3$ ($\%V_{bur}$).[200] Additional examples of di-substituted carboranyl boranes include carboranyl diboranthracene ($(BR)_{2O}Cb_2$, R = H, Cl, Br, Me, Ph, N_3), though $(BH)_{2O}Cb_2$ was only observed *in situ*, and carboranyl borafluorene analogues ($RB_{(b,O)}Cb$, R = iPr_2N, Cl, Br, Ph, $_O$Cb; Fig. 17e). For the carboranyl diboranthracene analogues, RLAs (by FIA) compared to $B(C_6F_5)_3$ are 114%, 113%, 133%, 104%, and 110% for R being H, Cl, Br, Me, Ph, and N_3 (Table 2), respectively, showcasing the high Lewis acidity of these compounds.[214,216] The LUMO energy levels are also reported, albeit no calculations were done for $B(C_6F_5)_3$ so data cannot be compared, but are −1.50 eV, −1.57 eV, −1.03 eV, −1.18 eV, and −1.33 eV for R being Cl, Br, Me, Ph, and N_3 (Table 2), respectively.[214,216] In terms of sterics, again no $\%V_{bur}$ calculations (or relevant crystal structure data) for $B(C_6F_5)_3$ was provided so this data cannot be compared, but $\%V_{bur}$ are 55.6%, 60.6%, 61.4%, 61.5%, and 66.2%, and 59.2% for R being H, Cl, Br, Me, Ph, and N_3 (Table 2), respectively.[214,216] Notable is the thermal stability of these compounds, all isolated compounds were stable to at least 235 °C, with $(BMe)_{2O}Cb_2$ showing the highest melting point of 285 °C. The carboranyl borafluorene analogues exhibit increased Lewis acidity, except for the iPr_2N substituted carborane, with RLAs (by FIA) to that of $B(C_6F_5)_3$ being 87%, 118%, 119%, 108%, and 131% for R being iPr_2N, Cl, Br, Ph, and $_O$Cb (Table 2), respectively.[212,217] As is observed for classical borafluorenes, fusion of the substituents around the central boron atom results in an increase in Lewis acidity, resulting in an FIA increase of 39 kJ mol^{-1} for $_O$CbB($_{b,O}$Cb) relative to B_OCb_3. Only select LUMO energy levels are reported for these compounds for −2.05 eV, −1.17 eV, and −3.94 eV energies for the iPr_2N, Ph, and $_O$Cb analogues, respectively.[212,217] Furthermore, relative to $B(C_6F_5)_3$, the LUMO energy level of $_O$CbB($_{b,O}$Cb) is stabilized by 0.42 eV. Lastly, the buried volumes of this series of carboranyl borafluorenes were 67.7%, 55.5%, 56.3%, 61.2%, and 67.7% for R being iPr_2N, Cl, Br, Ph, and $_O$Cb, respectively.[212,217]

5. Conclusion

In summary, historical and emerging applications of $B(C_6F_5)_3$ has been presented which showcase the Lewis acid to be highly versatile. Compared to its halide counterparts, $B(C_6F_5)_3$ is unique in its stability and formation of analyzable crystalline structures appropriate for mechanistic studies, which has paved the way for improved chemical designs and applications. This is evident when reviewing the electronics field, where $B(C_6F_5)_3$ has recently emerged as a popular dopant for the active materials leading to higher performance devices, however, little understanding of the mechanisms and material interactions at play is evident. For example, $B(C_6F_5)_3$ is hygroscopic and is known to form water adducts, oxygen bridged borate complexes and can decompose into boronic acids and boroxines upon long-term exposure to water, oxygen, and heat. Such varied chemical species are likely to influence the long-term performance of organic electronic devices but have been rarely discussed within this field. Despite this, $B(C_6F_5)_3$ has shown great promise to date for applications in materials science and is an area that is seemingly ripe for future research. However, an interdisciplinary approach involving both inorganic chemists and materials scientists is needed. To start bridging this gap, we presented select triaryl boranes, triaryl borates, and carboranyl boranes and relevant properties for doping applications in organic electronics. Aluminum, indium, and pentavalent pnictogen (antinomy, phosphorus, bismuth) based Lewis acids were not covered but are notable alternatives. Looking towards future work, collaborations between the materials science and inorganic communities alongside the application of machine learning to identify and screen additional alternatives, in terms of predicted properties and interactions, would be of immense value to the materials science community.

Data availability

There is no original data. All work covered has been published prior.

Conflicts of interest

There are no conflicts to declare.

Acknowledgements

GCW acknowledges funding from the NSERC DG program (2019-04392), the Canada Foundation for Innovation, and the University of Calgary. KMW thanks NSERC for a CGS-D scholarship & IEP for a PGS-D scholarship. KMW, MJG, and IEP thank Alberta Student Aid for Alberta Graduate Excellence Scholarships.

References

1 W. E. Piers and T. Chivers, Pentafluorophenylboranes: From Obscurity to Applications, *Chem. Soc. Rev.*, 1997, **26**(5), 345, DOI: **10.1039/cs9972600345**.

2 A. G. Massey and A. J. Park, Tris(Pentafluorophenyl)Boron, *J. Organometal. Chem.*, 1964, **2**(3), 245–250, DOI: 10.1016/S0022-328X(00)80518-5.
3 X. Yang, C. L. Stern and T. J. Marks, Cation-like Homogeneous Olefin Polymerization Catalysts Based upon Zirconocene Alkyls and Tris(Pentafluorophenyl)Borane, *J. Am. Chem. Soc.*, 1991, **113**(9), 3623–3625, DOI: 10.1021/ja00009a076.
4 X. Yang, C. L. Stern and T. J. Marks, Cationic Zirconocene Olefin Polymerization Catalysts Based on the Organo-Lewis Acid Tris(Pentafluorophenyl)Borane. A Synthetic, Structural, Solution Dynamic, and Polymerization Catalytic Study, *J. Am. Chem. Soc.*, 1994, **116**(22), 10015–10031, DOI: 10.1021/ja00101a022.
5 M. Bochmann, Cationic Group 4 Metallocene Complexes and Their Role in Polymerisation Catalysis: The Chemistry of Well Defined Ziegler Catalysts, *J. Chem. Soc., Dalton Trans.*, 1996, (3), 255, DOI: 10.1039/dt9960000255.
6 E. Y.-X. Chen and T. J. Marks, Cocatalysts for Metal-Catalyzed Olefin Polymerization: Activators, Activation Processes, and Structure–Activity Relationships, *Chem. Rev.*, 2000, **100**(4), 1391–1434, DOI: 10.1021/cr980462j.
7 X. Sun, A Novel Lithium Battery Electrolyte Based on Lithium Fluoride and a Tris(Pentafluorophenyl) Borane Anion Receptor in DME, *Electrochem. Solid-State Lett.*, 1998, **1**(6), 239, DOI: 10.1149/1.1390698.
8 G. C. Welch, R. R. S. Juan, J. D. Masuda and D. W. Stephan, Reversible, Metal-Free Hydrogen Activation, *Science*, 2006, **314**(5802), 1124–1126, DOI: 10.1126/science.1134230.
9 D. W. Stephan and G. Erker, Frustrated Lewis Pairs: Metal-Free Hydrogen Activation and More, *Angew. Chem., Int. Ed.*, 2010, **49**(1), 46–76, DOI: 10.1002/anie.200903708.
10 D. W. Stephan, Frustrated Lewis Pairs, *J. Am. Chem. Soc.*, 2015, **137**(32), 10018–10032, DOI: 10.1021/jacs.5b06794.
11 D. W. Stephan, Frustrated Lewis Pairs: From Concept to Catalysis, *Acc. Chem. Res.*, 2015, **48**(2), 306–316, DOI: 10.1021/ar500375j.
12 K. Ishihara and H. Yamamoto, Arylboron Compounds as Acid Catalysts in Organic Synthetic Transformations, *Eur. J. Org. Chem.*, 1999, (3), 527–538, DOI: 10.1002/(SICI)1099-0690(199903)1999:3<527::AID-EJOC527>3.0.CO;2-R.
13 G. Kumar, S. Roy and I. Chatterjee, Tris(Pentafluorophenyl)Borane Catalyzed C–C and C–Heteroatom Bond Formation, *Org. Biomol. Chem.*, 2021, **19**(6), 1230–1267, DOI: 10.1039/D0OB02478C.
14 V. Nori, F. Pesciaioli, A. Sinibaldi, G. Giorgianni and A. Carlone, Boron-Based Lewis Acid Catalysis: Challenges and Perspectives, *Catalysts*, 2021, **12**(1), 5, DOI: 10.3390/catal12010005.
15 Frustrated Lewis Pairs II: Expanding the Scope, in *Topics in Current Chemistry*, ed. G. Erker and D. W. Stephan, Springer Berlin Heidelberg, Berlin, Heidelberg, 2013, vol. 334, DOI: 10.1007/978-3-642-37759-4.
16 K. Ishihara, N. Hananki and H. Yamamoto, Tris(Pentafluorophenyl)Boron as a New Efficient, Air Stable, and Water Tolerant Catalyst in the Adol-Type and Michael Reactions, *Syn. Lett.*, 1993, **8**, 577–579, DOI: 10.1055/s-1993-22535.
17 H. Gao, A. Battley and E. M. Leitao, The Ultimate Lewis Acid Catalyst: Using Tris(Pentafluorophenyl) Borane to Create Bespoke Siloxane Architectures, *Chem. Commun.*, 2022, **58**(54), 7451–7465, DOI: 10.1039/D2CC00441K.
18 T. Hackel and N. A. McGrath, Tris(Pentafluorophenyl)Borane-Catalyzed Reactions Using Silanes, *Molecules*, 2019, **24**(3), 432, DOI: 10.3390/molecules24030432.
19 M. A. Brook, New Control Over Silicone Synthesis Using SiH Chemistry: The Piers–Rubinsztajn Reaction, *Chem. – Eur. J.*, 2018, **24**(34), 8458–8469, DOI: 10.1002/chem.201800123.
20 X. Chen, M. Yi, S. Wu, L. Tan, X. Ge, M. He and G. Yin, Synthesis of Structurally Precise Polysiloxanes via the Piers–Rubinsztajn Reaction, *Materials*, 2019, **12**(2), 304, DOI: 10.3390/ma12020304.
21 J. M. Blackwell, W. E. Piers and M. Parvez, Mechanistic Studies on Selectivity in the $B(C_6F_5)_3$-Catalyzed Allylstannation of Aldehydes: Is Hypercoordination at Boron Responsible?, *Org. Lett.*, 2000, **2**(5), 695–698, DOI: 10.1021/ol0000105.
22 D. J. Morrison, J. M. Blackwell and W. E. Piers, Mechanistic Insights into Perfluoroaryl Borane-Catalyzed Allylstannations: Toward Asymmetric Induction with Chiral Boranes, *Pure Appl. Chem.*, 2004, **76**(3), 615–623, DOI: 10.1351/pac200476030615.
23 D. J. Morrison and W. E. Piers, Weaker Lewis Acid, Better Catalytic Activity: Dual Mechanisms in Perfluoroarylborane-Catalyzed Allylstannation Reactions, *Org. Lett.*, 2003, **5**(16), 2857–2860, DOI: 10.1021/ol034928i.
24 M. Ge, B. M. Stoltz and E. J. Corey, Mechanistic Insights into the Factors Determining *Exo–Endo* Selectivity in the Lewis Acid-Catalyzed Diels–Alder Reaction of 1,3-Dienes with 2-Cycloalkenones, *Org. Lett.*, 2000, **2**(13), 1927–1929, DOI: 10.1021/ol0060026.
25 J.-H. Zhou, B. Jiang, F.-F. Meng, Y.-H. Xu and T.-P. Loh, $B(C_6F_5)_3$: A New Class of Strong and Bulky Lewis Acid for *Exo*-Selective Intermolecular Diels–Alder Reactions of Unreactive Acyclic Dienes with α,β-Enals, *Org. Lett.*, 2015, **17**(18), 4432–4435, DOI: 10.1021/acs.orglett.5b02066.
26 M. Bakos, Z. Dobi, D. Fegyverneki, Á. Gyömöre, I. Fernández and T. Soós, Janus Face of the Steric Effect in a Lewis Acid Catalyst with Size-Exclusion Design: Steric Repulsion and Steric Attraction in the Catalytic Exo-Selective Diels–Alder Reaction, *ACS Sustainable Chem. Eng.*, 2018, **6**(8), 10869–10875, DOI: 10.1021/acssuschemeng.8b02099.
27 J. Wang, Z. Liu, J. Li, Z. Song, C. Hu and Z. Su, *Exo/Endo* Selectivity Control in Diels–Alder Reactions of Geminal Bis(Silyl) Dienes: Theoretical and Experimental Studies, *J. Org. Chem.*, 2019, **84**(7), 3940–3952, DOI: 10.1021/acs.joc.8b03090.
28 G. Erker, Tris(Pentafluorophenyl)Borane: A Special Boron Lewis Acid for Special Reactions, *Dalton Trans.*, 2005, 1883–1890, DOI: 10.1039/b503688g.
29 J. A. Ewen, M. J. Edler, R. L. Jones, L. Haspeslagh, J. L. Atwood, S. G. Bott and K. Robinson, Metallocene/Polypropylene Structural Relationships: Implications on Polymerization and Stereochemical Control Mechanisms, *Macromol. Symp.*, 1991, **48–49**(1), 253–295, DOI: 10.1002/masy.19910480121.

30 D. J. Parks and W. E. Piers, Tris(Pentafluorophenyl)Boron-Catalyzed Hydrosilation of Aromatic Aldehydes, Ketones, and Esters, *J. Am. Chem. Soc.*, 1996, **118**(39), 9440–9441, DOI: 10.1021/ja961536g.

31 T. Ooi, D. Uraguchi, N. Kagoshima and K. Maruoka, Hypercoordination of Boron and Aluminum: Synthetic Utility as Chelating Lewis Acids, *J. Am. Chem. Soc.*, 1998, **120**(21), 5327–5328, DOI: 10.1021/ja9736828.

32 D. Vagedes, R. Fröhlich and G. Erker, Treatment of Naphthols with $B(C_6F_5)_3$: Formation and Characterization of the Lewis Acid Adducts of Their Keto Isomers, *Angew. Chem., Int. Ed.*, 1999, **38**(22), 3362–3365, DOI: 10.1002/(SICI)1521-3773(19991115)38:22<3362::AID-ANIE3362>3.0.CO;2-N.

33 S. Rubinsztajn and J. A. Cella, A New Polycondensation Process for the Preparation of Polysiloxane Copolymers, *Macromolecules*, 2005, **38**(4), 1061–1063, DOI: 10.1021/ma047984n.

34 P. Thirupathi, L. N. Neupane and K.-H. Lee, Tris(Pentafluorophenyl)Borane $[B(C_6F_5)_3]$-Catalyzed Friedel–Crafts Reactions of Activated Arenes and Heteroarenes with α-Amidosulfones: The Synthesis of Unsymmetrical Triarylmethanes, *Tetrahedron*, 2011, **67**(38), 7301–7310, DOI: 10.1016/j.tet.2011.07.041.

35 J. M. Blackwell, E. R. Sonmor, T. Scoccitti and W. E. Piers, $B(C_6F_5)_3$-Catalyzed Hydrosilation of Imines via Silyliminium Intermediates, *Org. Lett.*, 2000, **2**(24), 3921–3923, DOI: 10.1021/ol006695q.

36 J. M. Blackwell, W. E. Piers and R. McDonald, Mechanistic Studies on the $B(C_6F_5)_3$ Catalyzed Allylstannation of Aromatic Aldehydes with *Ortho* Donor Substituents, *J. Am. Chem. Soc.*, 2002, **124**(7), 1295–1306, DOI: 10.1021/ja012028w.

37 I. Protsak, V. Gun'ko, Y. Morozov, I. M. Henderson, D. Zhang, Z. Yinjun and V. Turov, Intermediates of Tris(Pentafluorophenyl)Borane and Dimethyl Carbonate Pave the Way for Deeper Organosiloxane Depolymerization Reactions, *Polym. J.*, 2021, **53**(4), 573–579, DOI: 10.1038/s41428-020-00452-0.

38 G. Kehr, R. Fröhlich, B. Wibbeling and G. Erker, (*N*-Pyrrolyl)$B(C_6F_5)_2$-A New Organometallic Lewis Acid for the Generation of Group 4 Metallocene Cation Complexes, *Chem. – Eur. J.*, 2000, **6**(2), 258–266, DOI: 10.1002/(SICI)1521-3765(20000117)6:2<258::AID-CHEM258>3.0.CO;2-E.

39 G. Kehr, R. Roesmann, R. Fröhlich, C. Holst and G. Erker, Protonation of the Heterocyclic Cp-Anion Equivalent [Pyrrolyl-$B(C_6F_5)_3$]Li – Formation of a Useful Neutral Brønsted Acid for the Generation of Homogeneous Metallocene Ziegler Catalysts, *Eur. J. Inorg. Chem.*, 2001, (2), 535–538, DOI: 10.1002/1099-0682(200102)2001:2<535::AID-EJIC535>3.0.CO;2-6.

40 S. Guidotti, I. Camurati, F. Focante, L. Angellini, G. Moscardi, L. Resconi, R. Leardini, D. Nanni, P. Mercandelli, A. Sironi, T. Beringhelli and D. Maggioni, Synthesis and Reactivity of $(C_6F_5)_3$B-N-Heterocycle Complexes. 1. Generation of Highly Acidic Sp^3 Carbons in Pyrroles and Indoles, *J. Org. Chem.*, 2003, **68**(14), 5445–5465, DOI: 10.1021/jo020647x.

41 A. Bonazza, I. Camurati, S. Guidotti, N. Mascellari and L. Resconi, Synthesis and Reactivity of $(C_6F_5)_3$B-N-Heterocycle Complexes, *Macromol. Chem. Phys.*, 2004, **205**(3), 319–333, DOI: 10.1002/macp.200300132.

42 G. C. Welch, L. Cabrera, P. A. Chase, E. Hollink, J. D. Masuda, P. Wei and D. W. Stephan, Tuning Lewis Acidity Using the Reactivity of "Frustrated Lewis Pairs": Facile Formation of Phosphine–Boranes and Cationic Phosphonium–Boranes, *Dalton Trans.*, 2007, 3407–3414, DOI: 10.1039/b704417h.

43 J. S. J. McCahill, G. C. Welch and D. W. Stephan, Reactivity of "Frustrated Lewis Pairs": Three-Component Reactions of Phosphines, a Borane, and Olefins, *Angew. Chem., Int. Ed.*, 2007, **46**(26), 4968–4971, DOI: 10.1002/anie.200701215.

44 J. Paradies, Mechanisms in Frustrated Lewis Pair-Catalyzed Reactions, *Eur. J. Org. Chem.*, 2019, (2–3), 283–294, DOI: 10.1002/ejoc.201800944.

45 M. L. McGraw and E. Y.-X. Chen, Lewis Pair Polymerization: Perspective on a Ten-Year Journey, *Macromolecules*, 2020, **53**(15), 6102–6122, DOI: 10.1021/acs.macromol.0c01156.

46 J. S. Reddy, B.-H. Xu, T. Mahdi, R. Fröhlich, G. Kehr, D. W. Stephan and G. Erker, Alkenylborane-Derived Frustrated Lewis Pairs: Metal-Free Catalytic Hydrogenation Reactions of Electron-Deficient Alkenes, *Organometallics*, 2012, **31**(15), 5638–5649, DOI: 10.1021/om3006068.

47 L. Greb, P. Oña-Burgos, B. Schirmer, S. Grimme, D. W. Stephan and J. Paradies, Metal-Free Catalytic Olefin Hydrogenation: Low-Temperature H_2 Activation by Frustrated Lewis Pairs, *Angew. Chem., Int. Ed.*, 2012, **51**(40), 10164–10168, DOI: 10.1002/anie.201204007.

48 J. A. Nicasio, S. Steinberg, B. Inés and M. Alcarazo, Tuning the Lewis Acidity of Boranes in Frustrated Lewis Pair Chemistry: Implications for the Hydrogenation of Electron-Poor Alkenes, *Chem. – Eur. J.*, 2013, **19**(33), 11016–11020, DOI: 10.1002/chem.201301158.

49 A. Willms, H. Schumacher, T. Tabassum, L. Qi, S. L. Scott, P. J. C. Hausoul and M. Rose, Solid Molecular Frustrated Lewis Pairs in a Polyamine Organic Framework for the Catalytic Metal-free Hydrogenation of Alkenes, *ChemCatChem*, 2018, **10**(8), 1835–1843, DOI: 10.1002/cctc.201701783.

50 Y. Segawa and D. W. Stephan, Metal-Free Hydrogenation Catalysis of Polycyclic Aromatic Hydrocarbons, *Chem. Commun.*, 2012, **48**(98), 11963, DOI: 10.1039/c2cc37190a.

51 T. Mahdi and D. W. Stephan, Enabling Catalytic Ketone Hydrogenation by Frustrated Lewis Pairs, *J. Am. Chem. Soc.*, 2014, **136**(45), 15809–15812, DOI: 10.1021/ja508829x.

52 D. J. Scott, M. J. Fuchter and A. E. Ashley, Nonmetal Catalyzed Hydrogenation of Carbonyl Compounds, *J. Am. Chem. Soc.*, 2014, **136**(45), 15813–15816, DOI: 10.1021/ja5088979.

53 T. Mahdi and D. W. Stephan, Facile Protocol for Catalytic Frustrated Lewis Pair Hydrogenation and Reductive Deoxygenation of Ketones and Aldehydes, *Angew. Chem., Int. Ed.*, 2015, **54**(29), 8511–8514, DOI: 10.1002/anie.201503087.

54 P. A. Chase, G. C. Welch, T. Jurca and D. W. Stephan, Metal-Free Catalytic Hydrogenation, *Angew. Chem., Int. Ed.*, 2007, **46**(42), 8050–8053, DOI: 10.1002/anie.200702908.

55 P. A. Chase, T. Jurca and D. W. Stephan, Lewis Acid-Catalyzed Hydrogenation: $B(C_6F_5)_3$-Mediated Reduction of Imines and Nitriles with H_2, *Chem. Commun.*, 2008, 1701–1703, DOI: 10.1039/b718598g.

56 P. Spies, S. Schwendemann, S. Lange, G. Kehr, R. Fröhlich and G. Erker, Metal-Free Catalytic Hydrogenation of Enamines, Imines, and Conjugated Phosphinoalkenylboranes, *Angew. Chem., Int. Ed.*, 2008, **47**(39), 7543–7546, DOI: 10.1002/anie.200801432.

57 H. Wang, R. Fröhlich, G. Kehr and G. Erker, Heterolytic Dihydrogen Activation with the 1,8-Bis(Diphenylphosphino)Naphthalene/$B(C_6F_5)_3$ Pair and Its Application for Metal-Free Catalytic Hydrogenation of Silyl Enol Ethers, *Chem. Commun.*, 2008, 5966–5968, DOI: 10.1039/b813286k.

58 J. Mohr and M. Oestreich, $B(C_6F_5)_3$-Catalyzed Hydrogenation of Oxime Ethers without Cleavage of the N–O Bond, *Angew. Chem., Int. Ed.*, 2014, **53**(48), 13278–13281, DOI: 10.1002/anie.201407324.

59 T. Mahdi and D. W. Stephan, Frustrated Lewis Pair Catalyzed Hydroamination of Terminal Alkynes, *Angew. Chem., Int. Ed.*, 2013, **52**(47), 12418–12421, DOI: 10.1002/anie.201307254.

60 T. Mahdi and D. W. Stephan, Stoichiometric and Catalytic Inter- and Intramolecular Hydroamination of Terminal Alkynes by Frustrated Lewis Pairs, *Chem. – Eur. J.*, 2015, **21**(31), 11134–11142, DOI: 10.1002/chem.201501535.

61 R. Dobrovetsky and D. W. Stephan, Stoichiometric Metal-Free Reduction of CO in Syn-Gas, *J. Am. Chem. Soc.*, 2013, **135**(13), 4974–4977, DOI: 10.1021/ja401492s.

62 M. Sajid, L. Elmer, C. Rosorius, C. G. Daniliuc, S. Grimme, G. Kehr and G. Erker, Facile Carbon Monoxide Reduction at Intramolecular Frustrated Phosphane/Borane Lewis Pair Templates, *Angew. Chem., Int. Ed.*, 2013, **52**(8), 2243–2246, DOI: 10.1002/anie.201208750.

63 D. W. Stephan, Frustrated Lewis Pair Chemistry of CO, *Chem. Soc. Rev.*, 2023, **52**(14), 4632–4643, DOI: 10.1039/D3CS00294B.

64 C. M. Mömming, E. Otten, G. Kehr, R. Fröhlich, S. Grimme, D. W. Stephan and G. Erker, Reversible Metal-Free Carbon Dioxide Binding by Frustrated Lewis Pairs, *Angew. Chem., Int. Ed.*, 2009, **48**(36), 6643–6646, DOI: 10.1002/anie.200901636.

65 A. Ashley, A. Thompson and D. O'Hare, Non-Metal-Mediated Homogeneous Hydrogenation of CO_2 to CH_3OH, *Angew. Chem., Int. Ed.*, 2009, **48**(52), 9839–9843, DOI: 10.1002/anie.200905466.

66 A. Berkefeld, W. E. Piers and M. Parvez, Tandem Frustrated Lewis Pair/Tris(Pentafluorophenyl)Borane-Catalyzed Deoxygenative Hydrosilylation of Carbon Dioxide, *J. Am. Chem. Soc.*, 2010, **132**(31), 10660–10661, DOI: 10.1021/ja105320c.

67 I. Peuser, R. C. Neu, X. Zhao, M. Ulrich, B. Schirmer, J. A. Tannert, G. Kehr, R. Fröhlich, S. Grimme, G. Erker and D. W. Stephan, CO_2 and Formate Complexes of Phosphine/Borane Frustrated Lewis Pairs, *Chem. – Eur. J.*, 2011, **17**(35), 9640–9650, DOI: 10.1002/chem.201100286.

68 M. Harhausen, R. Fröhlich, G. Kehr and G. Erker, Reactions of Modified Intermolecular Frustrated P/B Lewis Pairs with Dihydrogen, Ethene, and Carbon Dioxide, *Organometallics*, 2012, **31**(7), 2801–2809, DOI: 10.1021/om201076f.

69 Md. N. Khan, Y. Van Ingen, T. Boruah, A. McLauchlan, T. Wirth and R. L. Melen, Advances in CO_2 Activation by Frustrated Lewis Pairs: From Stoichiometric to Catalytic Reactions, *Chem. Sci.*, 2023, 13661–13695, DOI: 10.1039/D3SC03907B.

70 E. Otten, R. C. Neu and D. W. Stephan, Complexation of Nitrous Oxide by Frustrated Lewis Pairs, *J. Am. Chem. Soc.*, 2009, **131**(29), 9918–9919, DOI: 10.1021/ja904377v.

71 A. J. P. Cardenas, B. J. Culotta, T. H. Warren, S. Grimme, A. Stute, R. Fröhlich, G. Kehr and G. Erker, Capture of NO by a Frustrated Lewis Pair: A New Type of Persistent *N*-Oxyl Radical, *Angew. Chem., Int. Ed.*, 2011, **50**(33), 7567–7571, DOI: 10.1002/anie.201101622.

72 M. Sajid, A. Klose, B. Birkmann, L. Liang, B. Schirmer, T. Wiegand, H. Eckert, A. J. Lough, R. Fröhlich, C. G. Daniliuc, S. Grimme, D. W. Stephan, G. Kehr and G. Erker, Reactions of Phosphorus/Boron Frustrated Lewis Pairs with SO_2, *Chem. Sci.*, 2013, **4**(1), 213–219, DOI: 10.1039/C2SC21161K.

73 M. A. Dureen and D. W. Stephan, Terminal Alkyne Activation by Frustrated and Classical Lewis Acid/Phosphine Pairs, *J. Am. Chem. Soc.*, 2009, **131**(24), 8396–8397, DOI: 10.1021/ja903650w.

74 M. A. Dureen, C. C. Brown and D. W. Stephan, Addition of Enamines or Pyrroles and $B(C_6F_5)_3$ "Frustrated Lewis Pairs" to Alkynes, *Organometallics*, 2010, **29**(23), 6422–6432, DOI: 10.1021/om1008346.

75 M. A. Dureen, C. C. Brown and D. W. Stephan, Deprotonation and Addition Reactions of Frustrated Lewis Pairs with Alkynes, *Organometallics*, 2010, **29**(23), 6594–6607, DOI: 10.1021/om1009044.

76 M. A. Dureen, G. C. Welch, T. M. Gilbert and D. W. Stephan, Heterolytic Cleavage of Disulfides by Frustrated Lewis Pairs, *Inorg. Chem.*, 2009, **48**(20), 9910–9917, DOI: 10.1021/ic901590s.

77 D. Voicu, M. Abolhasani, R. Choueiri, G. Lestari, C. Seiler, G. Menard, J. Greener, A. Guenther, D. W. Stephan and E. Kumacheva, Microfluidic Studies of CO_2 Sequestration by Frustrated Lewis Pairs, *J. Am. Chem. Soc.*, 2014, **136**(10), 3875–3880, DOI: 10.1021/ja411601a.

78 D. C. Bradley, I. S. Harding, A. D. Keefe, M. Motevalli and D. H. Zheng, Reversible Adduct Formation between Phosphines and Triarylboron Compounds, *J. Chem. Soc., Dalton Trans.*, 1996, (20), 3931, DOI: 10.1039/dt9960003931.

79 P. S. Marqués, G. Londi, B. Yurash, T.-Q. Nguyen, S. Barlow, S. R. Marder and D. Beljonne, Understanding How Lewis Acids Dope Organic Semiconductors: A "Complex" Story, *Chem. Sci.*, 2021, **12**(20), 7012–7022, DOI: 10.1039/D1SC01268A.

80 M. Dryzhakov, E. Richmond, G. Li and J. Moran, Catalytic $B(C_6F_5)_3H_2O$-Promoted Defluorinative Functionalization of Tertiary Aliphatic Fluorides, *J. Fluorine Chem.*, 2017, **193**, 45–51, DOI: 10.1016/j.jfluchem.2016.11.005.

81 H. H. San, S.-J. Wang, M. Jiang and X.-Y. Tang, Boron-Catalyzed O–H Bond Insertion of α-Aryl α-Diazoesters in

Water, *Org. Lett.*, 2018, **20**(15), 4672–4676, DOI: 10.1021/acs.orglett.8b01988.

82 H. Zhang, X.-Y. Zhan, Y. Dong, J. Yang, S. He, Z.-C. Shi, X.-M. Zhang and J.-Y. Wang, Dehydration in Water: Frustrated Lewis Pairs Directly Catalyzed Allylization of Electron-Rich Arenes and Allyl Alcohols, *RSC Adv.*, 2020, **10**(29), 16942–16948, DOI: 10.1039/D0RA02912B.

83 K. M. Rabanzo-Castillo, V. B. Kumar, T. Söhnel and E. M. Leitao, Catalytic Synthesis of Oligosiloxanes Mediated by an Air Stable Catalyst, $(C_6F_5)_3B(OH_2)$, *Front. Chem.*, 2020, **8**, 477, DOI: 10.3389/fchem.2020.00477.

84 L. Winfrey, L. Yun, G. Passeri, K. Suntharalingam and A. P. Pulis, $H_2O{\cdot}B(C_6F_5)_3$-Catalyzed *Para*-Alkylation of Anilines with Alkenes Applied to Late-Stage Functionalization of Non-Steroidal Anti-Inflammatory Drugs, *Chem. – Eur. J.*, 2024, **30**(13), e202303130, DOI: 10.1002/chem.202303130.

85 M. Dryzhakov and J. Moran, Autocatalytic Friedel–Crafts Reactions of Tertiary Aliphatic Fluorides Initiated by $B(C_6F_5)_3{\cdot}H_2O$, *ACS Catal.*, 2016, **6**(6), 3670–3673, DOI: 10.1021/acscatal.6b00866.

86 G.-M. Zhang, H. Zhang, B. Wang and J.-Y. Wang, Boron-Catalyzed Dehydrative Allylation of 1,3-Diketones and β-Ketone Esters with 1,3-Diarylallyl Alcohols in Water, *RSC Adv.*, 2021, **11**(28), 17025–17031, DOI: 10.1039/D1RA01922H.

87 F. Jäkle, Advances in the Synthesis of Organoborane Polymers for Optical, Electronic, and Sensory Applications, *Chem. Rev.*, 2010, **110**, 3985–4022, DOI: 10.1021/cr100026f.

88 M. J. D. Bosdet and W. E. Piers, B–N as a C–C Substitute in Aromatic Systems, *Can. J. Chem.*, 2009, **87**, 8–29, DOI: 10.1139/V08-110.

89 J.-Y. Wang and J. Pei, BN-Embedded Aromatics for Optoelectronic Applications, *Chin. Chem. Lett.*, 2016, **27**, 1139–1146, DOI: 10.1016/j.cclet.2016.06.014.

90 S. K. Mellerup and S. Wang, Boron-Based Stimuli Responsive Materials, *Chem. Soc. Rev.*, 2019, **48**, 3537, DOI: 10.1039/c9cs00153k.

91 Y.-S. Duh, K. H. Lin and C.-S. Kao, Experimental Investigation and Visualization on Thermal Runaway of Hard Prismatic Lithium-Ion Batteries Used in Smart Phones, *J. Therm. Anal. Calorim.*, 2018, **132**(3), 1677–1692, DOI: 10.1007/s10973-018-7077-2.

92 J. Duan, X. Tang, H. Dai, Y. Yang, W. Wu, X. Wei and Y. Huang, Building Safe Lithium-Ion Batteries for Electric Vehicles: A Review, *Electrochem. Energy Rev.*, 2020, **3**(1), 1–42, DOI: 10.1007/s41918-019-00060-4.

93 B. Diouf and R. Pode, Potential of Lithium-Ion Batteries in Renewable Energy, *Renewable Energy*, 2015, **76**, 375–380, DOI: 10.1016/j.renene.2014.11.058.

94 Y. Chen, Y. Kang, Y. Zhao, L. Wang, J. Liu, Y. Li, Z. Liang, X. He, X. Li, N. Tavajohi and B. Li, A Review of Lithium-Ion Battery Safety Concerns: The Issues, Strategies, and Testing Standards, *J. Energy Chem.*, 2021, **59**, 83–99, DOI: 10.1016/j.jechem.2020.10.017.

95 X. Wu, K. Song, X. Zhang, N. Hu, L. Li, W. Li, L. Zhang and H. Zhang, Safety Issues in Lithium Ion Batteries: Materials and Cell Design, *Front. Energy Res.*, 2019, **7**, 65, DOI: 10.3389/fenrg.2019.00065.

96 X. Liu, D. Ren, H. Hsu, X. Feng, G.-L. Xu, M. Zhuang, H. Gao, L. Lu, X. Han, Z. Chu, J. Li, X. He, K. Amine and M. Ouyang, Thermal Runaway of Lithium-Ion Batteries without Internal Short Circuit, *Joule*, 2018, **2**(10), 2047–2064, DOI: 10.1016/j.joule.2018.06.015.

97 M. Herstedt, M. Stjerndahl, T. Gustafsson and K. Edström, Anion Receptor for Enhanced Thermal Stability of the Graphite Anode Interface in a Li-Ion Battery, *Electrochem. Commun.*, 2003, **5**(6), 467–472, DOI: 10.1016/S1388-2481(03)00106-1.

98 J. Xiang, Y. Zhang, B. Zhang, L. Yuan, X. Liu, Z. Cheng, Y. Yang, X. Zhang, Z. Li, Y. Shen, J. Jiang and Y. Huang, A Flame-Retardant Polymer Electrolyte for High Performance Lithium Metal Batteries with an Expanded Operation Temperature, *Energy Environ. Sci.*, 2021, **14**(6), 3510–3521, DOI: 10.1039/D1EE00049G.

99 Y. M. Lee, J. E. Seo, N.-S. Choi and J.-K. Park, Influence of Tris(Pentafluorophenyl) Borane as an Anion Receptor on Ionic Conductivity of $LiClO_4$-Based Electrolyte for Lithium Batteries, *Electrochim. Acta*, 2005, **50**(14), 2843–2848, DOI: 10.1016/j.electacta.2004.11.058.

100 C.-C. Chang and T.-K. Chen, Tris(Pentafluorophenyl) Borane as an Electrolyte Additive for $LiFePO_4$ Battery, *J. Power Sources*, 2009, **193**(2), 834–840, DOI: 10.1016/j.jpowsour.2009.04.033.

101 Y. M. Lee, Y.-G. Lee, Y.-M. Kang and K. Y. Cho, Nature of Tris(Pentafluorophenyl)Borane as a Functional Additive and Its Contribution to High Rate Performance in Lithium-Ion Secondary Battery, *Electrochem. Solid-State Lett.*, 2010, **13**(5), A55, DOI: 10.1149/1.3329703.

102 G.-B. Han, J.-N. Lee, J. W. Choi and J.-K. Park, Tris(Pentafluorophenyl) Borane as an Electrolyte Additive for High Performance Silicon Thin Film Electrodes in Lithium Ion Batteries, *Electrochim. Acta*, 2011, **56**(24), 8997–9003, DOI: 10.1016/j.electacta.2011.07.136.

103 S. Wu and A. Huang, Effects of Tris(Pentafluorophenyl) Borane (TPFPB) as an Electrolyte Additive on the Cycling Performance of $LiFePO_4$ Batteries, *J. Electrochem. Soc.*, 2013, **160**(4), A684–A689, DOI: 10.1149/2.074304jes.

104 H. Yue, Y. Yang, Y. Xiao, Z. Dong, S. Cheng, Y. Yin, C. Ling, W. Yang, Y. Yu and S. Yang, Boron Additive Passivated Carbonate Electrolytes for Stable Cycling of 5 V Lithium–Metal Batteries, *J. Mater. Chem. A*, 2019, **7**(2), 594–602, DOI: 10.1039/C8TA09380F.

105 K. Xu, Y. Lam, S. S. Zhang, T. R. Jow and T. B. Curtis, Solvation Sheath of Li^+ in Nonaqueous Electrolytes and Its Implication of Graphite/Electrolyte Interface Chemistry, *J. Phys. Chem. C*, 2007, **111**(20), 7411–7421, DOI: 10.1021/jp068691u.

106 S. J. An, J. Li, C. Daniel, D. Mohanty, S. Nagpure and D. L. Wood, The State of Understanding of the Lithium-Ion-Battery Graphite Solid Electrolyte Interphase (SEI) and Its Relationship to Formation Cycling, *Carbon*, 2016, **105**, 52–76, DOI: 10.1016/j.carbon.2016.04.008.

107 A. Wang, S. Kadam, H. Li, S. Shi and Y. Qi, Review on Modeling of the Anode Solid Electrolyte Interphase (SEI) for Lithium-Ion Batteries, *npj Comput. Mater.*, 2018, **4**(1), 15, DOI: **10.1038/s41524-018-0064-0**.

108 Z. Chen and K. Amine, Tris(Pentafluorophenyl) Borane as an Additive to Improve the Power Capabilities of Lithium-Ion Batteries, *J. Electrochem. Soc.*, 2006, **153**(6), A1221, DOI: **10.1149/1.2194633**.

109 T. Li, X.-Q. Zhang, N. Yao, Y.-X. Yao, L.-P. Hou, X. Chen, M.-Y. Zhou, J.-Q. Huang and Q. Zhang, Stable Anion-Derived Solid Electrolyte Interphase in Lithium Metal Batteries, *Angew. Chem., Int. Ed.*, 2021, **60**(42), 22683–22687, DOI: **10.1002/anie.202107732**.

110 S. Li, W. Zhang, Q. Wu, L. Fan, X. Wang, X. Wang, Z. Shen, Y. He and Y. Lu, Synergistic Dual-Additive Electrolyte Enables Practical Lithium-Metal Batteries, *Angew. Chem., Int. Ed.*, 2020, **59**(35), 14935–14941, DOI: **10.1002/anie.202004853**.

111 M. Wu, Y. Li, X. Liu, S. Yang, J. Ma and S. Dou, Perspective on Solid-Electrolyte Interphase Regulation for Lithium Metal Batteries, *SmartMat*, 2021, **2**(1), 5–11, DOI: **10.1002/smm2.1015**.

112 H. Gao, Y. Li, R. Guo and B. M. Gallant, Controlling Fluoride-Forming Reactions for Improved Rate Capability in Lithium-Perfluorinated Gas Conversion Batteries, *Adv. Energy Mater.*, 2019, **9**(21), 1900393, DOI: **10.1002/aenm.201900393**.

113 M. Kartal, M. Uysal, A. Alp and H. Akbulut, Tris-(Pentafluorophenyl) Borane as an Electrolyte Additive for Li–O_2 Batteries, *Int. J. Hydrogen Energy*, 2016, **41**(18), 7600–7608, DOI: **10.1016/j.ijhydene.2016.02.092**.

114 T. Zhao, X. Zheng, D. Wang, L. Huang, B. Li, X. Liu, H. Yang, Y. Dai, Y. Huang and W. Luo, A Quasi-Solid-State Polyether Electrolyte for Low-Temperature Sodium Metal Batteries, *Adv. Funct. Mater.*, 2023, **33**(48), 2304928, DOI: **10.1002/adfm.202304928**.

115 X. Zhou, X. Chen, Z. Yang, X. Liu, Z. Hao, S. Jin, L. Zhang, R. Wang, C. Zhang, L. Li, X. Tan and S. Chou, Anion Receptor Weakens ClO_4^- Solvation for High-Temperature Sodium-Ion Batteries, *Adv. Funct. Mater.*, 2023, **34**(5), 2302281, DOI: **10.1002/adfm.202302281**.

116 A. Y. S. Eng, C. B. Soni, Y. Lum, E. Khoo, Z. Yao, S. K. Vineeth, V. Kumar, J. Lu, C. S. Johnson, C. Wolverton and Z. W. Seh, Theory-Guided Experimental Design in Battery Materials Research, *Sci. Adv.*, 2022, **8**(19), eabm2422, DOI: **10.1126/sciadv.abm2422**.

117 C. K. Chiang, C. R. Fincher, Y. W. Park, A. J. Heeger, H. Shirakawa, E. J. Louis, S. C. Gau and A. G. MacDiarmid, Electrical Conductivity in Doped Polyacetylene, *Phys. Rev. Lett.*, 1977, **39**(17), 1098–1101, DOI: **10.1103/PhysRevLett.39.1098**.

118 J. Blochwitz, M. Pfeiffer, T. Fritz and K. Leo, Low Voltage Organic Light Emitting Diodes Featuring Doped Phthalocyanine as Hole Transport Material, *Appl. Phys. Lett.*, 1998, **73**(6), 729–731, DOI: **10.1063/1.121982**.

119 D. T. Duong, C. Wang, E. Antono, M. F. Toney and A. Salleo, The Chemical and Structural Origin of Efficient P-Type Doping in P3HT, *Org. Electron.*, 2013, **14**(5), 1330–1336, DOI: **10.1016/j.orgel.2013.02.028**.

120 D. T. Duong, H. Phan, D. Hanifi, P. S. Jo, T. Nguyen and A. Salleo, Direct Observation of Doping Sites in Temperature-Controlled, p-Doped P3HT Thin Films by Conducting Atomic Force Microscopy, *Adv. Mater.*, 2014, **26**(35), 6069–6073, DOI: **10.1002/adma.201402015**.

121 I. E. Jacobs, E. W. Aasen, J. L. Oliveira, T. N. Fonseca, J. D. Roehling, J. Li, G. Zhang, M. P. Augustine, M. Mascal and A. J. Moulé, Comparison of Solution-Mixed and Sequentially Processed P3HT:F4TCNQ Films: Effect of Doping-Induced Aggregation on Film Morphology, *J. Mater. Chem. C*, 2016, **4**(16), 3454–3466, DOI: **10.1039/C5TC04207K**.

122 E. F. Aziz, A. Vollmer, S. Eisebitt, W. Eberhardt, P. Pingel, D. Neher and N. Koch, Localized Charge Transfer in a Molecularly Doped Conducting Polymer, *Adv. Mater.*, 2007, **19**(20), 3257–3260, DOI: **10.1002/adma.200700926**.

123 I. Salzmann, G. Heimel, M. Oehzelt, S. Winkler and N. Koch, Molecular Electrical Doping of Organic Semiconductors: Fundamental Mechanisms and Emerging Dopant Design Rules, *Acc. Chem. Res.*, 2016, **49**(3), 370–378, DOI: **10.1021/acs.accounts.5b00438**.

124 I. D. V. Ingram, D. J. Tate, A. V. S. Parry, R. Sebastian Sprick and M. L. Turner, A Simple Method for Controllable Solution Doping of Complete Polymer Field-Effect Transistors, *Appl. Phys. Lett.*, 2014, **104**(15), 153304, DOI: **10.1063/1.4871096**.

125 P. Zalar, M. Kuik, Z. B. Henson, C. Woellner, Y. Zhang, A. Sharenko, G. C. Bazan and T. Nguyen, Increased Mobility Induced by Addition of a Lewis Acid to a Lewis Basic Conjugated Polymer, *Adv. Mater.*, 2014, **26**(5), 724–727, DOI: **10.1002/adma.201303357**.

126 P. Pingel, M. Arvind, L. Kölln, R. Steyrleuthner, F. Kraffert, J. Behrends, S. Janietz and D. Neher, P-Type Doping of Poly(3-Hexylthiophene) with the Strong Lewis Acid Tris(Pentafluorophenyl)Borane, *Adv. Electron. Mater.*, 2016, **2**(10), 1600204, DOI: **10.1002/aelm.201600204**.

127 Y. Han, G. Barnes, Y.-H. Lin, J. Martin, M. Al-Hashimi, S. Y. AlQaradawi, T. D. Anthopoulos and M. Heeney, Doping of Large Ionization Potential Indenopyrazine Polymers via Lewis Acid Complexation with Tris(Pentafluorophenyl)Borane: A Simple Method for Improving the Performance of Organic Thin-Film Transistors, *Chem. Mater.*, 2016, **28**(21), 8016–8024, DOI: **10.1021/acs.chemmater.6b03761**.

128 G. C. Welch, R. Coffin, J. Peet and G. C. Bazan, Band Gap Control in Conjugated Oligomers via Lewis Acids, *J. Am. Chem. Soc.*, 2009, **131**(31), 10802–10803, DOI: **10.1021/ja902789w**.

129 G. C. Welch and G. C. Bazan, Lewis Acid Adducts of Narrow Band Gap Conjugated Polymers, *J. Am. Chem. Soc.*, 2011, **133**(12), 4632–4644, DOI: **10.1021/ja110968m**.

130 P. Zalar, Z. B. Henson, G. C. Welch, G. C. Bazan and T.-Q. Nguyen, Color Tuning in Polymer Light-Emitting Diodes with Lewis Acids, *Angew. Chem., Int. Ed.*, 2012, **51**(30), 7495–7498, DOI: **10.1002/anie.201202570**.

131 H. Yan, J. Chen, K. Zhou, Y. Tang, X. Meng, X. Xu and W. Ma, Lewis Acid Doping Induced Synergistic Effects on Electronic and Morphological Structure for Donor and

Acceptor in Polymer Solar Cells, *Adv. Energy Mater.*, 2018, **8**(19), 1703672, DOI: 10.1002/aenm.201703672.

132 H. Yan, Y. Tang, X. Sui, Y. Liu, B. Gao, X. Liu, S. F. Liu, J. Hou and W. Ma, Increasing Quantum Efficiency of Polymer Solar Cells with Efficient Exciton Splitting and Long Carrier Lifetime by Molecular Doping at Heterojunctions, *ACS Energy Lett.*, 2019, **4**(6), 1356–1363, DOI: 10.1021/acsenergylett.9b00843.

133 H. Yan, Y. Tang, X. Meng, T. Xiao, G. Lu and W. Ma, Achieving High Doping Concentration by Dopant Vapor Deposition in Organic Solar Cells, *ACS Appl. Mater. Interfaces*, 2019, **11**(4), 4178–4184, DOI: 10.1021/acsami.8b16162.

134 Z. Chen, Y. Tang, B. Lin, H. Zhao, T. Li, T. Min, H. Yan and W. Ma, Probe and Control of the Tiny Amounts of Dopants in BHJ Film Enable Higher Performance of Polymer Solar Cells, *ACS Appl. Mater. Interfaces*, 2020, **12**(22), 25115–25124, DOI: 10.1021/acsami.0c06127.

135 D. Zhang, Q. Li, J. Zhang, J. Wang, X. Zhang, R. Wang, J. Zhou, Z. Wei, C. Zhang, H. Zhou and Y. Zhang, Control of Nanomorphology in Fullerene-Free Organic Solar Cells by Lewis Acid Doping with Enhanced Photovoltaic Efficiency, *ACS Appl. Mater. Interfaces*, 2020, **12**(1), 667–677, DOI: 10.1021/acsami.9b17238.

136 J. Luo, J. Xia, H. Yang, L. Chen, Z. Wan, F. Han, H. A. Malik, X. Zhu and C. Jia, Toward High-Efficiency, Hysteresis-Less, Stable Perovskite Solar Cells: Unusual Doping of a Hole-Transporting Material Using a Fluorine-Containing Hydrophobic Lewis Acid, *Energy Environ. Sci.*, 2018, **11**(8), 2035–2045, DOI: 10.1039/C8EE00036K.

137 S. S. Reddy, V. M. Arivunithi, V. G. Sree, H. Kwon, J. Park, Y.-C. Kang, H. Zhu, Y.-Y. Noh and S.-H. Jin, Lewis Acid-Base Adduct-Type Organic Hole Transport Material for High Performance and Air-Stable Perovskite Solar Cells, *Nano Energy*, 2019, **58**, 284–292, DOI: 10.1016/j.nanoen.2019.01.041.

138 Y. J. Jeong, J. Jung, E. H. Suh, D.-J. Yun, J. G. Oh and J. Jang, Self-Healable and Stretchable Organic Thermoelectric Materials: Electrically Percolated Polymer Nanowires Embedded in Thermoplastic Elastomer Matrix, *Adv. Funct. Mater.*, 2020, **30**(9), 1905809, DOI: 10.1002/adfm.201905809.

139 E. H. Suh, J. G. Oh, J. Jung, S. H. Noh, T. S. Lee and J. Jang, Brønsted Acid Doping of P3HT with Largely Soluble Tris(Pentafluorophenyl)Borane for Highly Conductive and Stable Organic Thermoelectrics Via One-Step Solution Mixing, *Adv. Energy Mater.*, 2020, **10**(47), 2002521, DOI: 10.1002/aenm.202002521.

140 E. H. Suh, S. B. Kim, H. S. Yang and J. Jang, Regulating Competitive Doping in Solution-Mixed Conjugated Polymers for Dramatically Improving Thermoelectric Properties, *Adv. Funct. Mater.*, 2022, **32**(46), 2207413, DOI: 10.1002/adfm.202207413.

141 H. J. Cheon, T. S. Lee, J. E. Lee, S. B. Kim, E. H. Suh, S.-K. Kwon, Y. J. Jeong, J. Jang and Y.-H. Kim, Design of Donor–Acceptor Polymer Semiconductors for Optimizing Combinations with Dopants to Maximize Thermoelectric Performance, *Chem. Mater.*, 2023, **35**(4), 1796–1805, DOI: 10.1021/acs.chemmater.2c03739.

142 J. Kim, D. Ju, S. Kim and K. Cho, Disorder-Controlled Efficient Doping of Conjugated Polymers for High-Performance Organic Thermoelectrics, *Adv. Funct. Mater.*, 2024, **34**(6), 2309156, DOI: 10.1002/adfm.202309156.

143 C. Lee, H. Kim and Y. Kim, Short-Wave Infrared-Sensing Organic Phototransistors with a Triarylamine-Based Polymer Doped with a Lewis Acid-Type Small Molecule, *ACS Appl. Mater. Interfaces*, 2021, **13**(16), 19064–19071, DOI: 10.1021/acsami.1c00472.

144 W. Huang, K. Besar, R. LeCover, A. M. Rule, P. N. Breysse and H. E. Katz, Highly Sensitive NH_3 Detection Based on Organic Field-Effect Transistors with Tris(Pentafluorophenyl)Borane as Receptor, *J. Am. Chem. Soc.*, 2012, **134**(36), 14650–14653, DOI: 10.1021/ja305287p.

145 B. Wang, A. D. Scaccabarozzi, H. Wang, M. Koizumi, M. I. Nugraha, Y. Lin, Y. Firdaus, Y. Wang, S. Lee, T. Yokota, T. D. Anthopoulos and T. Someya, Molecular Doping of Near-Infrared Organic Photodetectors for Photoplethysmogram Sensors, *J. Mater. Chem. C*, 2021, **9**(9), 3129–3135, DOI: 10.1039/D0TC05549B.

146 Y. Kato, K. Fukuda, T. Someya and T. Yokota, An Ultra-Flexible Temperature-Insensitive Strain Sensor, *J. Mater. Chem. C*, 2023, **11**(41), 14070–14078, DOI: 10.1039/D3TC02960C.

147 A. A. Meresa and F. S. Kim, Selective Ammonia-Sensing Platforms Based on a Solution-Processed Film of Poly(3-Hexylthiophene) and p-Doping Tris(Pentafluorophenyl)-Borane, *Polymers*, 2020, **12**(1), 128, DOI: 10.3390/polym12010128.

148 A. D. Scaccabarozzi, A. Basu, F. Aniés, J. Liu, O. Zapata-Arteaga, R. Warren, Y. Firdaus, M. I. Nugraha, Y. Lin, M. Campoy-Quiles, N. Koch, C. Müller, L. Tsetseris, M. Heeney and T. D. Anthopoulos, Doping Approaches for Organic Semiconductors, *Chem. Rev.*, 2022, **122**(4), 4420–4492, DOI: 10.1021/acs.chemrev.1c00581.

149 C. R. Bridges and T. Baumgartner, Lewis Acids and Bases as Molecular Dopants for Organic Semiconductors, *J. Phys. Org. Chem.*, 2020, **33**(9), e4077, DOI: 10.1002/poc.4077.

150 H. Méndez, G. Heimel, A. Opitz, K. Sauer, P. Barkowski, M. Oehzelt, J. Soeda, T. Okamoto, J. Takeya, J.-B. Arlin, J.-Y. Balandier, Y. Geerts, N. Koch and I. Salzmann, Doping of Organic Semiconductors: Impact of Dopant Strength and Electronic Coupling, *Angew. Chem., Int. Ed.*, 2013, **52**(30), 7751–7755, DOI: 10.1002/anie.201302396.

151 B. Yurash, D. X. Cao, V. V. Brus, D. Leifert, M. Wang, A. Dixon, M. Seifrid, A. E. Mansour, D. Lungwitz, T. Liu, P. J. Santiago, K. R. Graham, N. Koch, G. C. Bazan and T.-Q. Nguyen, Towards Understanding the Doping Mechanism of Organic Semiconductors by Lewis Acids, *Nat. Mater.*, 2019, **18**(12), 1327–1334, DOI: 10.1038/s41563-019-0479-0.

152 F. Pallini, S. Mattiello, N. Manfredi, S. Mecca, A. Fedorov, M. Sassi, K. Al Kurdi, Y.-F. Ding, C.-K. Pan, J. Pei, S. Barlow, S. R. Marder, T.-Q. Nguyen and L. Beverina, Direct Detection of Molecular Hydrogen upon P- and n-Doping of Organic Semiconductors with Complex Oxidants or Reductants, *J. Mater. Chem. A*, 2023, **11**(15), 8192–8201, DOI: 10.1039/D3TA00231D.

153 C. E. Tait, A. Reckwitz, M. Arvind, D. Neher, R. Bittl and J. Behrends, Spin–Spin Interactions and Spin Delocalisation in a Doped Organic Semiconductor Probed by EPR Spectroscopy, *Phys. Chem. Chem. Phys.*, 2021, **23**(25), 13827–13841, DOI: **10.1039/D1CP02133H**.

154 D. M. Stoltzfus, J. E. Donaghey, A. Armin, P. E. Shaw, P. L. Burn and P. Meredith, Charge Generation Pathways in Organic Solar Cells: Assessing the Contribution from the Electron Acceptor, *Chem. Rev.*, 2016, **116**(21), 12920–12955, DOI: **10.1021/acs.chemrev.6b00126**.

155 L. Guo, K. Liu, X. Tan, X. Wang, J. Huang, Z. Wei and G. Chen, B ← N Coordination Enables Efficient P-Doping in a Pyrazine-Based Polymer Donor Toward Enhanced Photovoltaic Performance, *Macromolecules*, 2021, **54**(23), 10758–10766, DOI: **10.1021/acs.macromol.1c01793**.

156 A. Markina, K.-H. Lin, W. Liu, C. Poelking, Y. Firdaus, D. R. Villalva, J. I. Khan, S. H. K. Paleti, G. T. Harrison, J. Gorenflot, W. Zhang, S. De Wolf, I. McCulloch, T. D. Anthopoulos, D. Baran, F. Laquai and D. Andrienko, Chemical Design Rules for Non-Fullerene Acceptors in Organic Solar Cells, *Adv. Energy Mater.*, 2021, **11**(44), 2102363, DOI: **10.1002/aenm.202102363**.

157 Z. Li, K. Jiang, G. Yang, J. Y. L. Lai, T. Ma, J. Zhao, W. Ma and H. Yan, Donor Polymer Design Enables Efficient Non-Fullerene Organic Solar Cells, *Nat. Commun.*, 2016, **7**(1), 13094, DOI: **10.1038/ncomms13094**.

158 Y. Li, Z. Zhang, X. Han, T. Li and Y. Lin, Fine-Tuning Contact via Complexation for High-Performance Organic Solar Cells, *CCS Chem.*, 2022, **4**(3), 1087–1097, DOI: **10.31635/ccschem.021.202100832**.

159 Y. Zhang, W. Wang, F. Zhang, K. Dai, C. Li, Y. Fan, G. Chen and Q. Zheng, Soft Organic Thermoelectric Materials: Principles, Current State of the Art and Applications, *Small*, 2022, **18**(12), 2104922, DOI: **10.1002/smll.202104922**.

160 M. Mukherjee, A. Srivastava and A. K. Singh, Recent Advances in Designing Thermoelectric Materials, *J. Mater. Chem. C*, 2022, **10**(35), 12524–12555, DOI: **10.1039/D2TC02448A**.

161 H. Wang and C. Yu, Organic Thermoelectrics: Materials Preparation, Performance Optimization, and Device Integration, *Joule*, 2019, **3**(1), 53–80, DOI: **10.1016/j.joule.2018.10.012**.

162 O. Bubnova, Z. U. Khan, A. Malti, S. Braun, M. Fahlman, M. Berggren and X. Crispin, Optimization of the Thermoelectric Figure of Merit in the Conducting Polymer Poly(3,4-Ethylenedioxythiophene), *Nat. Mater.*, 2011, **10**(6), 429–433, DOI: **10.1038/nmat3012**.

163 T. Park, C. Park, B. Kim, H. Shin and E. Kim, Flexible PEDOT Electrodes with Large Thermoelectric Power Factors to Generate Electricity by the Touch of Fingertips, *Energy Environ. Sci.*, 2013, **6**(3), 788, DOI: **10.1039/c3ee23729j**.

164 G.-H. Kim, L. Shao, K. Zhang and K. P. Pipe, Engineered Doping of Organic Semiconductors for Enhanced Thermoelectric Efficiency, *Nat. Mater.*, 2013, **12**(8), 719–723, DOI: **10.1038/nmat3635**.

165 W. Lee, H. Kim and Y. Kim, Contact/Noncontact-Mode Thermoelectric Characteristics of Polytriarylamine/Lewis Acid Complex Films in Horizontal Device Geometry, *Adv. Energy Sustainable Res.*, 2023, **4**(9), 2300009, DOI: **10.1002/aesr.202300009**.

166 Y. J. Jeong, J. Jung, E. H. Suh, D. Yun, J. G. Oh and J. Jang, Self-Healable and Stretchable Organic Thermoelectric Materials: Electrically Percolated Polymer Nanowires Embedded in Thermoplastic Elastomer Matrix, *Adv. Funct. Mater.*, 2020, **30**(9), 1905809, DOI: **10.1002/adfm.201905809**.

167 P. Lin and F. Yan, Organic Thin-Film Transistors for Chemical and Biological Sensing, *Adv. Mater.*, 2012, **24**(1), 34–51, DOI: **10.1002/adma.201103334**.

168 J. Panidi, A. F. Paterson, D. Khim, Z. Fei, Y. Han, L. Tsetseris, G. Vourlias, P. A. Patsalas, M. Heeney and T. D. Anthopoulos, Remarkable Enhancement of the Hole Mobility in Several Organic Small-Molecules, Polymers, and Small-Molecule:Polymer Blend Transistors by Simple Admixing of the Lewis Acid p-Dopant $B(C_6F_5)_3$, *Adv. Sci.*, 2018, **5**(1), 1700290, DOI: **10.1002/advs.201700290**.

169 W. Huang, K. Besar, R. LeCover, A. M. Rule, P. N. Breysse and H. E. Katz, Correction to Highly Sensitive NH_3 Detection Based on Organic Field-Effect Transistors with Tris(Pentafluorophenyl)Borane as Receptor, *J. Am. Chem. Soc.*, 2012, **134**(43), 18149, DOI: **10.1021/ja309862d**.

170 H. Ren, J. Chen, Y. Li and J. Tang, Recent Progress in Organic Photodetectors and Their Applications, *Adv. Sci.*, 2021, **8**(1), 2002418, DOI: **10.1002/advs.202002418**.

171 A. E. Mansour, D. Lungwitz, T. Schultz, M. Arvind, A. M. Valencia, C. Cocchi, A. Opitz, D. Neher and N. Koch, The Optical Signatures of Molecular-Doping Induced Polarons in Poly(3-Hexylthiophene-2,5-Diyl): Individual Polymer Chains *versus* Aggregates, *J. Mater. Chem. C*, 2020, **8**(8), 2870–2879, DOI: **10.1039/C9TC06509A**.

172 A. R. Jupp, Evidence for the Encounter Complex in Frustrated Lewis Pair Chemistry, *Dalton Trans.*, 2022, **51**(28), 10681–10689, DOI: **10.1039/D2DT00655C**.

173 T. Ikeda, K. Tahara, R. Ishimatsu, T. Ono, L. Cui, M. Maeda, Y. Ozawa and M. Abe, Lewis Pairing-Induced Electrochemiluminescence Enhancement from Electron Donor-Acceptor Diads Decorated with Tris(Pentafluorophenyl)Borane as an Electrochemical Protector, *Angew. Chem., Int. Ed.*, 2023, **63**(21), e202301109, DOI: **10.1002/anie.202301109**.

174 T. C. Hidalgo Castillo, M. Moser, C. Cendra, P. D. Nayak, A. Salleo, I. McCulloch and S. Inal, Simultaneous Performance and Stability Improvement of a P-Type Organic Electrochemical Transistor through Additives, *Chem. Mater.*, 2022, **34**(15), 6723–6733, DOI: **10.1021/acs.chemmater.2c00632**.

175 X. An, C. Wei, L. Bai, J. Zhou, L. Wang, Y. Han, L. Sun, J. Lin, H. Liu, J. Li, M. Xu, H. Ling, L. Xie and W. Huang, Photoexcitation Dynamics and Energy Engineering in Supramolecular Doping of Organic Conjugated Molecules, *Light: Sci. Appl.*, 2023, **12**(1), 30, DOI: **10.1038/s41377-022-01062-6**.

176 P. A. Albrecht, S. M. Rupf, M. Sellin, J. Schlögl, S. Riedel and M. Malischewski, Increasing the Oxidation Power of

TCNQ by Coordination of $B(C_6F_5)_3$, *Chem. Commun.*, 2022, **58**(32), 4958–4961, DOI: 10.1039/D2CC00314G.

177 A. E. Mansour, R. Warren, D. Lungwitz, M. Forster, U. Scherf, A. Opitz, M. Malischewski and N. Koch, Coordination of Tetracyanoquinodimethane-Derivatives with Tris(Pentafluorophenyl)Borane Provides Stronger p-Dopants with Enhanced Stability, *ACS Appl. Mater. Interfaces*, 2023, **15**(39), 46148–46156, DOI: 10.1021/acsami.3c10373.

178 O. Zapata-Arteaga, A. Perevedentsev, M. Prete, S. Busato, P. S. Floris, J. Asatryan, R. Rurali, J. Martín and M. Campoy-Quiles, A Universal, Highly Stable Dopant System for Organic Semiconductors Based on Lewis-Paired Dopant Complexes, *ACS Energy Lett.*, 2024, **9**(7), 3567–3577, DOI: 10.1021/acsenergylett.4c01278.

179 L. O. Müller, D. Himmel, J. Stauffer, G. Steinfeld, J. Slattery, G. Santiso-Quiñones, V. Brecht and I. Krossing, Simple Access to the Non-Oxidizing Lewis Superacid $Ph^F \rightarrow Al(OR^F)_3(R^F = C(CF_3)_3)$, *Angew. Chem., Int. Ed.*, 2008, **47**(40), 7659–7663, DOI: 10.1002/anie.200800783.

180 L. Greb, Lewis Superacids: Classifications, Candidates, and Applications, *Chem. – Eur. J.*, 2018, **24**(68), 17881–17896, DOI: 10.1002/chem.201802698.

181 L. Zapf, M. Riethmann, S. A. Föhrenbacher, M. Finze and U. Radius, An Easy-to-Perform Evaluation of Steric Properties of Lewis Acids, *Chem. Sci.*, 2023, **14**(9), 2275–2288, DOI: 10.1039/D3SC00037K.

182 G. J. P. Britovsek, J. Ugolotti and A. J. P. White, From $B(C_6F_5)_3$ to $B(OC_6F_5)_3$: Synthesis of $(C_6F_5)_2BOC_6F_5$ and $C_6F_5B(OC_6F_5)_2$ and Their Relative Lewis Acidity, *Organometallics*, 2005, **24**(7), 1685–1691, DOI: 10.1021/om049091p.

183 L. Xiang, J. Wang, A. Matler and Q. Ye, Structure-Constraint Induced Increase in Lewis Acidity of Tris(*Ortho*-Carboranyl)Borane and Selective Complexation with Bestmann Ylides, *Chem. Sci.*, 2024, **15**(43), 17944–17949, DOI: 10.1039/D4SC06144F.

184 S. Mummadi and C. Krempner, Triphenylborane in Metal-Free Catalysis, *Molecules*, 2023, **28**(3), 1340, DOI: 10.3390/molecules28031340.

185 L. Greb, C.-G. Daniliuc, K. Bergander and J. Paradies, Functional-Group Tolerance in Frustrated Lewis Pairs: Hydrogenation of Nitroolefins and Acrylates, *Angew. Chem., Int. Ed.*, 2013, **52**(22), 5876–5879, DOI: 10.1002/anie.201210175.

186 M. N. Bhagat, G.-F. Chang, C. K. Bennett, A. Raghuraman, M. E. Belowich, L. J. Broadbelt, S. T. Nguyen and J. M. Notestein, Improving and Stabilizing Fluorinated Aryl Borane Catalysts for Epoxide Ring-Opening, *Appl. Catal., A*, 2022, **636**, 118601, DOI: 10.1016/j.apcata.2022.118601.

187 K. M. Marczenko, S. Jee and S. S. Chitnis, High Lewis Acidity at Planar, Trivalent, and Neutral Bismuth Centers, *Organometallics*, 2020, **39**, 4287–4296, DOI: 10.1021/acs.organomet.0c00378.

188 F. Holtrop, C. Helling, M. Lutz, N. P. van Leest, B. de Bruin and J. C. Slootweg, Enhancement of London Dispersion in Frustrated Lewis Pairs: Towards a Crystalline Encounter Complex, *Syn. Lett.*, 2023, **34**, 1122–1128, DOI: 10.1055/a-1928-4902Art ID: ST-2022-07-0325-C.

189 M. O. Akram, J. R. Tidwell, J. L. Dutton and C. D. Martin, Tris(*Ortho*-carboranyl)Borane: An Isolable, Halogen-Free, Lewis Superacid, *Angew. Chem., Int. Ed.*, 2022, **61**(46), e202212073, DOI: 10.1002/anie.202212073.

190 A. E. Ashley, T. J. Herrington, G. G. Wildgoose, H. Zaher, A. L. Thompson, N. H. Rees and T. Kr, Separating Electrophilicity and Lewis Acidity: The Synthesis, Characterization, and Electrochemistry of the Electron Deficient Tris(Aryl)Boranes $B(C_6F_5)_{3-n}(C_6Cl_5)_n$ (n = 1–3), *J. Am. Chem. Soc.*, 2011, **133**, 14727–14740, DOI: 10.1021/ja205037t.

191 H. Zhao, J. H. Reibenspies and F. P. Gabbaï, Lewis Acidic Behavior of $B(C_6Cl_5)_3$, *Dalton Trans.*, 2013, **42**(3), 608–610, DOI: 10.1039/C2DT31482G.

192 M. Sultana, A. Paul and L. Roy, Computational Investigation of the Mechanism of FLP Catalyzed H_2 Activation and Lewis Base Assisted Proton Transfer, *ChemistrySelect*, 2020, **5**, 13397–13406, DOI: 10.1002/slct.202003794.

193 T. J. Herrington, A. J. W. Thom, A. J. P. White and A. E. Ashley, Novel H_2 Activation by a Tris[3,5-Bis(Trifluoromethyl)Phenyl]Borane Frustrated Lewis Pair, *Dalton Trans.*, 2012, **41**(30), 9019, DOI: 10.1039/c2dt30384a.

194 L. A. Körte, J. Schwabedissen, M. Soffner, S. Blomeyer, C. G. Reuter, Y. V. Vishnevskiy, B. Neumann, H. Stammler and N. W. Mitzel, Tris(Perfluorotolyl)Borane—A Boron Lewis Superacid, *Angew. Chem., Int. Ed.*, 2017, **56**(29), 8578–8582, DOI: 10.1002/anie.201704097.

195 M. Galdeano, F. Ruipérez and J. M. Matxain, Theoretical Characterization of New Frustrated Lewis Pairs for Responsive Materials, *Polymers*, 2021, **13**(10), 1573, DOI: 10.3390/polym13101573.

196 S. Yruegas, J. J. Martinez and C. D. Martin, Intermolecular Insertion Reactions of Azides into 9-Borafluorenes to Generate 9,10-B,N-Phenanthrenes, *Chem. Commun.*, 2018, **54**(50), 6808–6811, DOI: 10.1039/c8cc01529e.

197 H. Böhrer, N. Trapp, D. Himmel, M. Schleep and I. Krossing, From Unsuccessful H_2-Activation with FLPs Containing $B(Ohfip)_3$ to a Systematic Evaluation of the Lewis Acidity of 33 Lewis Acids Based on FLuoride, Chloride, Hydride and Methyl Ion Affinities, *Dalton Trans.*, 2015, **44**, 7489–7499, DOI: 10.1039/c4dt02822h.

198 M. M. Alharbi, Y. Ingen, A. van; Roldan, T. Kaehler and R. L. Melen, Synthesis and Lewis Acidity of Fluorinated Triaryl Borates, *Dalton Trans.*, 2023, **52**(6), 1820–1825, DOI: 10.1039/D2DT04095F.

199 L. Falivene, Z. Cao, A. Petta, L. Serra, A. Poater, R. Oliva, V. Scarano and L. Cavallo, Towards the Online Computer-Aided Design of Catalytic Pockets, *Nat. Chem.*, 2019, **11**(10), 872–879, DOI: 10.1038/s41557-019-0319-5.

200 M. O. Akram, C. D. Martin and J. L. Dutton, The Effect of Carborane Substituents on the Lewis Acidity of Boranes, *Inorg. Chem.*, 2023, **62**(33), 13495–13504, DOI: 10.1021/acs.inorgchem.3c01872.

201 J. O. Huh, H. Kim, K. M. Lee, Y. S. Lee, Y. Do and M. H. Lee, *O*-Carborane-Assisted Lewis Acidity Enhancement of Triarylboranes, *Chem. Commun.*, 2010, **46**(7), 1138–1140, DOI: 10.1039/B918263B.

202 K. M. Lee, J. O. Huh, T. Kim, Y. Do and M. H. Lee, A Highly Lewis Acidic Triarylborane Bearing Peripheral *O*-Carborane Cages, *Dalton Trans.*, 2011, **40**(44), 11758, DOI: 10.1039/c1dt11064k.

203 B. H. Choi, J. H. Lee, H. Hwang, K. M. Lee and M. H. Park, Novel Dimeric *o*-Carboranyl Triarylborane: Intriguing Ratiometric Color-Tunable Sensor via Aggregation-Induced Emission by Fluoride Anions, *Organometallics*, 2016, **35**(11), 1771–1777, DOI: 10.1021/acs.organomet.6b00172.

204 J. Kahlert, L. Böhling, A. Brockhinke, H.-G. Stammler, B. Neumann, L. M. Rendina, P. J. Low, L. Weber and M. A. Fox, Syntheses and Reductions of *C*-Dimesitylboryl-1,2-Dicarba-Closo-Dodecaboranes, *Dalton Trans.*, 2015, **44**, 9766–9781, DOI: 10.1039/C5DT00758E.

205 H. Wang, J. Zhang and Z. Xie, Reversible Photothermal Isomerization of Carborane-Fused Azaborole to Borirane: Synthesis and Reactivity of Carbene-Stabilized Carborane-Fused Borirane, *Angew. Chem., Int. Ed.*, 2017, **56**(31), 9198–9201, DOI: 10.1002/anie.201704642.

206 H. Zhang, J. Wang, W. Yang, L. Xiang, W. Sun, W. Ming, Y. Li, Z. Lin and Q. Ye, Solution-Phase Synthesis of a Base-Free Benzoborirene and a Three-Dimensional Inorganic Analogue, *J. Am. Chem. Soc.*, 2020, **142**(41), 17243–17249, DOI: 10.1021/jacs.0c06538.

207 Y. Wei, J. Wang, W. Yang, Z. Lin and Q. Ye, Boosting Ring Strain and Lewis Acidity of Borirane: Synthesis, Reactivity and Density Functional Theory Studies of an Uncoordinated Arylborirane Fused to *o*-Carborane, *Chem. – Eur. J.*, 2022, **29**(5), e202203265, DOI: 10.1002/chem.202203265.

208 J. Wang, P. Jia, W. Sun, Y. Wei, Z. Lin and Q. Ye, Synthesis of Iminoboryl *O*-Carboranes by Lewis Base Promoted Aminoborirane-to-Iminoborane Isomerization, *Inorg. Chem.*, 2022, **61**(23), 8879–8886, DOI: 10.1021/acs.inorgchem.2c00944.

209 J. Krebs, A. Häfner, S. Fuchs, X. Guo, F. Rauch, A. Eichhorn, I. Krummenacher, A. Friedrich, L. Ji, M. Finze, Z. Lin, H. Braunschweig and T. B. Marder, Backbone-Controlled LUMO Energy Induces Intramolecular C–H Activation in *Ortho*-Bis-9-Borafluorene-Substituted Phenyl and *o*-Carboranyl Compounds Leading to Novel 9,10-Diboraanthracene Derivatives, *Chem. Sci.*, 2022, **13**(47), 14165–14178, DOI: 10.1039/D2SC06057D.

210 T. Bischof, X. Guo, I. Krummenacher, L. Beßler, Z. Lin, M. Finze and H. Braunschweig, Alkene Insertion Reactivity of a *O*-Carboranyl-Substituted 9-Borafluorene, *Chem. Sci.*, 2022, **13**(25), 7492–7497, DOI: 10.1039/D2SC02750J.

211 A. Benton, J. D. Watson, S. M. Mansell, G. M. Rosair and A. J. Welch, The Lewis Acidity of Borylcarboranes, *J. Organomet. Chem.*, 2020, **907**, 121057, DOI: 10.1016/j.jorganchem.2019.121057.

212 L. Xiang, J. Wang, A. Matler and Q. Ye, Structure-Constraint Induced Increase in Lewis Acidity of Tris(*Ortho*-Carboranyl)Borane and Selective Complexation with Bestmann Ylides, *Chem. Sci.*, 2024, **15**(43), 17944–17949, DOI: 10.1039/D4SC06144F.

213 S. Yruegas, J. C. Axtell, K. O. Kirlikovali, A. M. Spokoyny and C. D. Martin, Synthesis of 9-Borafluorene Analogues Featuring a Three-Dimensional 1,10-Bis(*o*-Carborane) Backbone, *Chem. Commun.*, 2019, **55**(20), 2892–2895, DOI: 10.1039/C8CC10087J.

214 C. Zhang, J. Wang, W. Su, Z. Lin and Q. Ye, Synthesis, Characterization, and Density Functional Theory Studies of Three-Dimensional Inorganic Analogues of 9,10-Diboraanthracene—A New Class of Lewis Superacids, *J. Am. Chem. Soc.*, 2021, **143**(23), 8552–8558, DOI: 10.1021/jacs.1c03057.

215 J. Krebs, M. Haehnel, I. Krummenacher, A. Friedrich, H. Braunschweig, M. Finze, L. Ji and T. B. Marder, Synthesis and Structure of an *o*-Carboranyl-Substituted Three-Coordinate Borane Radical Anion, *Chem. – Eur. J.*, 2021, **27**(31), 8159–8167, DOI: 10.1002/chem.202100938.

216 C. Zhang, X. Liu, J. Wang and Q. Ye, A Three-Dimensional Inorganic Analogue of 9,10-Diazido-9,10-Diboraanthracene: A Lewis Superacidic Azido Borane with Reactivity and Stability, *Angew. Chem., Int. Ed.*, 2022, **61**(36), e202205506, DOI: 10.1002/anie.202205506.

217 C. Zhang, J. Wang, Z. Lin and Q. Ye, Synthesis, Characterization, and Properties of Three-Dimensional Analogues of 9-Borafluorenes, *Inorg. Chem.*, 2022, **61**(45), 18275–18284, DOI: 10.1021/acs.inorgchem.2c03111.

218 M. O. Akram, J. R. Tidwell, J. L. Dutton and C. D. Martin, Bis(1-Methyl-ortho-Carboranyl)Borane, *Angew. Chem., Int. Ed.*, 2023, **62**(34), e202307040, DOI: 10.1002/anie.202307040.

219 M. Diab, K. Jaiswal, D. Bawari and R. Dobrovetsky, The Chemistry of [1,1′-bis(o-Carboranyl)]Borane η^2-σ-Silane Adduct, *Isr. J. Chem.*, 2023, **63**(7–8), e202300010, DOI: 10.1002/ijch.202300010.

220 L. Xiang, J. Wang, I. Krummenacher, K. Radacki, H. Braunschweig, Z. Lin and Q. Ye, Persistent and Predominantly Localized Boron Radical from the Reduction of a Three-Dimensional Analogue of NHC-Stabilized Borafluorenium, *Chem. – Eur. J.*, 2023, **29**(42), e202301270, DOI: 10.1002/chem.202301270.

221 K. Vashisth, S. Dutta, M. O. Akram and C. D. Martin, Examining the Reactivity of Tris(*Ortho*-Carboranyl)Borane with Lewis Bases and Application in Frustrated Lewis Pair Si–H Bond Cleavage, *Dalton Trans.*, 2023, **52**(28), 9639–9645, DOI: 10.1039/D3DT01557B.

222 J. Wang, L. Xiang, X. Liu, A. Matler, Z. Lin and Q. Ye, Avenue to Novel *O*-Carboranyl Boron Compounds – Reactivity Study of *o*-Carborane-Fused Aminoborirane towards Organic Azides, *Chem. Sci.*, 2024, **15**(13), 4839–4845, DOI: 10.1039/D4SC00489B.

223 J. Wang and Q. Ye, Borirenes and Boriranes: Development and Perspectives, *Chem. – Eur. J.*, 2024, **30**(11), e202303695, DOI: 10.1002/chem.202303695.

